University of Louisville

ThinkIR: The University of Louisville's Institutional Repository

Electronic Theses and Dissertations

5-2023

Chemosensory processing by the mediodorsal thalamus.

Kelly E. Fredericksen
University of Louisville

Follow this and additional works at: https://ir.library.louisville.edu/etd

Part of the Systems Neuroscience Commons

CHEMOSENSORY PROCESSING BY THE MEDIODORSAL THALAMUS

By

Kelly E. Fredericksen
B.S., Elmhurst University, 2015
M.S., University of Louisville, 2020

A Dissertation
Submitted to the Faculty of the
School of Medicine of the University of Louisville
in Partial Fulfillment of the Requirements
for the Degree of

Doctor of Philosophy
in Anatomical Sciences and Neurobiology

Department of Anatomical Sciences and Neurobiology
University of Louisville
Louisville, Kentucky

May 2023

CHEMOSENSORY PROCESSING BY THE MEDIODORSAL THALAMUS

By

Kelly E. Fredericksen
B.S., Elmhurst University, 2015
M.S., University of Louisville, 2020

A Dissertation Approved on

April 14, 2023

by the following members of the Dissertation Committee:

_____
Dissertation Director
Chad Samuelsen, Ph.D.

_____
Martha Bickford, Ph.D.

_____
Robin Krimm, Ph.D.

_____
Robert Lundy, Ph.D.

_____
Roberto Vincis, Ph.D.

ACKNOWLEDGMENTS

First and foremost, I would like to thank my husband, my parents, my siblings, and my in-laws for the pocket of love and support that they envelope me in. I am truly grateful to have such a strong and encouraging family behind me in all that I do. I could not have done this without them. I would like to thank my friends who have become my family along the way– I am so lucky. I am thankful to my fellow lab members and departmental students, who have contributed greatly to my science and lifted my spirits more times than I can count. A big thank you goes to my mentor, Dr. Chad Samuelsen, for helping me become a better scientist and encouraging my experimental ideas. I am thankful for the support of my committee members: Dr. Robin Krimm, Dr. Roberto Vincis, Dr. Martha Bickford, and Dr. Robert Lundy. I am lucky to have such brilliant science advisors to guide me. To all, my sincerest thank you.

ABSTRACT

CHEMOSENSORY PROCESSING BY THE MEDIODORSAL THALAMUS

Kelly E. Fredericksen

April 14, 2023

The mediodorsal thalamus (MD) is thought to be key component of the network that processes chemosensory information to guide our consummatory choices. Previous studies show that the mediodorsal thalamus receives projections from both the piriform cortex (PC) and gustatory cortex (GC), suggesting that it may process chemosensory information from both areas. Although the mediodorsal thalamus has been shown to respond to odors detected by sniffing, it remains unknown how its neurons represent experienced odors, tastes, and odor-taste mixtures originating from the mouth. Importantly, humans and animals with mediodorsal thalamic lesions do not suffer from anosmia, but experience deficits in odor attention, and the hedonic perceptions of odors and odor-taste mixtures. To gain a better understanding of the role of the mediodorsal thalamus in processing chemosensory information, my dissertation project focused on investigating its connectivity, physiology, and behavioral relevance in the context of consummatory choice.

I used an intersectional viral approach and found that a greater proportion of neurons in the mediodorsal thalamus form cortico-thalamic connections with the gustatory cortex than with the posterior piriform cortex. This result suggests that input from the gustatory cortex may more broadly influence processing in the mediodorsal thalamus than the posterior piriform cortex.

Next, I recorded responses of neurons in the mediodorsal thalamus to experienced odors, tastes, and odor-taste mixtures delivered into the mouth. I found that neurons in the mediodorsal thalamus encode the identity of individual odors, tastes, and odor-taste mixtures. Additionally, subpopulations of neurons represent taste palatability and represent odor-taste mixtures differently than their odor or taste component. These results are the first to show the mediodorsal thalamus encodes taste and odor-taste information.

Finally, I used pharmacological inactivation during a two-bottle brief-access task to determine the role of the mediodorsal thalamus in the consummatory choice. I found that inactivation of the mediodorsal thalamus decreases overall consumption and increases the amount of switching between two stimuli, suggesting its importance in sensory attention and stimulus value during consummatory choice tasks. Taken together, these data indicate that the mediodorsal thalamus is important to the network that processes chemosensory signals and informs consummatory choice.

TABLE OF CONTENTS

LIST OF FIGURES

CHAPTER 1

INTRODUCTION

The food choices we make can have long-term health benefits or consequences. These choices are influenced by various sensations, particularly a food's aroma, taste, and texture. The perception of flavor is the result of the interplay between these different sensations. For example, the perception of a strawberry depends on the combination of a strawberry odor, the taste of sugar (sweet), and the texture of rough seeds. However, it is the multisensory integration of olfactory and gustatory information that is essential for the perception of flavor (Verhagen and Engelen, 2006; Small, 2012). Sampling an odor-taste mixture associates the odor with the taste's quality (chemical identity) and hedonic value (pleasantness/unpleasantness) (Stevenson et al., 1995; Sakai and Imada, 2003; Prescott et al., 2004; Gautam and Verhagen, 2010; Green et al., 2012). These powerful associations lead to preferences for odors that have been experienced with pleasant tastes, and the avoidance of odors that have been experienced with unpleasant tastes (Fanselow and Birk, 1982; Holder, 1991; Schul et al., 1996; Sakai and Yamamoto, 2001; Gautam and Verhagen, 2010; Green et al., 2012; McQueen et al., 2020). Therefore, our prior experiences with flavors (i.e. odor-taste mixtures) guides our consumption or avoidance of food. There are many

brain regions involved in processing the components of flavor. My dissertation research focuses on understanding how the mediodorsal thalamus, a higher-order thalamic area that receives input from the chemosensory cortices for smell and taste, processes olfactory and gustatory information to inform chemosensory consumption.

The olfactory system plays an essential role in our eating experience. The different combinations of odor molecules we encounter each day can influence our food choices; for example, the alluring aroma exuded from a chocolate shop can be difficult to resist. The olfactory system plays an essential role in our eating experience. Odors are detected by means of orthonasal or retronasal olfaction. Orthonasal olfaction is what is generally thought of as smelling or sniffing through the nose (chocolate shop as you walk by). Retronasal olfaction occurs when odors from the mouth enter the nasal cavity via the oropharynx during exhalation (chocolate during consumption). In both routes, odor molecules activate the olfactory system by binding to olfactory receptor neurons in the nasal epithelium. However, retronasal olfaction is fundamental for forming flavor perceptions (Rozin, 1982; Verhagen and Engelen, 2006; Lim and Johnson, 2011; Green et al., 2012; Small and Green, 2012; Bartoshuk et al., 2019). Olfactory receptor neurons send projections to glomeruli in the olfactory bulb and synapse with mitral and tufted neurons that project to various regions important in olfactory processing, including the piriform cortex, olfactory tubercle, amygdala, and entorhinal cortex (Scalia and Winans, 1975; Haberly and Price, 1977; Ghosh et al., 2011; Miyamichi et al., 2011; Wesson and Wilson, 2011; Witter et al., 2017). The olfactory system is unique

among the sensory modalities in that olfactory signals reach the cortex without first being relayed through the thalamus. Most projections from the olfactory bulb are to the piriform cortex (Ghosh et al., 2011), a region long considered to be the "primary" olfactory cortex.

The piriform cortex is the largest cortical area receiving direct input from the main olfactory bulb (Ghosh et al., 2011). It is comprised of at least two functionally distinct subregions based on differences in cytoarchitecture, connectivity, and function (Wilson and Sullivan, 2011). The leading theory of cortical processing of olfactory information posits that neurons in the anterior piriform cortex represent the identity of individual odors (e.g. the smell of lavender) while neurons in posterior piriform cortex encode the similarity, category, or quality of the odors (e.g., floral) (Litaudon et al., 2003; Kadohisa and Wilson, 2006; Wilson et al., 2020). This theory is also supported by anatomical studies showing that the dense innervation from the main olfactory bulb in anterior piriform cortex is reduced and replaced by association fibers in the posterior piriform cortex (Haberly and Price, 1977; Neville and Haberly, 2003). While piriform cortex has been thought of as a primary olfactory cortex, inputs from orbitofrontal cortex and basolateral amygdala to the region suggest it could have an associative function (Datiche and Cattarelli, 1996; Johnson et al., 2000; Majak et al., 2004; Illig, 2005; Calu et al., 2007). In an associative piriform cortex, processing would reflect learned information, such as odor-taste mixture associations. Electrophysiological studies show multimodal activity in individual neurons in the posterior piriform cortex that respond to single odors and tastes (Maier et al., 2012), and represent odor-taste mixtures uniquely

from their odor and taste components (Idris et al., 2023). Importantly, this indicates the convergence of odor and taste information to single multisensory neurons in the piriform cortex. Further supporting piriform cortex as a site of multisensory processing, the piriform cortex has reciprocal connections to the insular (gustatory) cortex, a region known mainly for taste processing that is thought to be a site of flavor integration. A study by Maier et al. (2015) found that inactivating the gustatory cortex altered taste-evoked responses in the piriform cortex. However, this effect extended to odor stimuli as well. Specifically, they found that perturbing the gustatory cortex significantly altered odor-evoked responses in the piriform cortex (Maier et al., 2015). The neural connections between piriform cortex and gustatory cortex could be essential for the integration of odors and tastes, yet this pathway is understudied. The flavor network needs to be further studied as it is vital to the everyday process of consuming foods.

When consuming a meal, we can experience up to five different taste qualities: sweet, salty, sour, bitter, and umami. Taste information is received through taste receptor cells located on the taste buds in the oral cavity. The taste buds are innervated by intragemmal fibers that stem from either the facial nerve, the glossopharyngeal nerve, or the vagus nerve, depending on the location of the taste bud (Norgren, 1983). These three cranial nerves communicate information to the nucleus of the solitary tract in the brainstem (Norgren, 1983). Gustatory signals from the nucleus of the solitary tract project to the amygdala, hypothalamus, and the parabrachial nucleus in non-primates (Norgren, 1978; Tokita et al., 2009). The parabrachial nucleus is considered the first region to

integrate gustatory and visceral information important for conditioned taste aversions and other types of gut feedback (Reilly, 1999; Iwai et al., 2015). Because primates do not have a parabrachial nucleus, signals transmit straight from the nucleus of the solitary tract to the parvacellular portion of the ventral posteromedial (VPMpc) nucleus of the thalamus (Beckstead et al., 1980). Neurons in the VPMpc, also known as the gustatory thalamus, can encode taste quality and taste palatability (the pleasantness or unpleasantness of a taste) indicating a higher level of processing than strictly representing taste identity (Liu and Fontanini, 2015). The VPMpc sends projections to the insular cortex, more specifically, the anterior insular area comprising the gustatory cortex. The gustatory cortex is considered the first area of the brain where taste and olfactory inputs are integrated for flavor perception (Small, 2012). This region contains single neurons that respond to both olfactory and gustatory stimuli (Samuelsen and Fontanini, 2017), and has reciprocal connections with the piriform cortex (Krushel and van Der Kooy, 1988; Shi and Cassell, 1998; Johnson et al., 2000; Sewards and Sewards, 2001). Our lab also has preliminary research showing that individual neurons in the gustatory cortex respond to odor-taste mixtures, indicating multimodal activity. The multisensory function and anatomical connections between the chemosensory cortices, piriform cortex and gustatory cortex, support the idea that cortico-cortical interactions contribute to the integration of odors and tastes.

The integration of smell and taste

The cortico-cortical interactions between the piriform cortex and gustatory cortex are thought to contribute to the processing of flavor. As previously discussed, the chemosensory cortices are multisensory, rather than being exclusively dedicated to processing either odor or taste information. Responses to olfactory, oral somatosensory, and gustatory stimuli overlap temporally in both the gustatory cortex and piriform cortex (Katz et al., 2001; Fontanini et al., 2009; Jezzini et al., 2013; Bolding and Franks, 2017; Maier, 2017; Samuelsen and Fontanini, 2017; Bouaichi and Vincis, 2020). Combining electrophysiology and optogenetics, Maier and colleagues (2015) found that optogenetic perturbation of the gustatory cortex suppressed taste responses and modulated odor responses in the piriform cortex, indicating functional cortico-cortical connections. Perturbation of the gustatory cortex additionally resulted in behavioral deficits: rats failed to express a preference for an odor stimulus previously associated with a sweetener (Maier et al., 2015). Blankenship et al. (2019) looked further and found that inactivating gustatory cortex impairs the expression of retronasal odor preferences. Because retronasal olfaction is essential for the association of odor-taste mixtures, this finding supports the gustatory cortex being a key region involved in odor-taste mixture processing (Rozin, 1982; Verhagen and Engelen, 2006; Lim and Johnson, 2011; Green et al., 2012; Small and Green, 2012; Bartoshuk et al., 2019). Together, these studies suggest that the integration of odor and taste information may depend on the cortico-cortical connectivity between the two chemosensory cortices.

Brain regions often require direct interactions for optimal function, but indirect pathways offer redundancy, enabling adaptation and compensation in case of damage (MacKinnon, 2018; Bonanomi, 2019; Hikosaka et al., 2019; Prillwitz et al., 2021). Many sensory cortico-cortical pathways have parallel cortico-thalamo-cortical routes that involve higher-order thalamic regions. These higher-order thalamic areas are thought to modulate, synchronize, and transmit sensory information from primary cortex to higher-order areas like the prefrontal cortex (Theyel et al., 2010; Saalmann et al., 2012; Stroh et al., 2013; Mease et al., 2016; Zhou et al., 2016; Schmitt et al., 2017; Rikhye et al., 2018). Investigating the visual sensory system, Saalmann and colleagues (2012) simultaneously recorded from layer 4 of the visual cortex, temporal occipital cortical area (TEO), and the pulvinar nucleus of the thalamus in monkeys during a visual task where a spatial cue indicated a target location. Their hypothesis that the pulvinar regulates cortical synchrony during selective attention was based on its anatomically central cortico-pulvinar-cortico connectivity and functional studies linking lesions of the pulvinar with attentional deficits (Petersen et al., 1987; Snow et al., 2009). Results showed that spatial attention increased the coherence between the neural spiking activity in pulvinar and the local field potentials of both cortical areas (Saalmann et al., 2012). The various studies supporting higher-order thalamic synchrony of sensory cortical information encourages investigation of the higher-order thalamic area that may modulate and synchronize chemosensory information. The mediodorsal thalamus is a higher-order thalamic area that receives input from primary areas of the olfactory and gustatory systems, piriform cortex and gustatory cortex,

respectively, and is reciprocally connected to prefrontal cortical areas important for decision making (Price and Slotnick, 1983; Kuroda et al., 1992; Ray and Price, 1992; Shi and Cassell, 1998; Kuramoto et al., 2017; Pelzer et al., 2017). Increased excitatory input from the mediodorsal thalamus has been shown to amplify prefrontal cortical activity, while improving sensory-based behavioral performance (Schmitt et al., 2017). The mediodorsal thalamus, like the pulvinar, has functional cortico-thalamo-cortical connectivity and plays a crucial role in attention (Plailly et al., 2008; Tham et al., 2009, 2011a, 2011b; Veldhuizen and Small, 2011; Schmitt et al., 2017; Rikhye et al., 2018). The mediodorsal thalamus, with its connectivity and function, is likely to synchronize smell and taste information, but its cortico-thalamic connections with chemosensory cortices and its role in processing chemosensory signals remain understudied.

The mediodorsal thalamus

According to the current literature, the mediodorsal thalamus is likely a key thalamic region in the cortico-thalamo-cortical pathway for chemosensory processing. The mediodorsal thalamus is a multisensory area capable of representing auditory, somatosensory, and visual information, but its most studied for its role in olfaction due to the dense olfactory inputs to the mediodorsal thalamus's central region (Kuroda et al., 1992; Courtiol and Wilson, 2015). Studies have investigated its role in olfactory-dependent behaviors (Yarita et al., 1980; Eichenbaum et al., 1980; Imamura et al., 1984; Slotnick and Risser, 1990; Oyoshi et al., 1996; Kawagoe et al., 2007; Sela et al., 2009; Tham et al., 2011b, 2011a;

Courtiol and Wilson, 2014, 2015), processing reward associations (Oyoshi et al., 1996; Kawagoe et al., 2007; Courtiol and Wilson, 2016; Schmitt et al., 2017; Rikhye et al., 2018; Chakraborty et al., 2019), and multisensory information (Schmitt et al., 2017; Rikhye et al., 2018; Fredericksen et al., 2019). Additionally, psychophysical experiments show that people with lesions of mediodorsal thalamus have an altered hedonic perception of odors and odor-taste mixtures, exhibiting a reduction in consumption (Rousseaux et al., 1996; Asai et al., 2008; Sela et al., 2009). The mediodorsal thalamus (MD) is also integral to general cognitive functions, like attention (Plailly et al., 2008; Tham et al., 2009, 2011a, 2011b; Veldhuizen and Small, 2011; Schmitt et al., 2017; Rikhye et al., 2018), valuation (Rousseaux et al., 1996; Sela et al., 2009; Tham et al., 2011a), and stimulus-outcome associations (Oyoshi et al., 1996; Kawagoe et al., 2007; Courtiol and Wilson, 2016) that need to be further studied in the context of processing chemosensory signals.

Anatomical studies suggest that the mediodorsal thalamus (MD) may be a crossroad of chemosensory input related to consummatory choice. Traditional tract-tracing studies show that projections from the piriform cortex (PC) and gustatory cortex (GC) overlap in the central and medial subregions of the mediodorsal thalamus (Price and Slotnick, 1983; Kuroda et al., 1992; Ray and Price, 1992; Shi and Cassell, 1998). Electron microscopy studies approximated that two-thirds of projections from the piriform cortex to mediodorsal thalamus were small round terminals (Kuroda et al., 1992). However, projections from piriform cortex also form "driver-like" giant synapses with neurons in the central segment

of the mediodorsal thalamus (Pelzer et al., 2017). The projections from gustatory cortex to the mediodorsal thalamus have not yet been characterized. Therefore, the pervasiveness of connectivity between cortical neurons from the piriform cortex or the gustatory cortex to the mediodorsal thalamus may differ.

Electrophysiological experiments investigating the functional properties of the mediodorsal thalamus focused on its role in olfaction due to its involvement in olfactory-dependent behaviors (Yarita et al., 1980; Eichenbaum et al., 1980; Imamura et al., 1984; Slotnick and Risser, 1990; Oyoshi et al., 1996; Kawagoe et al., 2007; Sela et al., 2009; Tham et al., 2011b, 2011a; Courtiol and Wilson, 2014, 2015). Individual mediodorsal thalamic neurons respond to orthonasal odors (Yarita et al., 1980; Imamura et al., 1984; Courtiol and Wilson, 2014) and display odor selectivity (Kawagoe et al., 2007; Courtiol and Wilson, 2015, 2016). Kawagoe et al. (2007) recorded in the mediodorsal thalamus during an odor discrimination task where odors cues were either associated with a reward or not. Even though odors were associated with the same reinforcement category, 10% of the neurons displayed differences in odor stimulus responses (Kawagoe et al., 2007). These results support that neurons in the mediodorsal thalamus are capable of encoding odor identity. The implications of this role can be observed in subjects with damage to the mediodorsal thalamus that experience deficits in odor discrimination as well as odor identification (Sela et al., 2009; Tham et al., 2011b). Importantly, this impairment in olfactory function is not due to anosmia or deficits in odor detection (Eichenbaum et al., 1980; Potter and Butters, 1980; Sapolsky and Eichenbaum, 1980; Sela et al., 2009). Interestingly, in anesthetized rabbits and behaving

monkeys, the majority of odor responsive neurons are sensory specific, as they do not respond to visual, auditory, or somatosensory stimulation (Yarita et al., 1980; Imamura et al., 1984). But would these odor responsive neurons in the mediodorsal thalamus respond to taste stimuli? To my knowledge, only one study has delivered taste stimuli while recording single-unit activity in the mediodorsal thalamus (Oyoshi et al., 1996). However, this neural activity was collected during the presentation of a single taste as a reward stimulus and was not compared across tastes (Oyoshi et al., 1996). My previous work revealed differences in immediate early gene expression in the mediodorsal thalamus dependent upon experience with an odor, taste, or odor-taste mixture (Fredericksen et al., 2019). We found that a novel odor elicited significantly greater c-Fos expression than an experienced odor. Conversely, we observed that a previously experienced taste, or odor-taste mixture evoked greater c-Fos expression than a novel taste, or odor-taste mixture (Fredericksen et al., 2019). These differences in c-Fos expression suggest the possible involvement of the mediodorsal thalamus in taste and odor-taste mixture processing. However, how neuronal activity in the mediodorsal thalamus represents individual intraorally delivered odors, tastes, and odor-taste mixtures remains unknown.

The mediodorsal thalamus and decision making

      The mediodorsal thalamus forms dense reciprocal connections with higher-order cortical areas, such as the orbitofrontal cortex, that are important for chemosensory-based decision-making (Schoenbaum et al., 2011; Alcaraz et al.,

2016). While one study showed that pharmacological inactivation of the mediodorsal thalamus significantly disrupted working memory for olfactory-dependent foraging (Scott et al., 2020), few others have investigated the involvement of the mediodorsal thalamus in consummatory behaviors. The mediodorsal thalamus is important for three main behaviors that influence chemosensory decision making: action/reward outcome associations, sensory attention, and chemosensory-stimulus value.

Acquiring appropriate action/reward outcome associations are important for making accurate choices of what to consume or what to avoid. Electrophysiology studies have demonstrated that the activity of neurons in the mediodorsal thalamus exhibits strong response preferences to an odor associated with a reward (Kawagoe et al., 2007) and the activity prior to odor sampling encodes the location associated with the odor (Courtiol and Wilson, 2016). Further evidence for the role of the mediodorsal thalamus in processing action-outcome associations important for decision-making is supported by studies showing that lesions of the mediodorsal thalamus impair the learning of new associations and discriminations (Slotnick and Kaneko, 1981; Gaffan and Murray, 1990; Slotnick and Risser, 1990; Corbit et al., 2003; Mitchell and Gaffan, 2008). For example, neurotoxic lesions to the mediodorsal thalamus in rhesus monkeys showed that the mediodorsal thalamus was required for new learning of visual discriminations, but the retention or retrieval of previous visual discriminations were intact (Mitchell and Gaffan, 2008). Bilateral optogenetic suppression of the mediodorsal thalamus results in incorrect sensory selection based on learned associations, but excitation of the

mediodorsal thalamus improved performance (Schmitt et al., 2017). However, how the mediodorsal thalamus processes odor-taste mixtures and how those associations inform consummatory choices remains unknown.

Sensory attention and task engagement are critical for making daily decisions. For example, we stop our vehicles at the visual stimulus of a red light and go when the light turns green. Because our auditory system is also engaged during the task of driving, we also stop when we hear an ambulance siren. The mediodorsal thalamus is important for processing this type of information, enabling attention to a specific sensory stimulus when engaging in a task. Interestingly, a study by Schmitt et al. (2017) found that the firing rates of mediodorsal thalamic neurons were modulated by the level of engagement in a forced sensory choice task. This study used bilateral optogenetic suppression of the mediodorsal thalamus and found that suppression resulted in mice attending to the incorrect auditory or visual stimulus (Schmitt et al., 2017). When people were asked to attend to an odor, not a taste, fMRI scans showed brain activation of the piriform cortex and the mediodorsal thalamus (Veldhuizen and Small, 2011). Additionally, neural coupling between the piriform cortex to the mediodorsal thalamus, and the mediodorsal thalamus to orbitofrontal cortex, increased during olfactory attention (Plailly et al., 2008). Human studies show damage of the mediodorsal thalamus results in varying impairments in olfactory attention that coincides with heightened oral capture, or localization to the mouth, possibly enhancing flavor binding in these individuals (Tham et al., 2011a). Therefore, it is possible that the involvement of the mediodorsal thalamus in olfactory attention may influence the

consummatory behaviors of orally-delivered chemosensory stimuli including tastes, retronasal odors, or odor-taste mixtures.

Part of what makes an odor smell "good" or "bad" is its associated value from previous experiences. For example, the smell of cocoa is pleasant for most people due to their past experiences eating a sweet chocolate bar. The perception of pleasantness or unpleasantness is also referred to as hedonic value. Psychophysical experiments show that people with lesions of mediodorsal thalamus have an altered hedonic perception of odors (Rousseaux et al., 1996; Asai et al., 2008; Sela et al., 2009). Further investigation found individuals exhibited a less positive hedonic judgment of both odors and odor-taste mixtures (Tham et al., 2011a). In this study it is unclear whether the altered hedonic perceptions of odor-taste mixtures are based on the alteration of the odor component alone. A case study of an adult woman revealed that olfactory and gustatory stimuli that were previously very pleasant were no longer positive after bilateral mediodorsal thalamic damage, while neutral or less pleasant stimuli were perceived as unpleasant (Rousseaux et al., 1996). These altered perceptions can be associated with a reduction of food intake and severe weight loss (Rousseaux et al., 1996). These findings underscore the need to determine the role of the mediodorsal thalamus in processing the hedonic value of odors, tastes, and odor-taste mixtures.

Chemosensory processing by the mediodorsal thalamus

My dissertation aims to elucidate the anatomical connections, neuronal function, and behavioral impact of the mediodorsal thalamus in multimodal chemosensory processing and consummatory choice. In chapter 2, I used an intersectional viral approach to characterize the direct cortico-thalamic connectivity from the chemosensory cortices (piriform cortex and gustatory cortex) to neurons in the mediodorsal thalamus. In chapter 3, I used awake behaving electrophysiology to characterize single-unit responses in the mediodorsal thalamus to intraorally delivered odors, tastes, and odor-taste mixtures. In chapter 4, I used pharmacological inactivation during a two-bottle brief-access task to determine the role of the mediodorsal thalamus in the consummatory choice of odors, tastes, and odor-taste mixtures. In chapter 5, I discuss the overall findings from my dissertation in relation to the chemosensory field.

CHAPTER 2

DIRECT CORTICO-THALAMIC CONNECTIONS FROM THE
CHEMOSENSORY CORTICES TO NEURONS IN THE MEDIODORSAL
THALAMUS

Introduction

The mediodorsal thalamus (MD) is a multisensory hub thought to synchronize, modulate and relay contextually relevant sensory information between primary and higher-order cortical areas (Theyel et al., 2010; Saalmann et al., 2012; Stroh et al., 2013; Mease et al., 2016; Schmitt et al., 2017; Rikhye et al., 2018). Through its dense connections with sensory and limbic regions, the mediodorsal thalamus plays a crucial role in the coordination and synchronization of neural activity across distributed cortical networks involved in many cognitive functions, including attention (Plailly et al., 2008; Tham et al., 2009, 2011a, 2011b; Veldhuizen and Small, 2011; Schmitt et al., 2017; Rikhye et al., 2018), valuation (Rousseaux et al., 1996; Sela et al., 2009; Tham et al., 2011a), and stimulus-outcome associations (Oyoshi et al., 1996; Kawagoe et al., 2007; Courtiol and Wilson, 2016). It is a target of all the primary olfactory areas (e.g., piriform cortex) (Courtiol and Wilson, 2015) and has been extensively studied for its role in olfactory-related behaviors (Yarita et al., 1980; Eichenbaum et al., 1980; Imamura

et al., 1984; Slotnick and Risser, 1990; Oyoshi et al., 1996; Kawagoe et al., 2007; Sela et al., 2009; Tham et al., 2011b, 2011a; Courtiol and Wilson, 2014, 2015), reward associations (Oyoshi et al., 1996; Kawagoe et al., 2007; Courtiol and Wilson, 2016; Schmitt et al., 2017; Rikhye et al., 2018; Chakraborty et al., 2019), and processing multisensory information (Schmitt et al., 2017; Rikhye et al., 2018; Fredericksen et al., 2019). Recent electrophysiological studies found that neurons in the mediodorsal thalamus encode the sensory and affective properties of orally-sourced odors, tastes, and odor-taste combinations (Fredericksen and Samuelsen, 2022), suggesting it may play role in processing olfactory and gustatory signals to guide food choice. Traditional tract tracing studies show that the mediodorsal thalamus receives overlapping projections from the chemosensory cortices (e.g., piriform cortex and gustatory cortex) (Price and Slotnick, 1983; Kuroda et al., 1992; Ray and Price, 1992; Shi and Cassell, 1998). However, the prevalence of their cortico-thalamic connections is unclear.

In this study, we used an intersectional viral approach to compare the proportion of cortico-thalamic connections from the posterior piriform cortex and the gustatory cortex to mediodorsal thalamic neurons. We hypothesized that the posterior piriform cortex would directly connect to more neurons in the mediodorsal thalamus, given its role in olfactory-dependent behaviors and the high density of piriform cortical fibers in the central region of the mediodorsal thalamus. However, our findings demonstrated that a greater proportion of neurons in the mediodorsal thalamus receive projections from gustatory cortex. These results offer new insights into the cortico-thalamic connections between the chemosensory cortices

17

and mediodorsal thalamus, suggesting that the gustatory cortex may broadly impact processing in the mediodorsal thalamus. Further research examining the anatomical and functional relationship between the gustatory cortex and mediodorsal thalamus will help to determine the role of this circuitry in chemosensory processing.

Materials and Methods

Animals. All procedures were performed in accordance with university, state, and federal regulations regarding research animals and were approved by the University of Louisville Institutional Animal Care and Use Committee. Female Long-Evans rats (~250-350 g, Charles Rivers) were single-housed and maintained on a 12 h light/dark cycle with *ad libitum* food and water. All rats had at least 3 days of experience with odor-taste mixtures in a two-bottle brief-access rig during a chemosensory choice task.

Viral Constructs and Surgery. We utilized an intersectional viral technique to evaluate the direct cortico-thalamic connections from the chemosensory cortices to the mediodorsal thalamus (Fig. 1). Specifically, we employed an anterograde transsynaptic virus, AAV1-hSyn-Cre-WPRE-hGH (1×10^{13} vg/ml; Addgene, 105553-AAV1), to induce expression of Cre-recombinase in postsynaptic neurons (Zingg et al., 2017). One week later, we introduced a second viral vector, pOTTC1032-pAAV5-EF1a-Nuc-flox(mCherry)-EGFP (7×10^{12} vg/ml; Addgene, 112677-AAV5), to transduce a Cre-dependent color-changing reporter. By default, infected neurons produce nuclear-localized mCherry, but neurons that co-transduce the color changing AAV-Nuc-flox-(mCherry)-EGFP and the transneuronally transported AAV-Cre viruses express EGFP (Zingg et al., 2017) allowing us to quantify the proportion of neurons that received direct cortico-thalamic projections.

Briefly, rats were anesthetized with isoflurane (induction: 5%, maintenance: 2-5%). Animals were secured in a stereotaxic device (KOPF) and given subcutaneous injections of atropine sulfate (0.03 mg/kg), dexamethasone (0.2 mg/kg), and the analgesic buprenorphine HCl (0.03 mg/kg). The scalp was shaved, cleaned with 70% ethanol and povidone-iodine solution, and excised to reveal the skull. For Group 1 (MD/PC), we unilaterally injected 200 nl (flowrate: 50 nl/min) of AAV1-hSyn-Cre-WPRE-hGH into the posterior piriform cortex (coordinates: AP: -1.4 mm, ML: +5.8 mm, DV: -6.9 mm from dura) using a 10 μl Micro4 micro-syringe pump (UMP3-3, World Precision Instruments) with a 34 ga beveled needle in a 10 μl Hamilton syringe (NANOFIL, World Precision Instruments). For Group 2 (MD/GC), rats received a unilateral injection of 200 nl of AAV1-hSyn-Cre-WPRE-hGH into the gustatory cortex (coordinates: AP: +1.4 mm, ML: +5.0 mm, DV: -4.9 mm from dura). One week later, rats in Group 1 (MD/PC) and Group 2 (MD/GC) underwent a second surgery. For Group 1 (MD/PC), we injected 200 nl of pOTTC1032-pAAV5-EF1a-Nuc-flox(mCherry)-EGFP into the posterior piriform cortex and 200 nl into the mediodorsal thalamus (coordinates: 10° angle, AP: -3.3 mm, ML: +1.6 mm, DV: -5.6 mm from dura). We targeted viral injections to the central and medial subregions of the mediodorsal thalamus to account for overlapping projections from piriform cortex and gustatory cortex (Price and Slotnick, 1983; Kuroda et al., 1992; Ray and Price, 1992; Shi and Cassell, 1998). For Group 2 (MD/GC), we injected 200 nl of pOTTC1032-pAAV5-EF1a-Nuc-flox(mCherry)-EGFP into the gustatory cortex and 200 nl into the mediodorsal thalamus. For Group 3 (MD-only), we unilaterally injected 200 nl of pOTTC1032-

pAAV5-EF1a-Nuc-flox(mCherry)-EGFP into the mediodorsal thalamus. Following the viral injections, craniotomies were covered with bone wax and the scalp was closed with wound clips (7 mm, Reflex 7). We administered an additional subcutaneous injection of buprenorphine HCl and monitored the rats for signs of pain and discomfort for a minimum of 4 days.

Histology. Three-weeks after injections of AAV-Nuc-flox(mCherry)-EGFP, rats were euthanized, and brains were processed for confocal microscopy. The rats were anesthetized with a mixture of ketamine, xylazine, and acepromazine (100 mg/kg, 5.2 mg/kg, and 1 mg/kg) and transcardially perfused with cold 0.1M phosphate buffer saline (PBS) and cold 4% paraformaldehyde. Brains were removed, post-fixed for 24 hours, and cryoprotected in 30% sucrose solution. Using a cryostat, sections were cut to the thickness of 70 microns and stored at 4°C. Sections used for staining were each ~70 microns apart. Tissue was blocked in a 0.1M PBS and tritonX-100 solution (1:1000; IBI Scientific) for 10 minutes. This was followed by 2 hours of incubation in the dark in a 0.1M PBS and Nissl stain solution (Neurotrace, 1:500; Invitrogen, N21483). The sections were washed three times (5 mins, 5 mins, 1 hr) in 0.1M PBS and mounted using Fluormount-G medium (SouthernBiotech).

Image analysis and cell counting. Using an Olympus FluoView1000/Olympus FluoView3000 microscope, confocal images of neurons expressing mCherry, EGFP, and Nissl fluorescence were captured from three consecutive sections

centered around the injection sites in the mediodorsal thalamus, posterior piriform cortex, or gustatory cortex. The center 11 images (~3.79 microns each) were compressed into a single Z-projection (~50 microns of depth) using Fiji/ImageJ2 (National Institutes of Health) and the threshold was set as a black and white image with black background and white cells as consistently as possible. Images were coded to ensure the experimenter was blind to condition before outlining the region of interest (ROI; presented as mean pixels^2) on the Nissl image, which were saved and opened on the corresponding black and white mCherry and EGFP images. The number of fluorescent-labeled neurons were quantified using automatic particle analysis in Fiji and verified by an experimenter blind to condition. Since the loxP sites of the FLEX vector recombine during DNA amplification, a small number of neurons can express both mCherry and EGFP. Therefore, co-labeled cells were counted and subtracted from both mCherry and EGFP counts. The number of mCherry+ neurons and EGFP+ neurons were counted within each region of interest and averaged across the three sections.

Statistical analysis. The cortical injection sites were verified by examining the expression of EGFP (Fig. 2A). Only rats exhibiting EGFP expression within the targeted cortical region were included in the analysis (n = 9), while those with significant EGFP expression outside the targeted cortical area were excluded from the study (n = 19/28).

Statistical analyses were performed using GraphPad Prism (Version 9.5.0, GraphPad Software, Inc.). One-way ANOVAs were used to determine whether the

ROI sizes of either the piriform cortex, the gustatory cortex, or the mediodorsal thalamus differed across groups. Unpaired t-tests were used to compare the total number of mCherry+ neurons or EGFP+ neurons. One-way ANOVAs and Tukey's HSD test for multiple comparisons were used to compare the total number of fluorescent expressing neurons (mCherry+ or EGFP+ neurons) in the thalamus across the three experimental groups.

Totals for proportional measures were calculated by adding the total mCherry+, EGFP+, and co-labeled neurons across the three sections of the mediodorsal thalamus from rats with AAV-Cre injections in the posterior piriform cortex (MD/PC), the gustatory cortex (MD/GC), or no AAV-Cre injections (MD-only). We compared the proportion of mCherry+ neurons to the proportion of non-mCherry neurons (EGFP+ and co-label). Similarly, we tested the proportion of EGFP+ neurons to the proportion of non-EGFP neurons (mCherry+ and co-label). χ^2 with Fisher's exact tests were used to compare proportions across experimental groups.

Results

We employed an intersectional viral technique to investigate the direct synaptic connectivity between the chemosensory cortices and the mediodorsal thalamus (Figure 1). For this approach, we injected the anterograde transsynaptic virus AAV-Cre into cortex, which drove the expression of Cre-recombinase in cortical neurons and postsynaptic neurons in the mediodorsal thalamus. A second virus, the Cre-dependent color-changing reporter AAV-Nuc-flox(mCherry)-EGFP drove EGFP expression in the presence of Cre-recombinase and mCherry expression in its absence (Bäck et al., 2019). EGFP+ neurons in the mediodorsal thalamus co-transduced both viruses, indicating that they receive direct synaptic input from cortex. Conversely, mCherry+ neurons were not synaptically connected to cortex. We injected AAV-Nuc-flox(mCherry)-EGFP into the cortex to visualize and quantify EGFP expression across cortical regions (Fig. 2). To ensure targeted injections, only rats with EGFP+ neurons within the cortical area were included in the analysis (n = 9).

Transduction of AAV-Nuc-flox(mCherry)-EGFP in the cortex

First, we tested whether the size of the region of interest (ROIs) outlining cortical areas were consistent across animals. The results of a one-way ANOVA revealed no difference in the ROI sizes for posterior piriform cortex [$F_{(2,6)}$ = 0.2314, p = 0.8002], or gustatory cortex [$F_{(2,6)}$ = 0.8232, p = 0.4831] (Table 1). However, due to cell-type specific differences across brain regions, it is plausible that the viruses could differentially infect the neuronal populations of the posterior

piriform cortex and gustatory cortex. Therefore, we quantified the number of mCherry+ and EGFP+ neurons in both cortical areas to determine if co-transduction of AAV-Cre and AAV-Nuc-flox(mCherry)-EGFP yielded similar levels of expression (Fig. 2A). Unpaired t-tests showed no significant difference between the total number of fluorescent-labeled neurons in the piriform cortex or gustatory cortex (PC: 516.11 ± 127.21 vs. GC: 534 ± 216.98; $t_{(4)}$ = 0.07112, p = 0.9467), indicating consistent transduction of AAV-Cre and AAV-Nuc-flox(mCherry)-EGFP virus in both cortical areas. Furthermore, the number of mCherry+ neurons (PC: 2.56 ± 2.56 vs. GC: 0.56 ± 0.56; $t_{(4)}$ = 0.7647, p = 0.487) and EGFP+ neurons (PC: 508.67 ± 130.46 vs. GC: 531.67 ± 215.51; $t_{(4)}$ = 0.0913, p = 0.9316) were similar between the two chemosensory cortical areas (Fig. 2B). It is worth noting that loxP sites in FLEX plasmids can recombine during DNA amplification and viral vector production, which could lead to a small number of neurons exhibiting Cre-independent transgene expression. Consequently, some neurons could express both mCherry and EGFP. Therefore, we compared the number of co-labeled neurons and found no significant difference between the two chemosensory cortices (PC: 4.89 ± 3.56 vs. GC: 1.78 ± 1.44; $t_{(4)}$= 0.8096 , p = 0.4636). Together, these findings indicate that the intersectional viral technique resulted in comparable levels of fluorescent expression in the posterior piriform cortex and gustatory cortex.

Transduction of AAV-Nuc-flox(mCherry)-EGFP in the mediodorsal thalamus

Just as with the cortical areas, we first examined whether the ROI sizes of

the mediodorsal thalamus differed across experimental groups. A one-way ANOVA revealed no significant difference in the ROI sizes among the groups [F (2,6) = 0.2545, p = 0.7833] (Table 1). Next, we investigated whether the cortico-thalamic connections formed with the mediodorsal thalamus differed between the chemosensory cortices by counting the number of mCherry+ neurons and EGFP+ neurons in the mediodorsal thalamus from rats with AAV-Cre injections in the posterior piriform cortex (MD/PC), the gustatory cortex (MD/GC), and those that did not receive an injection of AAV-Cre (MD-only) (Fig. 3). The expression of EGFP in the mediodorsal thalamus indicated transneuronal transport of the AAV-Cre virus via cortico-thalamic connections with the cortex. First, we investigated the total number of fluorescent-labeled neurons in the mediodorsal thalamus to ensure consistent viral transduction of AAV-Nuc-flox(mCherry)-EGFP across experimental groups. A one-way ANOVA showed no difference in the number of fluorescent-labeled neurons in the mediodorsal thalamus among experimental groups (MD/PC: 423.33 ± 175.29; MD/GC: 560.22 ± 179.32; MD-only: 234.11 ± 49.12; F (2,6) = 1.232, p = 0.3562) (Fig. 4A).

After observing no difference in the total number of fluorescent-labeled neurons in the mediodorsal thalamus among experimental groups, we compared the number of mCherry+ neurons, EGFP+ neurons, and co-labeled neurons (Fig. 4B). We found no significant differences in the number of mCherry+ neurons (MD/PC: 365.44 ± 173.89; MD/GC: 36.44 ± 10.68; MD-only: 216.11 ± 51.51; F (2,6) = 2.467, p = 0.1653) or number of co-labeled neurons (MD/PC: 16.56 ± 8.59; MD/GC: 3.33 ± 1.35; MD-only: 14.56 ± 6.17; F (2,6) = 1.340, p = 0.3302). However,

26

there was a significant difference in the number of EGFP+ neurons in the mediodorsal thalamus (MD/PC: 41.33 ± 11.51; MD/GC: 520.44 ± 188.28; MD-only: 3.44 ± 2.95; F (2,6) = 7.000, p = 0.0270). *Post hoc* analysis using a Tukey's HSD test showed that the rats injected with anterograde transsynaptic AAV-Cre in the gustatory cortex (MD/GC) had significantly more EGFP+ neurons compared to both the MD/PC group (p = 0.048) and the MD-only group (p = 0.035). Surprisingly, there was no difference in the number of EGFP+ neurons between the MD/PC group and the MD-only group.

Next, we examined the proportion of mCherry+ and EGFP+ neurons within the mediodorsal thalamus to control for the total number of fluorescent-labeled neurons across each experimental group (Table 2, Fig. 4C-D). The results of a χ^2 test showed that the proportion of mCherry+ neurons to non-mCherry neurons (EGFP+ and co-label) in the mediodorsal thalamus significantly differed across the three experimental groups (χ^2_2 = 7334, p < 0.001) (Fig. 4C). *Post hoc* analyses revealed that the MD-only group, that did not receive any AAV-Cre, had a significantly higher proportion of mCherry+ neurons (92.3%) than either the MD/PC (86.3%; Fisher's exact test, p < 0.001) or the MD/GC groups (6.5%; Fisher's exact test, p < 0.001), while the MD/PC group had a significantly higher proportion of mCherry+ neurons than the MD/GC group (Fisher's exact test, p < 0.001). Additionally, the proportion of EGFP+ neurons to non-EGFP+ neurons (mCherry+ and co-label) in the mediodorsal thalamus significantly differed across the three experimental groups (χ^2_2 = 8149, p < 0.001) (Fig. 4D). The MD/GC group had a significantly higher proportion of EGFP+ neurons (92.9%) compared to either the

MD/PC (9.8%; Fisher's exact test, $p < 0.001$) or the MD-only groups (1.5%; Fisher's exact test, $p < 0.001$). The MD/PC group also had a significantly higher proportion of EGFP+ neurons than the MD-only experimental group (Fisher's exact test, $p < 0.001$). These results demonstrate that the proportion of neurons in the mediodorsal thalamus receiving projections from the gustatory cortex, indicated by the expression of EGFP due to transneuronal transport of AAV-Cre, is significantly higher than the proportion of neurons receiving projections from the piriform cortex. These findings highlight the importance of controlling for total number of fluorescent-labeled neurons, even in the absence of significant differences across the total fluorescent neuronal populations.

In summary, these results suggest that the gustatory cortex forms cortico-thalamic connections with significantly more neurons in the mediodorsal thalamus than the posterior piriform cortex. These findings, combined with electrophysiological experiments showing responses to odors, tastes, and odor-taste mixtures in the mediodorsal thalamus, support the possibility of its involvement in processing both olfactory and gustatory signals. While anatomical connectivity differences do not necessarily indicate functional differences, they highlight the need for further studies to explore the anatomical and functional relationship between the gustatory cortex and mediodorsal thalamus.

Table 1

The sizes of regions of interest (ROIs) were consistent across animals

Mean ROI ± SEM (pixels²)	
MD with Cre injection in PC	1427390.90 ± 84724.11 1422373.62 ± 187367.61 1350524.51 ± 167103.99
MD with Cre injection in GC	1248160.47 ± 97905.20 1392471.80 ± 92212.46 1419645.67 ± 75977.44
MD with no Cre injection in cortex	1510425.78 ± 86705.95 1336971.14 ± 21573.26 1147349.17 ± 47660.93
PC injection site	2633959.63 ± 255781.19 2597081.34 ± 26544.98 2489228.63 ± 84860.43
GC injection site	1329558.17 ± 109536.11 1217408.87 ± 78615.59 1111814.45 ± 158203.62

Table 2.

The number of fluorescently labeled neurons significantly differed across experimental groups

Total fluorescently labeled neurons			
	mCherry	EGFP	Colabel
MD/PC	3289	372	149
MD/GC	328	4684	30
MD only	1945	31	131
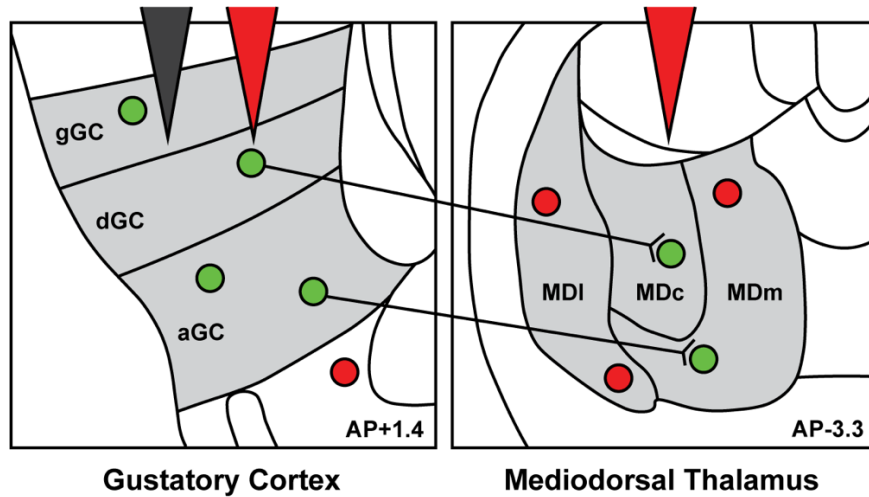
Figure 1. Schematic representation of intersectional viral method. Direct connections from the gustatory cortex (shown here) or piriform cortex to the mediodorsal thalamus will be determined by injecting transsynaptic anterograde AAV1-hsyn-Cre (grey triangle) into cortex, followed a week later by injections of AAV5-EF1a-Nuc-flox (mCherry)-EGFP (red triangles) into cortex and thalamus. Neurons in the thalamus that express EGFP receive transsynaptic AAV-Cre by a direct connection from the cortex. Neurons that express mCherry are infected by AAV-Nuc-flox only (red circles). Gustatory cortex: gGC [granular], dGC [disgranular], aGC [agranular]. Mediodorsal thalamus: MDm [medial], MDc [central], MDl [lateral].
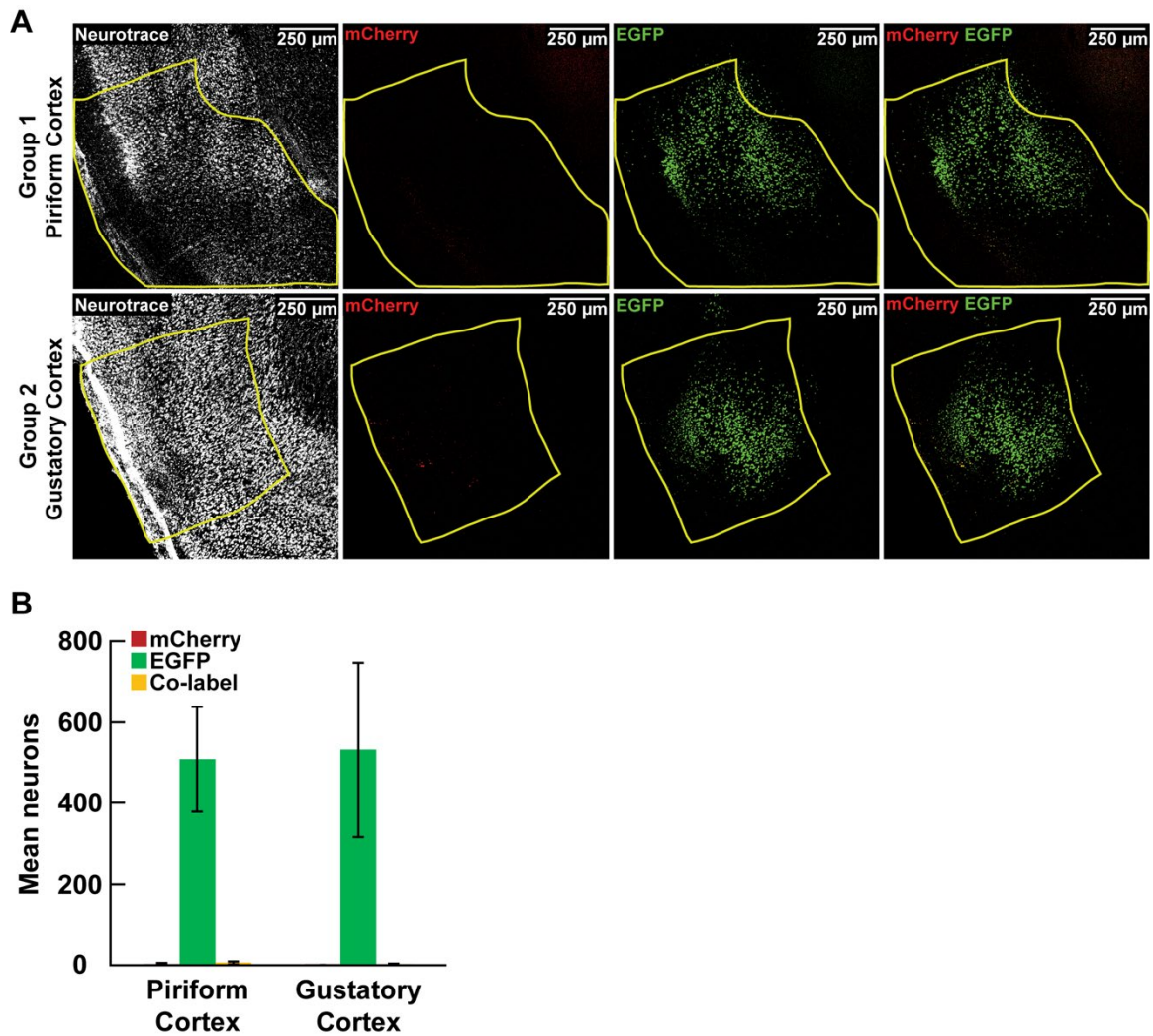
Figure 2. Virally-mediated fluorescent expression in cortex. A. Representative images and ROIs for the expression of mCherry and EGFP following injections of AAV-Cre in the piriform cortex (top) or gustatory cortex (bottom). Neurons infected with both AAV-Cre and AAV-Nuc-flox express EGFP (green). Neurons infected with AAV-Nuc-flox, but not AAV-Cre, express mCherry (red). Co-labeled neurons are yellow. Sections were stained with Neurotrace (nissl, white). There were no significant differences in ROI areas across sections (Table 1). Scale bar: 250 μm.

B. There was no difference in the number of neurons (mean ± SEM) expressing mCherry (red bars), EGFP (green bars), or co-label (yellow bars) across cortical areas.
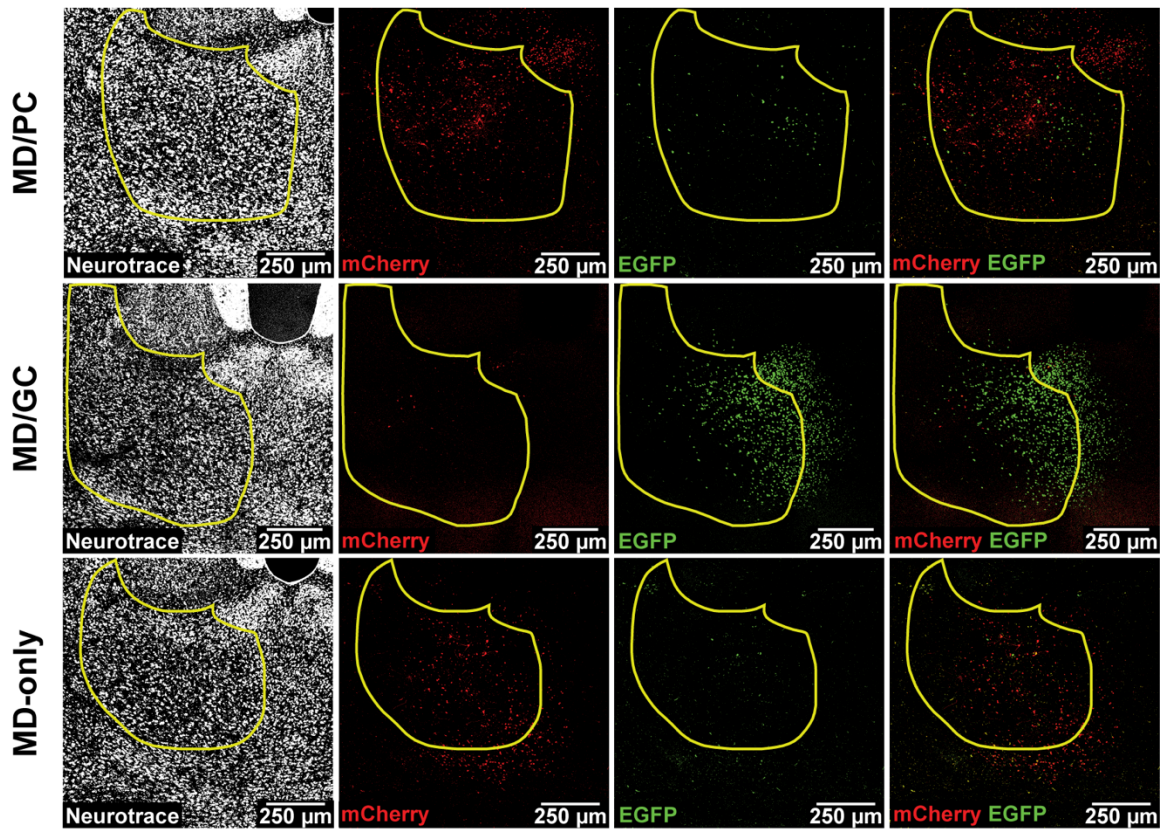
Figure 3. Representative images and ROIs of virally-mediated fluorescent expression in the mediodorsal thalamus. Expression of mCherry and EGFP following injection of AAV-Nuc-flox into the mediodorsal thalamus and AAV-Cre into the piriform cortex (top), gustatory cortex (middle), or no injection (bottom). Neurons expressing EGFP (green) in the mediodorsal thalamus receive transynaptic AAV-Cre by direct projections from cortex and are infected with AAV-Nuc-flox. All neurons infected with AAV-Nuc-flox, but not AAV-Cre, express mCherry (red). Co-labeled neurons are yellow. Sections were stained with Neurotrace (nissl, white). There were no significant differences in ROI areas across sections (Table 1). Scale bar: 250 μm.
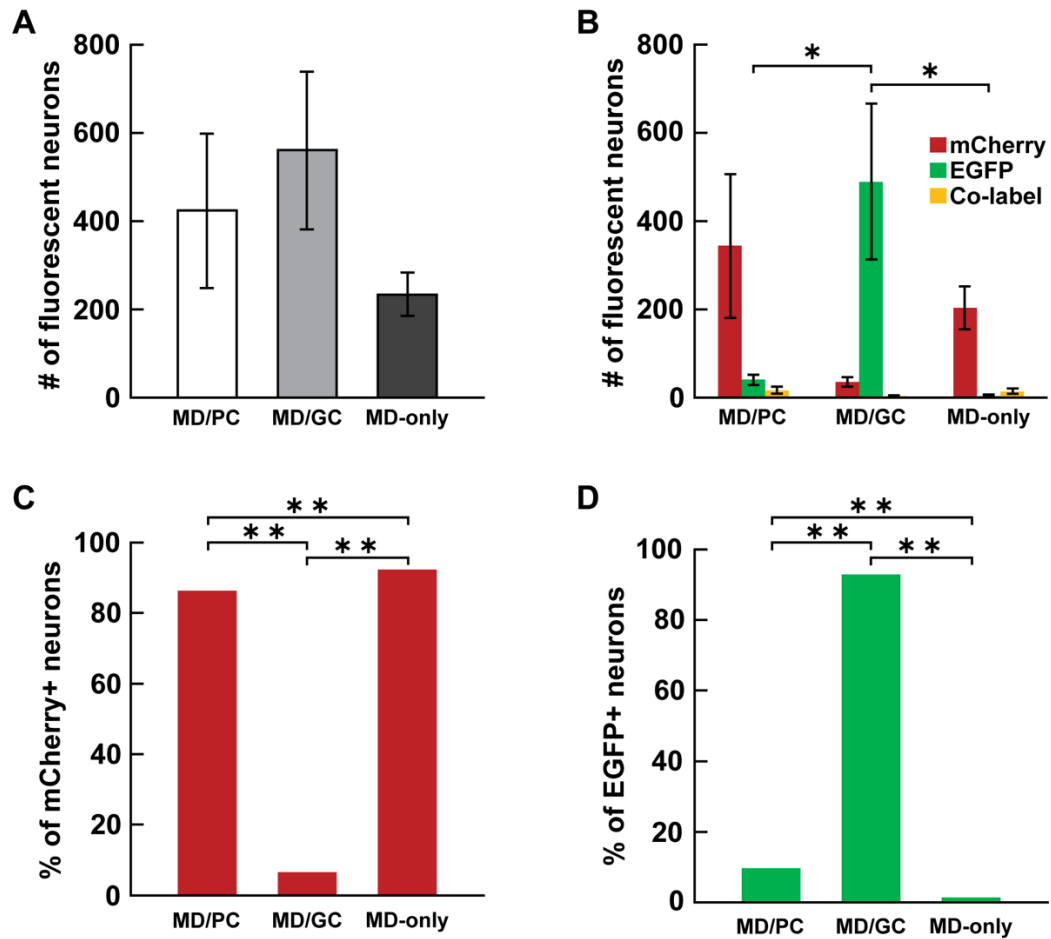
Figure 4. Expression of mCherry and EGFP in the mediodorsal thalamus following intersectional viral approach. A. There was no difference in the number of fluorescent-labeled neurons (mean ± SEM) in the mediodorsal thalamus across the three groups of MD/PC (white, AAV-Cre was injected into PC), MD/GC (light grey, AAV-Cre was injected into GC), or MD only (dark grey, no AAV-Cre injection). **B.** There were significantly more EGFP+ neurons (green bars) in the MD/GC group compared to MD/PC and MD-only. There was no difference in the number of mCherry+ neurons (red bars) or co-label (yellow bars) across groups.

C. The proportion of neurons in the mediodorsal thalamus expressing mCherry and **D.** the proportion of neurons expressing EGFP significantly differed across the three experimental groups. ***p < 0.001. *p < 0.05.

Discussion

In this study, we utilized an intersectional viral approach to identify and compare the number of neurons in the mediodorsal thalamus with cortico-thalamic connections from the chemosensory cortices. We hypothesized that the posterior piriform cortex would form more cortico-thalamic connections with the mediodorsal thalamus due to prior tracing studies (Price and Slotnick, 1983; Kuroda et al., 1992; Ray and Price, 1992; Shi and Cassell, 1998) and its known role in many olfactory-dependent behaviors (Yarita et al., 1980; Eichenbaum et al., 1980; Imamura et al., 1984; Slotnick and Risser, 1990; Oyoshi et al., 1996; Kawagoe et al., 2007; Sela et al., 2009; Tham et al., 2011b, 2011a; Courtiol and Wilson, 2014, 2015). Surprisingly, we found that more neurons in the mediodorsal thalamus have cortico-thalamic connections from the gustatory cortex than the posterior piriform cortex. It is important to note that the number of neurons forming cortico-thalamic connections alone does not directly translate to function. Our anatomical results encourage future studies of the connections between the gustatory cortex and the mediodorsal thalamus and the functional role of the mediodorsal thalamus neurons in the taste system.

Although the mediodorsal thalamus has been shown to play a significant role in olfactory processing, its involvement in gustatory processing is poorly understood. However, our findings that the gustatory cortex connects robustly to the mediodorsal thalamus suggests that taste information is also processed by this region. In a recent study, we demonstrated that neurons in the mediodorsal thalamus represent not only odors, but tastes and odor-taste mixtures, with more

neurons responding to tastes and odor-taste mixtures (Fredericksen and Samuelsen, 2022). This heavy taste-based physiology parallels our anatomical findings that gustatory cortex contacts more neurons in the mediodorsal thalamus. The gustatory cortex input to the mediodorsal thalamus could represent more than taste information, as the region functions as an associative area responsive to temperature (Kadohisa et al., 2005), visceral (Hanamori et al., 1998), somatosensory (Kadohisa et al., 2005; Vincis and Fontanini, 2016), visual (Ifuku et al., 2006; Vincis and Fontanini, 2016), auditory (Samuelsen et al., 2012; Gardner and Fontanini, 2014; Vincis and Fontanini, 2016), and olfactory signals (Vincis and Fontanini, 2016; Samuelsen and Fontanini, 2017). Further studies combining optogenetic tools with behaving electrophysiology will help to elucidate what role the circuitry between the gustatory cortex and the mediodorsal thalamus plays in chemosensory processing.

As the largest olfactory area, the piriform cortex is separated into anterior and posterior subregions based on differences in cytoarchitecture, connectivity, and function (Ghosh et al., 2011; Wilson and Sullivan, 2011). Where the anterior piriform cortex is primarily involved in the initial processing of olfactory signals, the posterior piriform cortex is associative and involved in higher-level processing of odor information (Litaudon et al., 2003; Kadohisa and Wilson, 2006; Wilson et al., 2020). We focused our investigation on the cortico-thalamic projections from posterior piriform cortex because, like the gustatory cortex, it responds to single odors and tastes (Maier et al., 2012; Samuelsen and Fontanini, 2017). Furthermore, it represents odor-taste mixtures uniquely from their odor and taste

components (Idris et al., 2023). However, it is possible that the cortico-thalamic connections from the anterior piriform cortex to the mediodorsal thalamus may be more prevalent than posterior piriform cortex. Future studies investigating the projections from the anterior piriform cortex to the mediodorsal thalamus are needed to determine the contribution of this circuitry to chemosensory processing in the thalamus.

The distinct cortico-thalamic connections between the posterior piriform cortex and gustatory cortex to the mediodorsal thalamus suggest several theories about their function. One potential explanation is that the circuitry differences relate to the types of synapses from cortex to thalamus. Electron microscopy studies have shown that a third of projections from the piriform cortex to mediodorsal thalamus form "driver-like" giant synapses (Kuroda et al., 1992; Pelzer et al., 2017). These large, circular synaptic contacts are thought to directly stimulate activity in post-synaptic neurons, while smaller "modulator-like" synapses exert subtle influences on the network (Sherman and Guillery, 1998; Kirchgessner et al., 2021). Additionally, "driver-like" inputs typically establish numerous synaptic connections with a single postsynaptic neuron, while small round "modulators" form single synapses with multiple postsynaptic neurons (Erişir et al., 1997; Budisantoso et al., 2012; Hammer et al., 2014, 2015). It is possible that the posterior piriform cortex forms more "driver-like" synapses with fewer neural targets to drive activity, and the gustatory cortex primarily forms "modulator-like" synapses with more neural targets to provide state-dependent modulation (Kuroda et al., 1992; Sherman and Guillery, 1998; Budisantoso et al., 2012; Bickford, 2015;

Pelzer et al., 2017). Future studies investigating the synaptic profiles of the projections from gustatory cortex to mediodorsal thalamic neurons are needed to define this cortico-thalamic circuit.

The intersectional viral method presents potential confounding factors that require consideration. Due to cell-type specific differences between brain regions, it is possible that the AAV viruses could have infected piriform cortex differently than gustatory cortex. This seems unlikely as we found no differences in total fluorescence expression across groups between the cortical areas or the mediodorsal thalamus. Another factor to consider is the differences in thalamo-cortical connectivity between the thalamus and each cortical area. Unlike piriform cortex, the mediodorsal thalamus reciprocally connects with the gustatory cortex (Krettek and Price, 1977; Allen et al., 1991; Kuramoto et al., 2017), making low-efficiency retrograde infection of thalamo-cortical projecting neurons by the transsynaptic anterograde AAV-Cre possible (Zingg et al., 2017). Therefore, any low-efficiency retrograde infection would increase the expression of EGFP+ neurons in the mediodorsal thalamus for the MD/GC experimental group. While future studies could parse apart directionality of these connections, our results characterize the direct connectivity between the gustatory cortex and the mediodorsal thalamus, albeit with the small possibility of multidirectional connectivity.

In summary, a greater number of neurons in the mediodorsal thalamus form cortico-thalamic connections with the gustatory cortex than with the posterior piriform cortex. This outcome suggests that input from the gustatory cortex may be

broadly influential to processing in the mediodorsal thalamus. Our findings underscore the importance of future investigations into the anatomical and functional relationship between gustatory cortex and mediodorsal thalamus.

CHAPTER 3

NEURAL REPRESENTATION OF INTRAORAL OLFACTORY AND
GUSTATORY SIGNALS BY THE MEDIODORSAL THALAMUS IN ALERT RATS

Introduction

The perception of food, and ultimately the decision whether to eat it, requires the integration and discrimination of multisensory signals from the mouth (Sclafani, 2001; Verhagen and Engelen, 2006). While all senses contribute, concurrent activation of the olfactory and gustatory systems is essential for giving food its flavor (Small, 2012; Prescott, 2015). This multisensory process generates enduring odor-taste associations that are crucial for guiding future food choices (Fanselow and Birk, 1982; Schul et al., 1996; Sakai and Yamamoto, 2001; Gautam and Verhagen, 2010; Green et al., 2012; McQueen et al., 2020). These experience-dependent behaviors rely upon a network of brain regions to integrate and process multimodal chemosensory signals to guide choice (Samuelsen and Vincis, 2021).

The thalamus receives inputs from various cortical and subcortical structures and is integral for communicating information across the brain (Roy et al., 2022). The thalamic subnuclei can be broadly divided into at least two categories: first-order and higher-order thalamic nuclei. First-order thalamic nuclei

are primarily responsible for processing sensory input from the periphery and relaying it to the sensory cortex, whereas higher-order thalamic nuclei process and communicate information between cortical areas (Sherman, 2016; Nakajima and Halassa, 2017; Halassa and Sherman, 2019). The mediodorsal thalamus is a higher-order thalamic nucleus involved in an array of cognitive functions, including attention (Plailly et al., 2008; Tham et al., 2009, 2011a, 2011b; Veldhuizen and Small, 2011; Schmitt et al., 2017; Rikhye et al., 2018), valuation (Rousseaux et al., 1996; Sela et al., 2009; Tham et al., 2011a), memory (Parnaudeau et al., 2013; Bolkan et al., 2017; Scott et al., 2020), and stimulus-outcome associations (Oyoshi et al., 1996; Kawagoe et al., 2007; Courtiol and Wilson, 2016). It receives projections from primary olfactory cortical areas (e.g., piriform cortex), is reciprocally connected with the gustatory cortex, and forms dense reciprocal connections with prefrontal cortical areas important for decision-making (Price and Slotnick, 1983; Kuroda et al., 1992; Ray and Price, 1992; Shi and Cassell, 1998; Kuramoto et al., 2017; Pelzer et al., 2017). Given its robust connectivity with olfactory areas, studies have examined the role of the mediodorsal thalamus in various experience-dependent olfactory behaviors, including olfactory attention (Plailly et al., 2008; Small et al., 2008; Tham et al., 2009; Veldhuizen and Small, 2011), odor discrimination (Eichenbaum et al., 1980; Staubli et al., 1987; Courtiol and Wilson, 2016; Courtiol et al., 2019), and odor-reward associations (Kawagoe et al., 2007). It is implicated in the hedonic perception of odors and flavors, as people with mediodorsal thalamus lesions report decreased hedonic ratings for experienced odors and odor-taste mixtures (Tham et al., 2011a).

Electrophysiological experiments in anesthetized and behaving rats have shown that neurons in the mediodorsal thalamus encode odors sampled by sniffing (i.e., orthonasal olfaction) (Courtiol and Wilson, 2014) and display odor selectivity during olfactory discrimination tasks (Courtiol and Wilson, 2016). However, it is unknown how mediodorsal thalamus neurons represent orally consumed odors, tastes, and odor-taste mixtures.

To address this question, we recorded single-unit activity in the mediodorsal thalamus of behaving rats during the intraoral delivery of three stimulus categories: individual odors, individual tastes, and odor-taste mixtures. This approach allowed odorized stimuli to be detected via retronasal olfaction, an essential factor for flavor perception (Verhagen and Engelen, 2006; Prescott, 2012). It also ensured that all chemosensory stimuli would share similar somatosensory and attentional attributes associated with the intraoral delivery of liquids. Our data provide novel insights into how the mediodorsal thalamus processes chemosensory signals originating from the mouth. Our findings demonstrate that mediodorsal thalamus neurons respond broadly across intraoral stimuli with time-varying multiphasic changes in activity. This chemoselective population reliably encodes unimodal and multimodal chemosensory signals over time, with a subpopulation representing the palatability-related features of tastes and associations between experienced odor-taste pairs. Our results are consistent with the mediodorsal thalamus being an integral component of the network processing of chemosensory signals by communicating information between sensory and prefrontal cortical areas important for ingestive behavior.

Materials and Methods

Experimental subjects. All procedures were performed in accordance with university, state, and federal regulations regarding research animals and were approved by the University of Louisville Institutional Animal Care and Use Committee. Female Long-Evans rats (~250–350 g, Charles Rivers) were single-housed and maintained on a 12 h light/dark cycle with *ad libitum* access to food and distilled water unless specified otherwise.

Surgery and tetrode implantation. Rats were anesthetized in an isoflurane gas anesthesia induction chamber with a 5% isoflurane/oxygen mix. Once sedated, rats were removed, and an isoflurane mask was placed on them. Rats received preoperative injections of buprenorphine HCl (0.05 mg/kg), atropine (0.03 mg/kg), dexamethasone (0.2 mg/kg), and lactated Ringers solution (5 ml). Once a surgical level of anesthesia was reached, the scalp was shaved, and the rat was placed into a stereotaxic frame. The depth of anesthesia was maintained with a 1.5–3.5% isoflurane/oxygen mix and monitored every 15 minutes by inspection of the breathing rate, whisking, and the toe-pinch withdrawal reflex. Ophthalmic ointment was placed on the eyes, and the scalp was swabbed with a povidone-iodine solution followed by a 70% ethanol solution. A midline incision was made, and the skull was cleaned with a 3% hydrogen peroxide solution. Cranial holes were drilled for the placement of seven anchoring screws (Microfasteners, SMPPS0002). A craniotomy was performed over the right mediodorsal thalamus (AP: −3.3 mm, ML: 1.4–1.6 mm from bregma) to implant a drivable bundle of eight tetrodes (Sandvik-

Kanthal, PX000004) with a final impedance of ~200–300 kΩ. The medial and central portions of the mediodorsal thalamus were targeted due to their connectivity with olfactory and gustatory cortical areas (Price and Slotnick, 1983; Kuroda et al., 1992; Ray and Price, 1992; Shi and Cassell, 1998; Pelzer et al., 2017). The tetrode bundle was inserted at a 10° angle, to avoid the superior sagittal sinus, and to a depth of ~4.7 mm from the brain surface. Ground wires were secured to multiple anchoring screws. Intraoral cannulas (IOCs) were bilaterally inserted to allow for the delivery of solutions containing stimuli directly into the oral cavity. All implants and a head-bolt (for head restraint) were cemented to the skull with dental acrylic. Injections of analgesic (buprenorphine HCl) were provided for 2–3 days after surgery. Rats were allowed a recovery period of 7–10 days before beginning water restriction.

Stimulus delivery and recording procedure. Following recovery from surgery, rats began a water restriction regime where they received access to a bottle containing distilled water for 1 h each day in their home cage. Once acclimated to the water restriction regime, rats were given 1 h access in their home cage for four consecutive days to two bottles containing different odor-taste mixtures: a palatable mixture of 0.01% isoamyl acetate-100 mM sucrose and an unpalatable mixture of 0.01% benzaldehyde-200 mM citric acid. Experience with odor-taste mixtures generates associations between the quality and value of an odor and a taste (Fanselow and Birk, 1982; Holder, 1991; Stevenson et al., 1995; Prescott et al., 2004; Gautam and Verhagen, 2010; Green et al., 2012; McQueen et al., 2020),

but it is unclear how many exposures to an odor-taste mixture are necessary to generate these associations. Therefore, we provided rats multiple days of exposure to odor-taste mixtures to establish odor-taste associations and limit possible variability across sessions related to learning odor-taste associations. Previous studies have shown that multiple days of exposure to odor-taste mixtures is sufficient to establish odor-taste associations (Sakai and Yamamoto, 2001; McQueen et al., 2020). This experience had the additional benefit of reducing the likelihood of rats rejecting odorized stimuli due to neophobia (Miller et al., 1986; Lin et al., 2009; Fredericksen et al., 2019; McQueen et al., 2020). After each recording session, rats were given 1 h access in their home cage to the two bottles containing the previously presented odor-taste mixtures to support experienced odor-taste associations throughout the experiment.

After odor-taste mixture experience, rats were trained to wait calmly in a head-restrained position for the intraoral delivery of liquids through the IOCs. All stimuli were mixed with distilled water and delivered via manifolds of polyimide tubes placed in the IOCs. Stimuli included distilled water, tastes (100 mM sucrose, 100 mM NaCl, 200 mM citric acid, and 1 mM quinine), odors (0.01% isoamyl acetate, 0.01% benzaldehyde, and 0.01% methyl valerate), the previously experienced odor-taste mixtures (isoamyl acetate-sucrose and benzaldehyde-citric acid), and mismatched pairings of those mixtures (isoamyl acetate-citric acid and benzaldehyde-sucrose). These odors have been used in previous studies investigating orally consumed odors (Aimé et al., 2007; Julliard et al., 2007; Gautam and Verhagen, 2010, 2012; Tong et al., 2011; Rebello et al., 2015;

Samuelsen and Fontanini, 2017; Bamji-Stocke et al., 2018; Fredericksen et al., 2019; McQueen et al., 2020). At these concentrations, isoamyl acetate and benzaldehyde lack a gustatory component (Aimé et al., 2007; Gautam and Verhagen, 2010; Samuelsen and Fontanini, 2017). A trial began with an intertrial interval of 20 ± 5 s followed by the pseudo-random delivery of ~25–30 µl (pressure infused via computer-controlled solenoid valves, opening time ~25 ms) of water, a single taste, a single odor, or an odor-taste mixture. Each stimulus delivery was followed 5 s later by a ~40 µl distilled water rinse. Although intraoral delivery directly infuses chemosensory stimuli into the oral cavity, rats can still reject stimuli by not swallowing and allowing fluids to leak from the mouth. If a rat failed to consume an intraoral stimulus, the session was immediately aborted. Only trials where rats consumed all 12 stimuli were included in the analysis. All recording sessions consisted of 120 trials (i.e., 12 stimuli × 10 trials), except for one session where a rat received only nine trials per stimulus. Tetrode bundles were lowered ~160 µm further after each recording session to obtain a new ensemble of neurons.

Electrophysiological recordings. Signals were sampled at 40 kHz, digitized, and band-pass filtered using the Plexon OmniPlex D system (Plexon, RRID:SCR_014803). Single units were isolated offline using a combination of template algorithms, cluster-cutting, and examination of interspike-interval plots using Offline Sorter (Plexon, Offline Sorter; RRID:SCR_000012). Single units were required to have interspike intervals longer than the biological constraints of a

neuronal refractory period (> 1 ms; 0% refractory period violations). Data analysis was performed using Neuroexplorer (Nex Technologies; RRID SCR 001818) and custom-written scripts in MATLAB (The MathWorks, RRID:SCR 001622).

Analysis of single units. For each neuron, single-trial activity and peristimulus time histograms (PSTHs) were aligned to the stimulus presentation through the IOCs. Responses to chemosensory stimuli were evaluated by analyzing changes in firing rates as in previous studies (Jezzini et al., 2013; Samuelsen et al., 2013; Gardner and Fontanini, 2014; Liu and Fontanini, 2015; Samuelsen and Fontanini, 2017; Levitan et al., 2019; Bouaichi and Vincis, 2020). Neurons were defined as "chemoselective" when two criteria were satisfied: (1) stimulus-evoked activity significantly differed from baseline for at least one stimulus and (2) there was a significant difference in the activity evoked by the twelve intraoral stimuli. A one-sample Kolmogorov-Smirnov test found that the spiking activity of neurons in the mediodorsal thalamus were not normally distributed. Therefore, significant difference from baseline for each stimulus was established using a nonparametric Wilcoxon rank-sum comparison between a 2 s baseline window (binned in 200 ms increments; 10-trial x 10-bin, concatenated into 100 x 1 baseline-array) immediately prior to stimulus delivery (i.e., baseline) and each 200 ms bin (10-trial x 1-bin array) following stimulus delivery (5 s post-stimulus) with correction for family-wise error (two consecutive significant bins, $p < 0.05$) (Gardner and Fontanini, 2014; Samuelsen and Fontanini, 2017; Bouaichi and Vincis, 2020).

Since a nonparametric statistic is not available to determine significant interactions between chemosensory-evoked activity and time, a two-way ANOVAs (stimulus × time) (Jezzini et al., 2013; Samuelsen et al., 2013; Gardner and Fontanini, 2014; Liu and Fontanini, 2015; Samuelsen and Fontanini, 2017; Levitan et al., 2019; Bouaichi and Vincis, 2020) was used to determine differences in the magnitude and time course of the chemosensory-evoked activity across the 12 stimuli (200 ms bins from 0 to 5 s after stimulus delivery) with a conservative alpha ($p < 0.01$). A neuron was considered to respond differently among the intraoral stimuli when the stimulus main effect or the interaction term (stimulus × time) had a value of $p < 0.01$. The distribution of responses and tuning of the chemoselective population were compared using a χ^2 test ($p < 0.05$) with post hoc comparisons performed using Fisher's exact test with Dunn–Sidak correction for family-wise error (Shan and Gerstenberger, 2017).

Area under the receiver operating characteristic (auROC) normalization method. To avoid potential confounds introduced by differences in baseline and evoked firing rates among neurons, stimulus-evoked activity was normalized to its baseline activity using the auROC method when comparing responses by groups of neurons (Cohen et al., 2012; Jezzini et al., 2013; Gardner and Fontanini, 2014; Liu and Fontanini, 2015; Vincis and Fontanini, 2016; Samuelsen and Fontanini, 2017; Bouaichi and Vincis, 2020). This method normalizes each neuron's stimulus-evoked activity to baseline activity using a scale of 0–1, where 0.5 represents the median of equivalence of the baseline activity. The auROC values represent the

probability that the spike counts during each 200 ms bin is significantly greater than the spike counts during the baseline period (-2 to 0 s). A score of 1 indicates that all values in the tested bin are greater than baseline, whereas a score of 0 indicates that all values are less than baseline. Therefore, a value greater than 0.5 indicates an excited response and a value less than 0.5 indicates a suppressed response. Population PSTHs were generated by averaging the auROC-normalized response to a given stimulus for each neuron in the observed population. Comparisons of the auROC-normalized population activity were performed using the Freidman's test ($p < 0.05$).

Excited and suppressed responses. To determine whether a chemoselective neuron exhibited an excited or a suppressed response to an intraoral stimulus, we calculated the mean auROC value of all bins that significantly differed from baseline. Responses with an average significant auROC value greater than 0.5 were defined as excited, and those with an average significant auROC value less than 0.5 were defined as suppressed. Comparisons in the time course between non-responses and responses that were excited or suppressed by chemosensory stimuli were performed using the Wilcoxon rank-sum test with correction for family-wise error (two consecutive significant bins, $p < 0.05$). Heat maps were generated that show all significant responses to each stimulus plotted from the lowest average significant auROC value (suppressed) to the greatest average significant auROC value (excited). The period during which a significant difference from baseline occurred was determined using a sliding window of 100 ms, stepped in

51

20 ms increments, until the firing rate was 2.58 standard deviations (99% confidence level) above or below the average baseline firing rate (2 s before stimulus delivery) (Bouaichi and Vincis, 2020). The response latency (i.e., time from stimulus delivery to first significant difference from baseline) was recorded as the trailing edge of the first significant bin. The response duration (i.e., total amount of time significantly different from baseline) was calculated as the total number of 20 ms bins significantly above (excited) or below (suppressed) the average baseline firing rate. Differences in response latency and response duration between excited and suppressed responses were compared using a two-sample Kolmogorov–Smirnov test ($p < 0.05$). Comparisons of response latency and response duration between stimulus categories were performed using the Kruskal–Wallis test corrected with the Tukey's HSD test ($p < 0.05$).

Population decoding analysis. Population decoding analyses were performed using an open source pattern classifier algorithm (for a detailed description of the Neural Decoding Toolbox see Meyers, 2013). This analysis uses the pattern of firing rates of a population of neurons to make predictions about which stimulus was delivered during a given trial. The accuracy of the classifier indicates how the population of neurons in the mediodorsal thalamus represents intraoral stimuli and how that chemosensory information is processed over time. For each subpopulation of neurons, a firing rate matrix of the spike times of each neuron (2 s before to 5 s after stimulus delivery) was realigned to the stimulus delivery, compiled into 250 ms bins, and normalized to the Z score. Four firing rate matrices

were constructed for each subpopulation: (1) all 12 stimuli, (2) water and the three odors, (3) water and the four tastes, and (4) water and the four odor-taste mixtures. Water was included in each category as a general non-chemosensory stimulus. Matrix activity was divided into nine sets: eight "training sets" were used by the classifier algorithm to "learn" the relationship between the population's neural activity pattern and the different stimuli; one "testing set" was used to predict which stimulus was delivered given the population's pattern of activity that was used to train the classifier. A max correlation coefficient classifier was used to assess stimulus-related information represented by the population activity. The max correlation coefficient classifier calculates the correlation coefficient between a test trial and each of the training set stimulus templates; the stimulus template with the largest correlation coefficient value is selected as the predicted stimulus. To compute the classification accuracy, this process was repeated ten times using different testing and training sets each time. The classification accuracy was defined as the fraction of trials during each bin for which the classifier correctly predicted the stimulus. Comparisons of the classification accuracy between neuron populations were performed using a permutation test ($p < 0.05$) (Ojala and Garriga, 2010).

A confusion matrix is a visual representation of the decoding performance for each stimulus, where columns represent the actual stimulus and rows represent the predicted stimulus. White squares represent classification accuracy less than chance, and darker hues indicate better performance. Diagonal squares represent the proportion of trials in which the classifier correctly assigned the predicted

stimulus to its true stimulus. Squares outside the diagonal represent the predicted stimuli that the classifier most often "confused" for each true stimulus (i.e., false predictions). Comparisons between populations of neurons in the proportion of trials where the predicted stimulus did not match the true stimulus were made with the Wilcoxon rank-sum test ($p < 0.05$). The Kruskal–Wallis test with Tukey's HSD correction for family-wise error ($p < 0.05$) was used to determine whether the classifier was more likely to confuse different groups of stimuli with each other.

Mixture-component difference (MCD) analysis. The MCD is equal to the difference in firing rate (−2 to 5 s; 200 ms bins) between the response to an odor-taste mixture (e.g., isoamyl acetate-sucrose) and the response to the odor component alone (e.g., isoamyl acetate) or the taste component alone (e.g., sucrose). A positive MCD score indicated that the mixture-evoked activity was higher than the component-evoked activity, while a negative MCD score indicated that the component-evoked activity was higher than the mixture-evoked activity. This analysis was used to examine eight mixture-stimulus differences (four mixture-odor and four mixture-taste) for each chemoselective neuron (n = 85) for a total of 680 mixture-component difference responses. Unlike the activity evoked by intraoral stimulus delivery, baseline activity is not directly related to an event. This variability in baseline activity can artificially enhance individual baseline MCD scores. To mitigate this variability, we calculated the mean and standard deviation using the baseline MCD scores of the eight mixture-stimulus differences for each chemoselective neuron. A response was considered significant when an evoked

MCD score exceeded the mean of the eight baseline MCD scores ± 6 times the standard deviation. The absolute difference in the MCD value was used to calculate the average MCD time course to account for the differences between mixtures and components irrespective of whether the mixture or the component had the greater firing rate. Significant changes from baseline in the average MCD time course were determined using a Wilcoxon rank-sum test with correction for family-wise error (two consecutive significant bins, $p < 0.05$).

Palatability index (PI) analysis. A PI was used to evaluate whether the activity of neurons in the mediodorsal thalamus represents the palatability-related features of tastes (Fontanini et al., 2009; Piette et al., 2012; Jezzini et al., 2013; Liu and Fontanini, 2015; Samuelsen and Fontanini, 2017; Bouaichi and Vincis, 2020). This analysis quantified differences in activity between tastes with similar hedonic values (sucrose/NaCl, citric acid/quinine) and tastes with opposite hedonic values (sucrose/quinine, sucrose/citric acid, NaCl/quinine, NaCl/citric acid). To control for differences in firing rates across the population of chemoselective neurons, the auROC-normalized activity (–2 to 5 s, 200 ms bins) was used to estimate the differences between taste pairs. The PI score was defined as the difference in the absolute value of the log-likelihood ratio of the auROC-normalized firing rate for

taste responses with opposite ($<|LR|>_{opposite}$) and similar ($<|LR|>_{same}$) hedonic values. The PI was defined as follows ($<|LR|>_{opposite} - <|LR|>_{same}$), where:

$$<|LR|>_{same} = 0.5 \times \left(\left| \ln \frac{sucrose}{NaCl} \right| + \left| \ln \frac{quinine}{citric\ acid} \right| \right)$$

$$<|LR|>_{opposite} = 0.25 \times \left(\left| \ln \frac{sucrose}{quinine} \right| + \left| \ln \frac{sucrose}{citric\ acid} \right| + \left| \ln \frac{NaCl}{quinine} \right| + \left| \ln \frac{NaCl}{citric\ acid} \right| \right)$$

A positive PI score indicates that a neuron responds similarly to tastes with similar palatability and differently to stimuli with opposite palatability. A chemoselective neuron was deemed palatability-related when the evoked PI score was positive and exceeded the mean + 6 times the standard deviation of the baseline (Bouaichi and Vincis, 2020). Significant changes from baseline in the average PI score time course were determined using a Wilcoxon rank-sum test with correction for family-wise error (two consecutive significant bins, $P < 0.05$).

Histology. After recordings were completed, rats were anesthetized with a ketamine/xylazine/acepromazine mixture (100, 5.2, and 1 mg/kg), and DC current (7 µA for 7 s) was applied to mark the tetrode locations. Rats were then transcardially perfused with cold phosphate buffer solution followed by 4% paraformaldehyde (PFA). Brains were extracted, post-fixed in 4% PFA, and then incubated in 30% sucrose. Sections were cut 70 µm thick using a cryostat, mounted, and stained with cresyl violet. Tetrode placement within the mediodorsal thalamus was required for recording sessions to be included in the data analysis (see Fig. 5).

Experimental design and statistical analysis. As with previous head-fixed recording experiments (Jones et al., 2007; Fontanini et al., 2009; Samuelsen et al., 2012, 2013; Gardner and Fontanini, 2014; Vincis and Fontanini, 2016; Samuelsen and Fontanini, 2017), only adult female rats were used because the size and strength of adult male rats significantly increases the risk of catastrophic head-cap failure. All chemosensory stimuli were delivered pseudo-randomly according to custom-written MATLAB (MathWorks) scripts. Experimenters had no control over the order of stimulus delivery. All statistical analyses were performed using GraphPad Prism (GraphPad Software, Inc.) and MATLAB (MathWorks), including population decoding analyses using the Neural Decoding Toolbox (Meyers, 2013). No statistical methods were used to predetermine sample sizes, but the numbers of recorded neurons and animals in this study are similar to those reported in previous studies.

Results

Previous electrophysiological studies have shown that neurons in the mediodorsal thalamus represent the identity of odors sampled via orthonasal olfaction (Yarita et al., 1980; Imamura et al., 1984; Courtiol and Wilson, 2014, 2016), but it is unclear how chemosensory signals originating from the mouth are processed by the mediodorsal thalamus. To this aim, we recorded single-unit activity in the mediodorsal thalamus of behaving rats during the intraoral delivery of distilled water, individual odors, individual tastes, and odor-taste mixtures. Figure 5 shows a representative example and a schematic illustration of the dorsal-ventral range of recording electrodes in the mediodorsal thalamus of each animal. A total of 135 single neurons were recorded from five rats across 27 sessions (5.4 ± 0.4 sessions per rat) with an average yield of 5.1 ± 0.9 neurons per session.

Neurons in the mediodorsal thalamus represent intraoral chemosensory signals

As a first step in evaluating chemosensory processing by the mediodorsal thalamus, we identified the population of neurons that responded differently to various odors, tastes, and odor-taste mixtures (i.e., chemoselective). Neurons defined as "chemoselective" exhibited a significant change in activity compared to baseline for at least one stimulus and responded differently across the various intraoral stimuli (see Materials and Methods for details). These two criteria were purposefully stringent because the intraoral delivery of solutions could introduce potential confounds related to the general effects of somatosensation or attention

rather than chemosensory-related activity. We found that 63% (85/135) of the neurons recorded from the mediodorsal thalamus met both criteria, and therefore we focused our analyses on this chemoselective population.

To better understand how intraoral chemosensory signals are processed by the mediodorsal thalamus, we analyzed the responses of the chemoselective population to odors, tastes, and odor-taste-mixtures (Fig. 6). Visual inspection of representative neurons and the average responses of the chemoselective population to water and the three odors (Fig. 6A), the four tastes (Fig. 6B), and the four odor-taste mixtures (Fig. 6C) suggested that responses differed between the chemosensory stimuli categories (i.e., odors, tastes, and odor-taste mixtures). A comparison of the auROC-normalized population activity showed an overall difference in the responses evoked by the 12 intraoral stimuli (Freidman's test, χ^2_{11} = 58.28, $p < 0.001$). Therefore, we next sought to determine whether the population responses differed within the three chemosensory stimuli categories. Although there was no significant difference in the responses to the three odors (Fig. 6A, Freidman's test, χ^2_2 = 2.02, $p = 0.364$), the chemoselective population's responses differed across the four tastes (Fig. 6B, Freidman's test, χ^2_3 = 31.08, $p < 0.001$) and the four odor-taste mixtures (Fig. 6C, Freidman's test, χ^2_3 = 15.12, $p = 0.002$).

Next, we examined whether different proportions of chemoselective neurons responded to the various intraoral stimuli. Figures 6D–F show the distribution of neurons that responded to water and each of the three odors (Fig. 6D), the four tastes (Fig. 6E), and the four odor-taste mixtures (Fig. 6F). There was an overall significant difference in the proportion of neurons responding to the

various intraoral stimuli (χ^2_{11} = 56.99, p < 0.001), with the majority of chemoselective neurons (60.0%, 51/85) responding to stimuli from all three categories. Analysis of the response distribution within each chemosensory category showed no difference in the proportion of neurons responding to the different odors (Fig. 6D, χ^2_2 = 0.028, p = 0.986) or odor-taste mixtures (Fig. 6F, χ^2_3 = 2.477, p = 0.480) but showed a significant difference among the taste stimuli (Fig. 6E, χ^2_3 = 22.38, p < 0.001). *Post hoc* analyses showed that significantly more neurons responded to citric acid (65.9%, 56/85) than responded to sucrose (38.8%, 33/85; Fisher's exact test, p < 0.001) or salt (31.7%, 27/85; Fisher's exact test, p < 0.001) but not quinine (48.2%, 41/85; Fisher's exact test, p > 0.05). More chemoselective neurons responded to the unpalatable citric acid than responded to either palatable taste.

Next, we evaluated the tuning profiles of chemoselective neurons within each stimulus category to determine the proportion of neurons that responded to only a single stimulus (i.e., sparsely tuned) or multiple stimuli (i.e., broadly tuned). Overall, most chemoselective neurons responded to at least one odor-taste mixture (92.9%, 79/85), followed by at least one taste (82.4%, 70/85), and then at least one odor (71.8%, 61/85). Within the odor category (Fig. 6G), there was no difference in the proportion of chemoselective neurons that did not respond to odors (28.2%, 24/85), responded to a single odor (31.8%, 27/85), or responded to multiple odors (40.0%, 34/85) (χ^2_2= 2.788, p = 0.25). Within the taste category (Fig. 6H), the proportion of chemoselective neurons that responded to multiple taste stimuli (χ^2_2 = 29.36, p < 0.0001, 55.3%, 47/85) was significantly greater than the

proportion that responded to only a single taste (27.1%, 23/85; Fisher's exact test, $p < 0.001$) or did not respond to tastes (17.6%, 15/85; Fisher's exact test, $p < 0.001$). Within the odor-taste mixture category (Fig. 6I), the proportion of chemoselective neurons that responded to multiple odor-taste mixtures ($\chi^2_2 = 114.0$, $p < 0.001$, 77.6%, 66/85) was significantly greater than the proportion that responded to only a single odor-taste mixture (15.3%, 13/85; Fisher's exact test, $p < 0.001$) or did not respond to mixtures (7.1%, 6/85; Fisher's exact test, $p < 0.001$). For all three chemosensory categories, there was no difference in the proportions of neurons that responded to only one, only two, only three, or all four stimuli (Table 3; odors: $\chi^2_2 = 4.439$, $p = 0.11$; tastes: $\chi^2_3 = 6.116$, $p = 0.11$; mixtures: $\chi^2_3 = 5.128$, $p = 0.16$). These analyses showed that chemoselective neurons in the mediodorsal thalamus respond broadly across tastes and odor-taste mixtures but include a similar proportion of sparsely tuned and broadly tuned neurons responding to intraoral odors.

These analyses revealed that most neurons in the mediodorsal thalamus respond to the intraoral delivery of chemosensory stimuli, are primarily broadly tuned within chemosensory categories, and respond differently to unimodal and multimodal chemosensory signals. These results are consistent with neurons in the mediodorsal thalamus processing sensory information across a range of chemosensory stimuli.

Temporal processing of chemosensory signals by the mediodorsal thalamus

Chemosensory processing in the olfactory and gustatory system is characterized by dynamic and time-varying modulations in activity (Katz et al., 2001; Fontanini et al., 2009; Maier et al., 2012; Samuelsen et al., 2012, 2013; Liu and Fontanini, 2015; Maier, 2017; Samuelsen and Fontanini, 2017). Although these areas primarily respond to chemosensory stimuli with excitation, a study by Liu and Fontanini (2015) examining another thalamic nucleus, the gustatory thalamus (i.e., the parvicellular portion of the ventroposteromedial nucleus), revealed a near balance between taste-evoked excitation and suppression. Visual inspection of raster plots and PSTHs (Fig. 6A–C) indicated that chemoselective neuron activity could be excited or suppressed by the intraoral delivery of chemosensory stimuli. To evaluate responses by the chemoselective neuron population, we sorted chemosensory-evoked activity into excited responses (when the significant evoked activity was greater than baseline), suppressed responses (when the significant evoked activity was less than baseline), and non-responses (activity that did not significantly differ from baseline). The auROC-normalized population averages of non-responses, excited responses, and suppressed responses (Fig. 7A–C) and the heat maps of each significant response (Fig. 7D–F) to odors, tastes, and odor-taste mixtures illustrate the heterogeneity of responses across the chemoselective population. There was no significant difference in the overall proportion of responses that were excited (27.2%, 254/935) or suppressed (23.7%, 222/935) by the different chemosensory stimuli (Fisher's exact test, p = 0.0998). This equivalence in stimulus-evoked excitation

and suppression was represented within each stimulus category. There was no difference in the proportion of odors that evoked excitation (23.5%, 60/255) or suppression (20.0%, 51/255; Fisher's exact test, p = 0.391), tastes that evoked excitation (24.1%, 82/340) or suppression (22.1%, 75/340; Fisher's exact test, p = 0.585), or odor-taste mixtures that evoked excitation (32.9%, 112/340) or suppression (28.2%, 96/340; Fisher's exact test, p = 0.212). Overall, chemosensory-evoked activity in the mediodorsal thalamus was balanced between excitation and suppression.

To determine whether temporal differences existed between excited and suppressed activity, we determined the response latency (i.e., time from stimulus delivery to first significant difference from baseline) and response duration (i.e., total amount of time the response was significantly different from baseline) for all chemosensory-evoked responses. Overall, responses suppressed by chemosensory stimuli (301.7 ± 30.1 ms) occurred significantly faster than those excited by chemosensory stimuli (443.9 ± 45.0 ms; two-sample Kolmogorov–Smirnov test, K-S stat = 0.23, p < 0.001). Next, we determined whether differences in response latency between excitation and suppression occurred across the chemosensory categories. While there was no difference among the stimulus categories in the response latency of excited activity (odors: 443.4 ± 82.8 ms, tastes: 471.6 ± 90.3 ms, odor-taste mixtures: 426.0 ± 65.5 ms; Kruskal–Wallis, H (2) = 0.1080, p = 0.948), this analysis revealed a significant difference among the stimulus categories for the response latency of suppression (Kruskal–Wallis, H (2) = 8.9704, p = 0.011). Tukey's HSD test for multiple comparisons showed that the

response latency of suppression occurred significantly faster with the intraoral delivery of odor stimuli (156.1 ± 36.1 ms) than that for either taste (341.0 ± 55.8 ms, p = 0.033) or odor-taste mixtures (349.2 ± 49.5 ms, p = 0.012). Next, we analyzed the duration of activity that was significantly greater than baseline (a measure of total excitation) or significantly lower than baseline (a measure of total suppression). Overall, the excited activity lasted significantly longer (716.2 ± 34.7 ms) than the responses suppressed by chemosensory stimuli (477.2 ± 27.5 ms; two-sample Kolmogorov–Smirnov test, K-S stat = 0.21, p < 0.001). Unlike response latency, there were no differences among stimulus categories in the duration of either excited activity (odors: 737.1 ± 74.5 ms, tastes: 742.6 ± 60.3 ms, mixtures: 685.0 ± 51.7 ms; Kruskal–Wallis, H (2) = 0.3723, p = 0.8301) or suppressed activity (odors: 528.2 ± 59.2 ms, tastes: 488.6 ± 49.9 ms, mixtures: 441.6 ± 39.3 ms; Kruskal–Wallis, H (2) = 1.4805, p = 0.4770). In summary, neuron activity was suppressed by stimuli more quickly, especially in response to odors, but exhibited excitation for a significantly longer time than suppression was observed.

Population decoding of chemosensory signals by the mediodorsal thalamus

Although the activity of individual neurons can represent specific features of chemosensory stimuli, neuronal networks are responsible for integrating and processing that information to guide behavior. We hypothesized that the heterogeneity displayed by the population of chemoselective neurons enables the accurate representation of the various chemosensory stimuli over time. We

performed a population decoding analysis (see Materials and Methods for details) to examine whether the firing patterns of the ensemble of chemoselective neurons in the mediodorsal thalamus accurately encodes stimulus identity over time (Jezzini et al., 2013; Meyers, 2013; Liu and Fontanini, 2015; Bouaichi and Vincis, 2020). We began by analyzing how well the population activity of chemoselective neurons (n = 85) and non-chemoselective neurons (n = 50) represented the 12 intraoral stimuli during the 5 s after stimulus delivery. Figure 8A shows the average decoding performance of the two populations over time. The classification accuracy of the chemoselective population exceeded the chance level (8.3%) and significantly differed from that of the non-chemoselective population beginning 250 ms after stimulus delivery (permutation test, $p < 0.05$) and continuing for the entire 5 s window. As expected, the decoding performance of the non-chemoselective neurons showed that its population activity does not represent information about intraoral stimuli. These results are consistent with the population of chemoselective neurons encoding the identity of chemosensory signals originating from the mouth.

The confusion matrices in Figure 8B show the two population's average classification performances for each stimulus over the 5 s after intraoral delivery. White squares represent a classification accuracy less than chance (8.3%), and darker hues indicate better performance. The diagonal squares represent the proportion of trials for which the classifier correctly assigned the predicted stimulus (rows) to its true stimulus (columns). Off-diagonal squares indicate the proportion of trials where the predicted stimulus did not match the true stimulus (i.e., false predictions). The confusion matrix of the chemoselective population (Fig. 8B, left)

shows that the classification accuracy for each stimulus is greatest along the diagonal (i.e., predicted stimulus matches the true stimulus) and reveals the predicted stimuli the classifier most often confused for each true stimulus. For example, the classifier most often correctly predicted citric acid but sometimes incorrectly predicted odor-taste mixtures containing citric acid. The proportion of trials where the predicted stimulus did not match the true stimulus (i.e., rows excluding the diagonal) was significantly greater for the non-chemoselective population (8.36% ± 0.17%) than that for the chemoselective population (6.09% ± 0.51%, Wilcoxon rank-sum, Z = 6.78, $p < 0.001$), indicating that the population activity of non-chemoselective neurons resulted in significantly more incorrect predictions than that for the chemoselective population.

Visual inspection of the confusion matrix for the chemoselective population (Fig. 8B) suggested that the classifier was more likely to "confuse" water, the odors, and the palatable stimuli (i.e., NaCl, sucrose, or an odor-taste mixture containing sucrose) with each other than with the unpalatable stimuli (i.e., citric acid, quinine, or an odor-taste mixture containing citric acid). This would suggest that the chemoselective population may represent palatability-related features of chemosensory stimuli. To determine whether false predictions were more likely to occur between similar groups of stimuli, we compared the proportion of trials where the predicted stimulus did not match the true stimulus (i.e., the off-diagonal squares) between the palatable stimuli, waters and odors, and unpalatable stimuli. When the classifier erroneously predicted a palatable stimulus (top four rows), the true stimulus was more likely to be another palatable stimulus (10.1% ± 1.4%, $p <$

66

0.001) or an odor or water (8.3% ± 1.1%, $p < 0.001$) than an unpalatable stimulus (1.8% ± 0.3%; Kruskal–Wallis, H (2) = 27.52, $p < 0.001$). When the classifier erroneously predicted an odor or water (middle four rows), the true stimulus was more likely to be another odor or water (8.1% ± 1.4%, $p = 0.002$) or a palatable stimulus (8.9% ± 1.2%, $p < 0.001$) than an unpalatable stimulus (1.5% ± 0.2%; Kruskal–Wallis, H (2) = 28.50, $p < 0.001$). However, when the classifier erroneously predicted an unpalatable stimulus (bottom four rows), the true stimulus was more likely to be another unpalatable stimulus (13.6% ± 2.9%; Kruskal–Wallis, H (2) = 12.48, $p < 0.001$) than either a palatable stimulus (3.1% ± 0.4%, $p = 0.022$) or an odor or water (2.8% ± 0.5%, $p = 0.002$). These results are consistent with the chemoselective population representing the palatability-related features of chemosensory stimuli.

Although the population activity of the chemoselective neurons accurately encoded the 12 intraoral stimuli, response similarities within the different chemosensory categories (e.g., tastes: NaCl and sucrose; odors: isoamyl acetate and methyl valerate; mixtures: benzaldehyde-citric acid and isoamyl acetate-citric acid) sometimes resulted in false predictions. Therefore, we next examined how well the population activity of chemoselective and non-chemoselective neurons decoded stimuli within each of the chemosensory categories. The odor decoding performance of the chemoselective population (Fig. 8C) showed an early onset, with a classification accuracy above chance level and significantly differing from that of the non-chemoselective population from the first bin after intraoral delivery (0–250 ms) (permutation test, $p < 0.05$). The significant difference in classification

accuracy between the two populations was briefly disrupted ~2 s after stimulus delivery before returning to significance for the remaining temporal window. The taste decoding performance of the chemoselective population (Fig. 8D) did not perform above the chance level until the second bin after intraoral delivery (250–500 ms) but significantly differed from that of the non-chemoselective population beginning from the first bin (0–250 ms) (permutation test, $p < 0.05$). The classification accuracy remained above chance level and significantly different from that of the non-chemoselective population for the remaining temporal window. Similar to the decoding performance of odors, the odor-taste mixture decoding performance of the chemoselective population (Fig. 8E) showed an early onset, with a classification accuracy above chance level and significantly differing from that of the non-chemoselective population from the first bin (0–250 ms) (permutation test, $p < 0.05$). Similar to the decoding performance of tastes, the classification accuracy for odor-taste mixtures remained above chance level and was significantly different from that of the non-chemoselective population for the entire 5 s time frame. This population decoding analysis showed that the activity of chemoselective neurons differently represents the four odor-taste mixtures, despite them being composed of only two tastes (sucrose and citric acid) and two odors (isoamyl acetate and benzaldehyde).

Together, these data indicate that the ensemble of chemoselective neurons in the mediodorsal thalamus reliably encodes unimodal and multimodal chemosensory signals over time. Furthermore, the population activity evoked by water, odors, and palatable stimuli is more similar than that of the responses to

unpalatable stimuli, suggesting that subpopulations of chemoselective neurons may preferentially represent information about stimulus identity or stimulus palatability.

Most chemoselective neurons respond to mixtures differently from one of their components

The odor-taste mixture decoding performance of the chemoselective population activity (Fig. 8E) suggested odor-taste mixtures are represented differently from their components. However, the activity evoked by the intraoral delivery of odor-taste mixtures may be similar to the odor and taste component alone. Visual inspection of raster plots and PSTHs suggested that a subset of chemoselective neurons responded differently to odor-taste mixtures compared to their individual odor or taste components (Fig. 9A). To determine which chemoselective neurons in the mediodorsal thalamus responded to odor-taste mixtures differently from their unimodal components, we performed an MCD analysis (see Materials and Methods for details). This analysis quantified the difference in firing rate across time between the neuronal response to an odor-taste mixture and the response to its odor component alone or its taste component alone. A response was considered significantly different when the evoked MCD score exceeded the mean of the eight baseline MCD scores ± 6 times the standard deviation. Figure 9B shows the representative neuron's MCD score for the difference between the activity evoked by the mixture of isoamyl acetate-sucrose

and isoamyl acetate alone (left) and the MCD score for the difference between the activity evoked by the mixture of benzaldehyde-sucrose and sucrose alone (right).

The MCD analysis revealed that nearly one-third of the odor-taste mixture responses (32.8%, 168/680) differed from at least one of their components (mixture-taste: isoamyl acetate-sucrose and sucrose: 19/85, 22.4%; benzaldehyde-sucrose and sucrose: 27/85, 31.8%; benzaldehyde-citric acid and citric acid: 16/85, 18.8%; isoamyl acetate-citric acid and citric acid: 14/85, 16.5%. mixture-odor: isoamyl acetate-sucrose and isoamyl acetate: 18/85, 21.2%; isoamyl acetate-citric acid and isoamyl acetate: 24/85, 28.2%; benzaldehyde-sucrose and benzaldehyde: 23/85, 27.1%; benzaldehyde-citric acid and benzaldehyde: 27/85, 31.8%). There was no difference between the proportion of mixture-taste MCD responses (76/168, 45.2%) and mixture-odor MCD responses (92/168, 54.8%; Fisher's exact test, $p = 0.102$). Because each MCD score represents the difference in firing rate between an odor-taste mixture and one of its components, a positive MCD score indicates that the mixture-evoked activity was higher than the component-evoked activity (example 9B right), while a negative MCD score indicates that the component-evoked activity was higher than the mixture-evoked activity (example 9B left). Next, we asked whether the significant response of each MCD score was due to higher mixture-evoked activity or higher component-evoked activity. We found that overall there were significantly more MCD responses with higher mixture-evoked activity (100/168; 59.5%) than higher component-evoked activity (68/168, 40.5%; Fisher's exact test, $p < 0.001$). There was a significant difference in the proportion of mixture-taste MCD responses with higher mixture-

evoked activity (56/76, 73.7%) compared to those mixture-taste MCD responses with higher taste-evoked activity (20/76, 26.3%; Fisher's exact test, $p < 0.001$). However, there was no difference in the proportion of mixture-odor MCD responses with higher mixture-evoked activity (44/92, 47.8%) compared to those mixture-odor MCD responses with higher odor-evoked activity (48/92, 52.2%; $p = 0.66$).

We next determined how many neurons represented the 168 significant MCD responses (a neuron could have a maximum of eight significant MCD responses; four odor-taste mixtures compared to their odor and taste component). We found that 53 of the 85 (62.4%) chemoselective neurons accounted for the significant MCD responses. Of the 53 neurons, 21 (39.6%, 21/53) had odor-taste mixture responses that differed from both odor and taste responses, 23 (43.4%, 23/53) differed from odor responses alone, and 9 (17.0%, 9/53) differed from taste responses alone. Interestingly, we found no difference in the number of MCD responses for neurons with odor-taste mixture responses that differed from both odor (2.23 ± 0.23) and taste responses (2.61 ± 0.26), differed from odor responses alone (1.96 ± 0.22), or differed from taste responses alone (2.33 ± 0.33, Kruskal–Wallis, H (3) = 3.904, $p = 0.272$). These results indicate that mixture-odor and mixture-taste MCD responses were distributed across this chemoselective population, with most neurons representing multiple mixture-component differences. A total of 18 (34.0%, 18/53) neurons responded to at least one mixture differently than both of that same mixture's components (isoamyl acetate-sucrose, isoamyl-acetate, and sucrose: 38.9%, 7/18; benzaldehyde-sucrose,

benzaldehyde, and sucrose: 72.2%,13/18; benzaldehyde-citric acid, benzaldehyde, and citric acid: 33.3%, 6/18; isoamyl acetate-citric acid, isoamyl-acetate, and citric acid: 33.3%, 6/18).

To examine the time course of MCD responses, we calculated the average absolute difference in MCD (−2 to 5 s; 200 ms bins) for the significant MCD responses and the non-MCD responses (Fig. 9C). The average absolute MCD score was used to account for differences between odor-taste mixtures and their components irrespective of whether the mixture or the component had the greater firing rate (Fig. 9B). This analysis revealed that significant MCD responses differed from baseline at 600 ms, peaked at 800 ms, and remained significantly above baseline for 3 s after stimulus delivery (Wilcoxon rank-sum, two consecutive significant bins, $p < 0.05$). The average absolute value of the non-MCD responses did not differ from baseline ($p > 0.05$). This analysis suggested that the difference between mixtures and their unimodal component is largely represented from ~0.5 to 3 s after stimulus delivery.

We used population decoding analysis to examine how well the activity of the neuron ensemble with odor-taste mixture responses that differed from at least one of its components (i.e., significant MCD) encoded the 12 intraoral stimuli over time. Figure 9D shows the average decoding performance over time of the population of chemoselective neurons with significant MCD responses (n = 53) and the non-MCD population (n = 32). The classification accuracy of the population with significant MCD responses exceeded the chance level beginning in the first bin (0–250 ms), while the non-MCD population did not exceed the chance level

until the second bin after intraoral delivery (250–500 ms). Both populations performed better than chance for the remainder of the temporal window, but the classification accuracy of the MCD population was significantly better than that of the non-MCD population for ~3 s after stimulus delivery (permutation test, $p <$ 0.05). The confusion matrices in Figure 9E show the average classification performance for each stimulus during the 5 s after stimulus delivery of the population with significant MCD responses (left) and the non-MCD population (right). The proportion of trials where the predicted stimulus did not match the true stimulus (i.e., the rows excluding the diagonal) was significantly greater for the non-MCD population (7.43 ± 0.35) than that for the population with significant MCD responses (6.32 ± 0.46, Wilcoxon rank-sum, Z = 3.79, $p <$ 0.001), indicating that the population activity of the non-MCD neurons resulted in significantly more incorrect predictions than that for neurons with significant MCD responses.

Next, we sought to determine whether the decoding performance of the two populations differed within each chemosensory category. Figure 9F–H shows the decoding performance of the population of chemoselective neurons with significant MCD responses and the non-MCD population for the three categories of chemosensory stimuli. Decoding performance by the population with significant MCD responses showed an early onset for all three chemosensory categories with classification accuracies above chance level and significantly differing from that of the non-MCD population beginning in the first bin (0–250 ms) (permutation test, p < 0.05). The classification accuracy of the non-MCD population did not exceed the chance level until the second bin (250–500 ms) for tastes (Fig. 9G) and odor-taste

mixtures (Fig. 9H) or until the third bin (500–750 ms) for odors (Fig. 9F). For all three stimulus categories, the significant differences in decoding performance between the MCD and non-MCD populations were maintained for ~3 s after stimulus delivery.

Taken together, these results show that most chemoselective neurons in the mediodorsal thalamus respond to odor-taste mixtures differently than their odor or taste component, with chemosensory information largely represented during the first 3 s after stimulus delivery.

A subset of chemoselective neurons represents the palatability-related features of tastes

Tastes have intrinsic value, and rodents consume palatable tastes and avoid unpalatable ones. It is well established that brain regions important for chemosensory processing and feeding-related behaviors represent the chemical and palatability-related features of tastes (Fontanini et al., 2009; Piette et al., 2012; Sadacca et al., 2012; Jezzini et al., 2013; Li et al., 2013; Liu and Fontanini, 2015; Samuelsen and Fontanini, 2017). The decoding performance and confusion matrix of the chemoselective population activity (Fig. 8A–B) suggested that a subset of neurons may encode the palatability-related features of chemosensory stimuli. Therefore, we calculated a palatability index (PI) (see Materials and Methods for details) to determine whether neurons in the mediodorsal thalamus represent the palatability-related features of tastes, meaning that tastes belonging to similar hedonic categories evoke similar responses (e.g., sucrose/NaCl vs. citric

acid/quinine). This analysis quantified the differences in activity between tastes of similar palatability (sucrose/NaCl, citric acid/quinine) and tastes of opposite palatability (sucrose/quinine, sucrose/citric acid, NaCl/quinine, NaCl/citric acid). A chemoselective neuron was considered to represent taste palatability when it had a positive PI score (i.e., it responded similarly to tastes with similar hedonic value but differently to tastes with opposite hedonic value) and the evoked PI score exceeded the mean + 6 times the standard deviation of the baseline (Bouaichi and Vincis, 2020).

This analysis revealed that the activity of more than a quarter (27.1%, 23/85) of the chemoselective neurons represented palatability-related features of tastes (Fig. 10A, representative examples auROC normalized firing rate (top) and PI scores (bottom)). To examine the temporal evolution of palatability-related activity, we calculated the average PI score (−2 to 5 s; 200 ms bins) for the populations of palatability-related (n = 23) and non-palatability-related neurons (n = 62). Figure 10B shows that the mean PI score of the palatability-related neurons began to significantly differ from baseline after 1.2 s and peaked 2 s after stimulus delivery (Wilcoxon rank-sum, two consecutive significant bins, $p < 0.05$). The mean PI score of the non-palatability-related population did not differ from baseline ($p > 0.05$).

Because, by definition, neurons in the palatability-related population must respond similarly to tastes with similar palatability, the non-palatability-related population of chemoselective neurons should better represent the identity of chemosensory stimuli over time. Figure 10C shows the average decoding

performance for all 12 stimuli over time for the palatability-related (n = 23) and non-palatability-related (n = 62) populations of chemoselective neurons. The classification accuracy of the non-palatability-related population exceeded the chance level beginning in the first bin (0–250 ms), but the classification accuracy of the palatability-related population did not exceed the chance level until the second bin after intraoral delivery (250–500 ms). Both populations performed better than chance level for the remainder of the 5 s window. However, the classification accuracy of the non-palatability-related population was significantly better than that of the palatability-related population between 0.25 and 1 s after stimulus delivery (permutation test, $p < 0.05$). The confusion matrices in Figure 10D show the average classification performance for each stimulus during the 5 s after intraoral delivery in the palatability-related (left) and non-palatability-related (right) populations of chemoselective neurons. There was no difference between the two populations in the proportion of trials in which the predicted stimulus did not match the true stimulus (i.e., the rows excluding the diagonal) (6.99% ± 0.48% vs. 6.74% ± 0.41%, Wilcoxon rank-sum, Z = 0.27, $p = 0.79$), indicating that the two populations performed similarly overall despite the differences in the classification accuracy between 0.25 and 1 s after stimulus delivery.

As predicted, the decoding performance of the non-palatability-related population activity was significantly better than that of the palatability-related population activity. Therefore, we expected that a comparison of the decoding performance of the two populations for each chemosensory category would reveal worse classification accuracy of the palatability-related population for tastes but

76

better accuracy for odors and odor-taste mixtures. Figure 10E–G shows the decoding performance for the three categories of chemosensory stimuli in the palatability-related and non-palatability-related populations. Counter to our prediction, the decoding performance of palatability-related population activity was significantly better than that of the non-palatability-related neuron activity for tastes (Fig. 10F) but worse for odors (Fig. 10E) and odor-taste mixtures (Fig. 10G).

Interestingly, these population decoding analyses revealed that the poorer decoding performance for all 12 stimuli by the palatability-related population (Fig. 10C) was not due to confusion between taste stimuli. In fact, the taste decoding performance of the palatability-related population was significantly better than that of the non-palatability population (Fig. 10F). An alternative reason for the poorer decoding performance by the palatability-related population could be due to similar population activity evoked by individual odor and taste stimuli previously experienced together as an odor-taste mixture. Behavioral studies have shown that multiple days of experience with odor-taste mixtures establishes odor-taste associations that inform consummatory choice (Sakai and Yamamoto, 2001; McQueen et al., 2020). For example, rats that are exposed to mixtures of isoamyl acetate-sucrose and benzaldehyde-citric acid prefer to consume water containing isoamyl acetate rather than water containing benzaldehyde. However, rats that are exposed to mixtures with the opposite pairs, such as isoamyl acetate-citric acid and benzaldehyde-sucrose, prefer to consume water containing benzaldehyde rather than water containing isoamyl acetate (McQueen et al., 2020). These powerful associations are resistant to extinction (Sakai and Imada, 2003; Albertella

and Boakes, 2006; Yeomans et al., 2006; González et al., 2016) and link the odor with the taste quality and value (Fanselow and Birk, 1982; Holder, 1991; Stevenson et al., 1995; Prescott et al., 2004; Gautam and Verhagen, 2010; Green et al., 2012; McQueen et al., 2020). To avoid variability across sessions related to learning of odor-taste associations, we provided rats with experience to isoamyl acetate-sucrose and benzaldehyde-citric acid mixtures. Because of this odor-taste mixture experience, it is possible that the poorer decoding performance by the palatability-related neurons was due to similarities in the population activity between isoamyl acetate and sucrose and those between benzaldehyde and citric acid.

To investigate the relationship between previously presented odor-taste pairs, we trained the classifier with the population activity evoked by sucrose and citric acid (true stimulus) and elicited predictions based on the population activity evoked by isoamyl acetate or benzaldehyde (predicted stimulus). The classification accuracy of the taste-trained classifier should exceed chance level if the activity evoked by a taste is similar to the activity evoked by its previously paired-odor. Figure 11A shows the taste-trained decoding performance of the palatability-related and non-palatability-related neurons. The classification accuracy of the palatability-related population performed better than chance and was significantly better than that of the non-palatability-related population during two time-frames, 0.25–1 s and 2–2.5 s after stimulus delivery (permutation test, $p < 0.05$). Next, we tested the opposite relationship by training the classifier with the population activity evoked by isoamyl acetate and benzaldehyde (true stimulus)

and elicited predictions based on the population activity evoked by sucrose and citric acid (predicted stimulus) (Fig. 11C). As with the taste-trained classifier above, the odor-trained classifier revealed that the classification accuracy of the palatability-related population performed better than chance and was significantly better than that of the non-palatability-related population during the time frames of 0.25–1 s and 1.75–2.5 s after stimulus delivery (permutation test, $p < 0.05$). The average classification accuracies of the two populations during the peak decoding performance (0.25–1 s) are represented by the confusion matrices in Figure 11B and 11D. Together, the results of the taste-trained classifier and odor-trained classifier showed that the proportion of trials during the initial peak (0.25–1 s after stimulus delivery), where the predicted stimulus did not match the true stimulus (i.e., false predictions), were significantly greater for the non-palatability-related population (55.4% ± 4.3%) than those for the palatability-related population (27.0% ± 3.6%, Wilcoxon rank-sum, Z = 3.47, $p < 0.001$). Thus, the population activity of the non-palatability-related neurons resulted in significantly more incorrect predictions than that of the palatability-related population. These results suggest that the poorer overall decoding performance by the palatability-related neurons during the 0.25–1 s after stimulus delivery (Fig. 10C) is related to the similar responses evoked by the components of previously experienced odor-taste mixtures.

In summary, the chemoselective population of neurons in the mediodorsal thalamus is broadly responsive to intraoral chemosensory stimuli and responds to odor-taste mixtures differently than an odor or taste alone. This chemoselective

population contains a subset of neurons that represents the palatability-related features of tastes that may also represent associations between experienced odor-taste pairs. Overall, the above findings demonstrate that chemoselective neurons in the mediodorsal thalamus dynamically encode chemosensory signals originating from the mouth.

Table 3

The proportion of neurons responding to only one, two, three, or all four stimuli

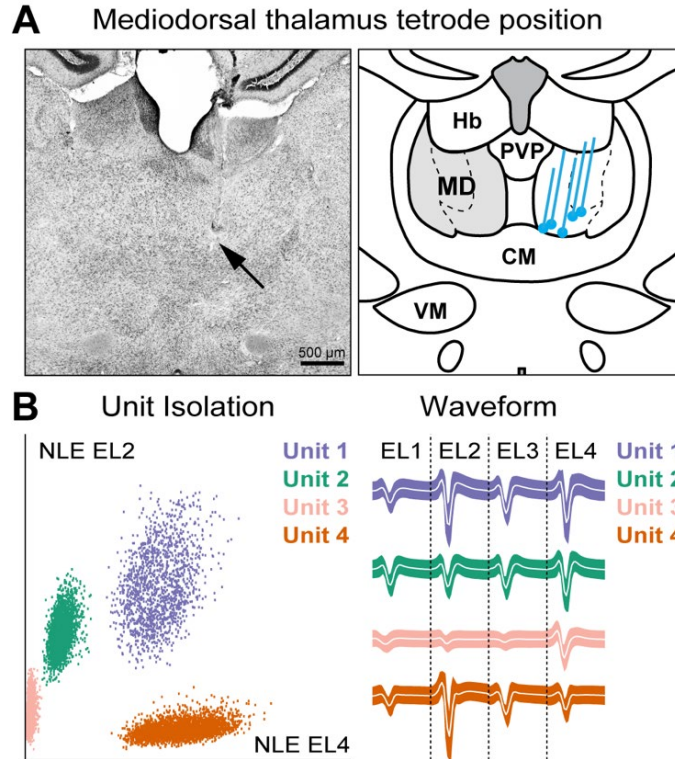|	Only 1	Only 2	Only 3	All 4
Odors	27/85 (31.8%)	18/85 (21.2%)	16/85 (18.8%)	-
Tastes	23/85 (27.1%)	21/85 (24.7%)	12/85 (14.1%)	14/85 (16.5%)
Odor-taste mixtures	13/85 (15.3%)	26/85 (30.6%)	17/85 (20.0%)	23/85 (27.1%)

Figure 5. Tetrode locations and representative single-unit recordings. A. *Left:* Example histological section showing the recording tetrode position (black arrow) in the mediodorsal thalamus. *Right:* Schematic summary of the reconstructed tetrode path in five rats. The blue lines correspond to the dorsoventral range of each drivable tetrode bundle. CM, central medial thalamic nucleus. Hb, habenular nucleus. MD, mediodorsal thalamus. PVP, paraventricular thalamic nucleus. VM, ventromedial thalamic nucleus. **B.** *Left:* Representative single-unit recordings in the mediodorsal thalamus showing the principal component analysis of waveform shapes of four individual neurons. EL, electrode; NLE, non-linear energy. *Right:* Average single-unit response for the same four neurons recorded from the four wires of the tetrode.
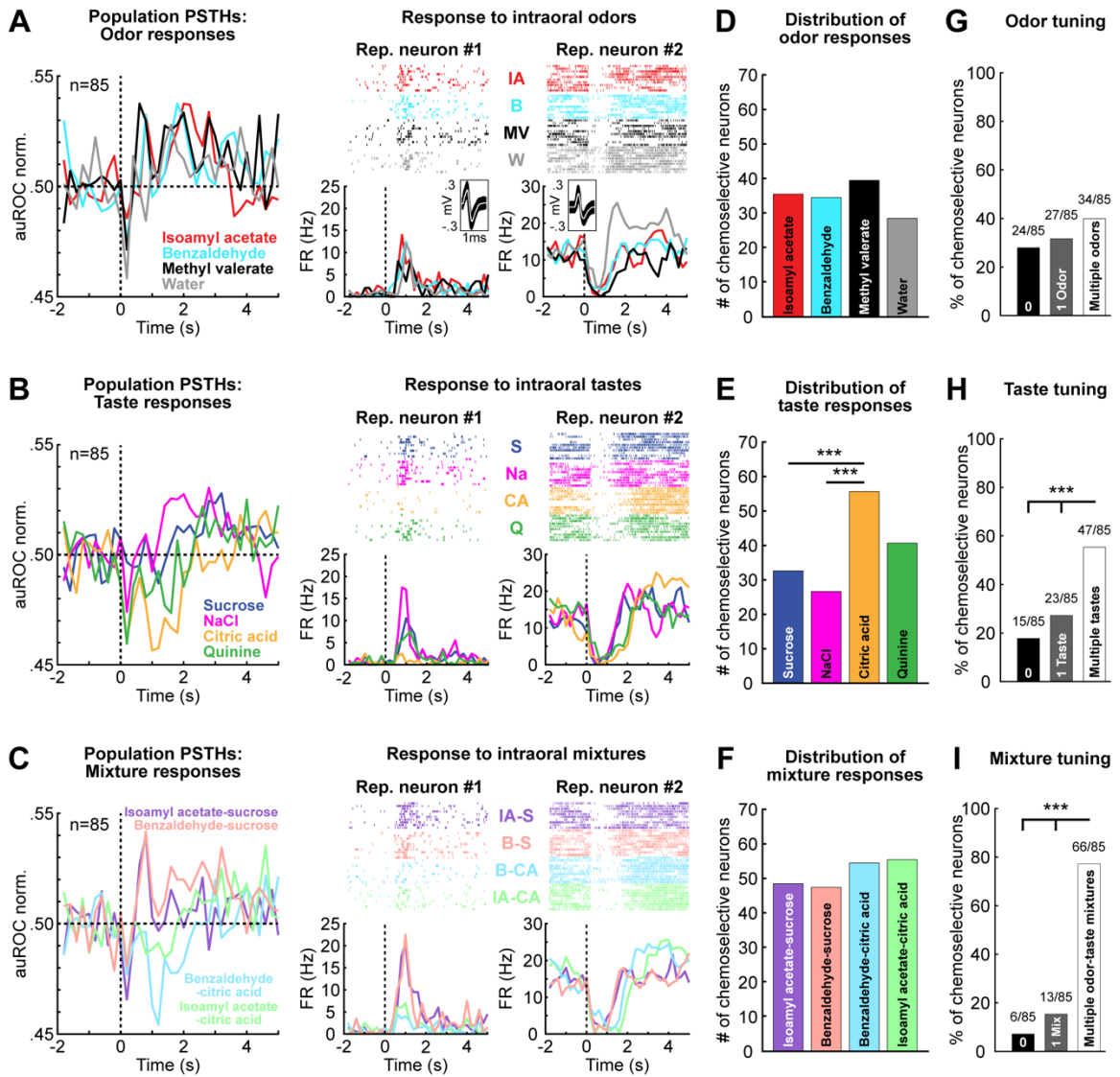
Figure 6. Neurons in the mediodorsal thalamus represent chemosensory signals originating in the mouth. A–C. *Left:* Peristimulus time histograms (PSTHs) of the chemoselective population's (n = 85) normalized response (auROC; area under the receiver-operating characteristic curve) to **A.** odors, **B.** tastes, and **C.** odor-taste mixtures. Vertical dashed lines indicate the stimulus delivery (time = 0). Horizontal dashed lines indicate baseline. *Right:* Representative chemoselective neurons firing rate raster plots and PSTHs in

response to intraoral delivery (time = 0, vertical dashed lines) of **A.** water and the three odors (isoamyl acetate [IA, red], benzaldehyde [B, cyan], methyl valerate [MV, black], water [W, gray]), **B.** the four tastes (sucrose [S, blue], NaCl [Na, magenta], citric acid [CA, yellow], quinine [Q, green]), and **C.** the four odor-taste mixtures (isoamyl acetate-sucrose [IA-S, purple], benzaldehyde-sucrose [B-S, peach], benzaldehyde-citric acid [B-CA, light blue], isoamyl acetate-citric acid [IA-CA, light green]). Insets: average action potential waveforms for each neuron. **D–F.** Distribution of the number of chemoselective neurons responding to **D.** water and the three odors, **E.** the four tastes, and **F.** the four odor-taste mixtures. **G–I.** Tuning profiles within each stimulus category show the proportion of chemoselective neurons that did not respond, responded to a single stimulus, or responded to multiple stimuli for **G.** odors, **H.** tastes, and **I.** odor-taste mixtures. *** $p < 0.001$.
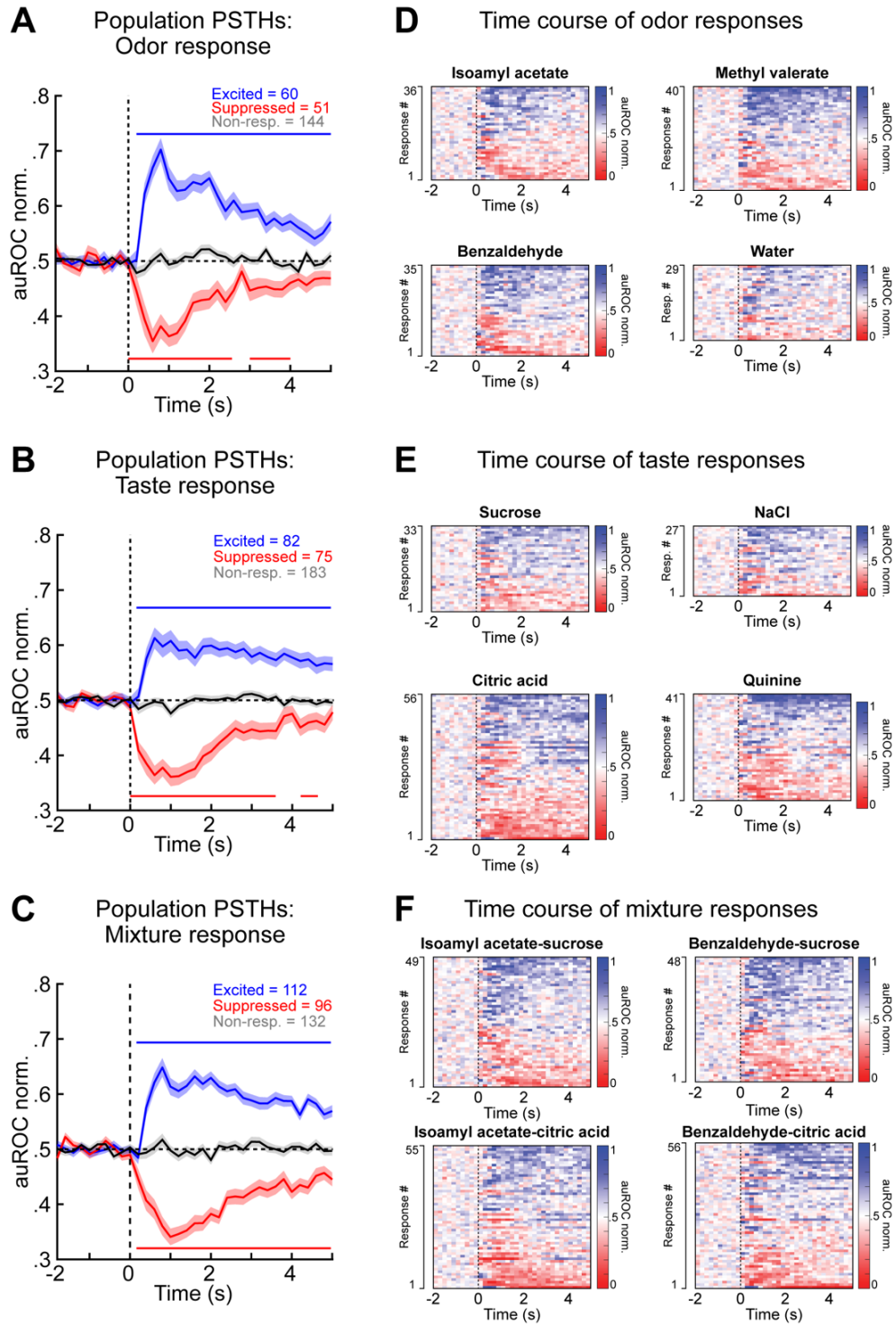
Figure 7. Intraoral chemosensory stimuli evoke excited and suppressed responses. A–C. auROC-normalized population PSTHs of the responses that

showed excited (blue) or suppressed (red) activity or were non-responsive (black) after the presentation of **A.** odors, **B.** tastes, and **C.** odor-taste mixtures. Vertical dashed lines indicate stimulus delivery (time = 0). Horizontal dashed lines indicate baseline. The shaded area represents the SEM. Horizontal lines above (blue) and below (red) traces indicate when responses significantly differed from non-responses (Wilcoxon rank-sum, $p < 0.05$). **D–F,** Pseudo colored heat maps of each significant response to **D.** odors, **E.** tastes, and **F.** odor-taste mixtures plotted in order from the most suppressed (red) to the most excited (blue) response for each stimulus.
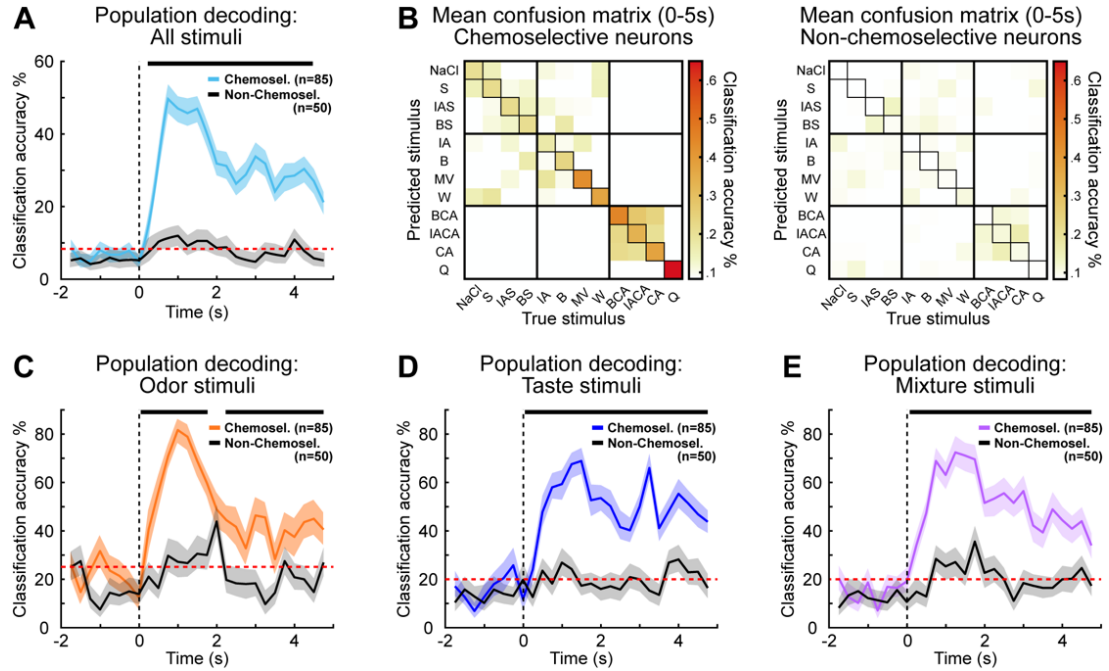
Figure 8. Population decoding of chemosensory signals by neurons in the mediodorsal thalamus. A. The population decoding performance over time by the chemoselective neurons (n = 85) and non-chemoselective neurons (n = 50) for all 12 intraoral stimuli. The red dashed line indicates chance level. The vertical dashed line indicates stimulus delivery (time = 0). The shaded area represents a 99.5% bootstrapped confidence interval. The horizontal black bar above the trace denotes bins when the classification accuracy significantly differed between the two populations (permutation test, $p < 0.05$). **B.** Confusion matrices of the chemoselective (left) and non-chemoselective (right) populations showing the average classification accuracy over the 5 s after stimulus delivery. Colors represent the classification accuracy, with white squares representing performance less than chance (8.3%) and darker hues indicating a greater fraction

of correct trials. The diagonal squares highlight the proportion of trials in which the classifier correctly assigned the predicted stimulus to the true stimulus. **C–E.** The population decoding performance over time by the chemoselective and non-chemoselective populations for the three categories of chemosensory stimuli: **C.** odors, **D.** tastes, and **E.** odor-taste mixtures.
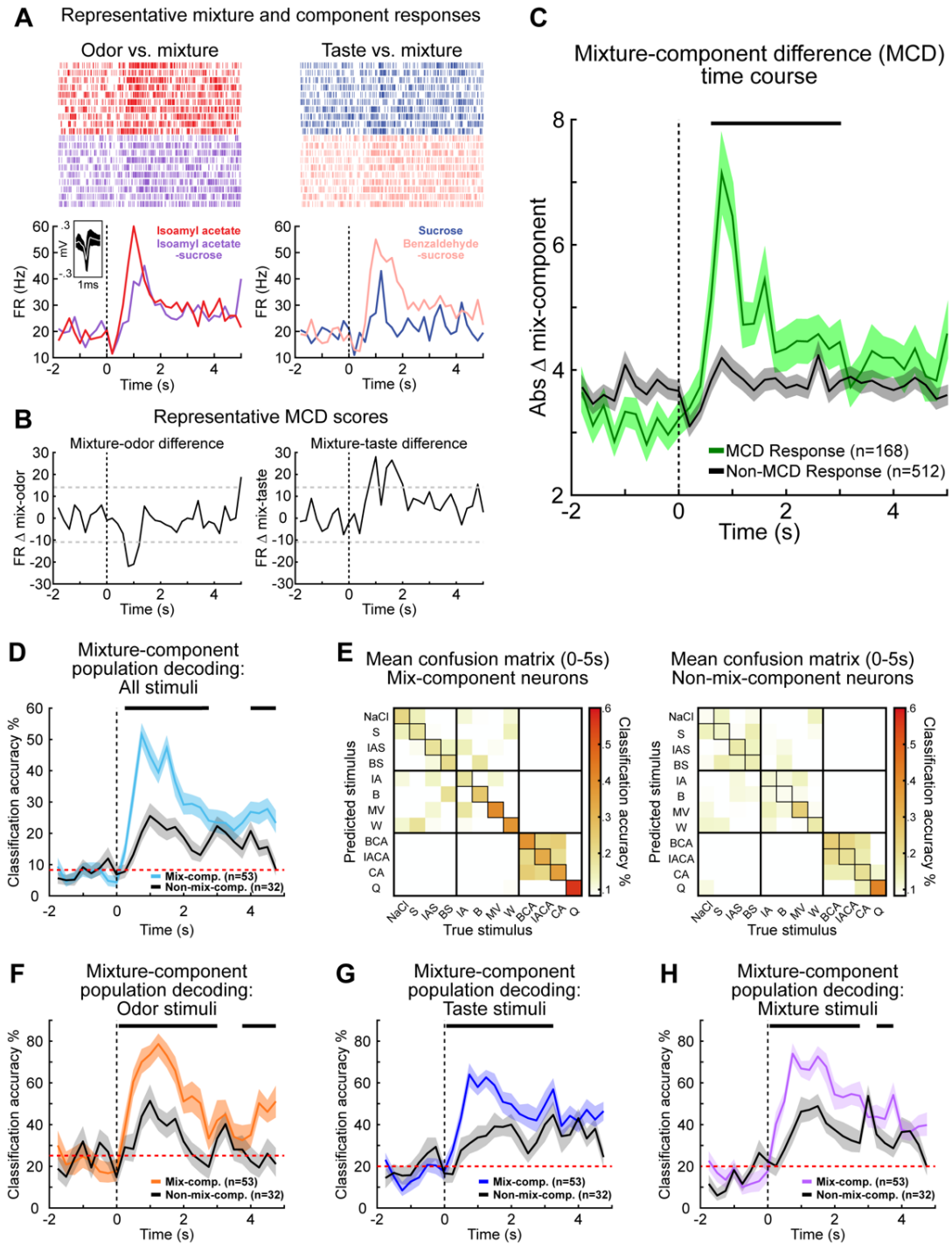
Figure 9. Most chemoselective neurons respond to mixtures differently than their odor or taste component. A. Raster plots and PSTHs from a representative neuron in the mediodorsal thalamus illustrating the differences in activity evoked

by mixtures and their components: isoamyl acetate-sucrose mixture vs. isoamyl acetate alone (left) and benzaldehyde-sucrose mixture and sucrose alone (right). Vertical dashed lines indicate stimulus delivery (time = 0). Inset: the average action potential waveform. **B.** The MCD scores for the responses by the representative neuron. *Left:* The MCD score is the difference between the activity evoked by the mixture of isoamyl acetate-sucrose and the isoamyl acetate alone. *Right:* The MCD score is the difference between the activity evoked by the mixture of benzaldehyde-sucrose and sucrose alone (right). Vertical dashed lines indicate stimulus delivery (time = 0). Grey dashed lines indicate the significance threshold (baseline MCD score ± 6 times the standard deviation). **C.** Time course of the average absolute mixture-component difference (MCD) score for the 168 significant MCD responses (green line) and the 512 non-MCD responses (black line) from 2 s before to 5 s after intraoral delivery (200 ms bins). The significant MCD responses differ from baseline from 0.6–3 s (black bar) after stimulus delivery, and the non-MCD responses never differ from baseline. The shaded area represents the SEM. **D.** The population decoding performance for all 12 intraoral stimuli over time by the ensembles of chemoselective neurons with MCD responses (n = 53) and non-MCD responses (n = 32). The red dashed line indicates chance level. The vertical dashed line indicates stimulus delivery (time = 0). The shaded area represents a 99.5% bootstrapped confidence interval. The horizontal black bar above the trace denotes bins when the classification accuracy significantly differed between the two populations (permutation test, $p < 0.05$). **E.** Confusion matrices of the MCD neurons (left) and non-MCD neurons (right)

showing the average classification accuracy over the 5 s after stimulus delivery. Color is used to represent the classification accuracy, with white squares representing performance less than chance and darker hues indicating a greater fraction of correct trials. The diagonal squares highlight the proportion of trials in which the classifier correctly assigned the predicted stimulus to its true stimulus. **F–H.** The population decoding performance over time by MCD neurons and non-MCD neurons for the three categories of chemosensory stimuli: **F.** odors, **G.** tastes, and **H.** odor-taste mixtures. Note that both populations had decoding performances above chance level (red dashed line) but with different temporal profiles.
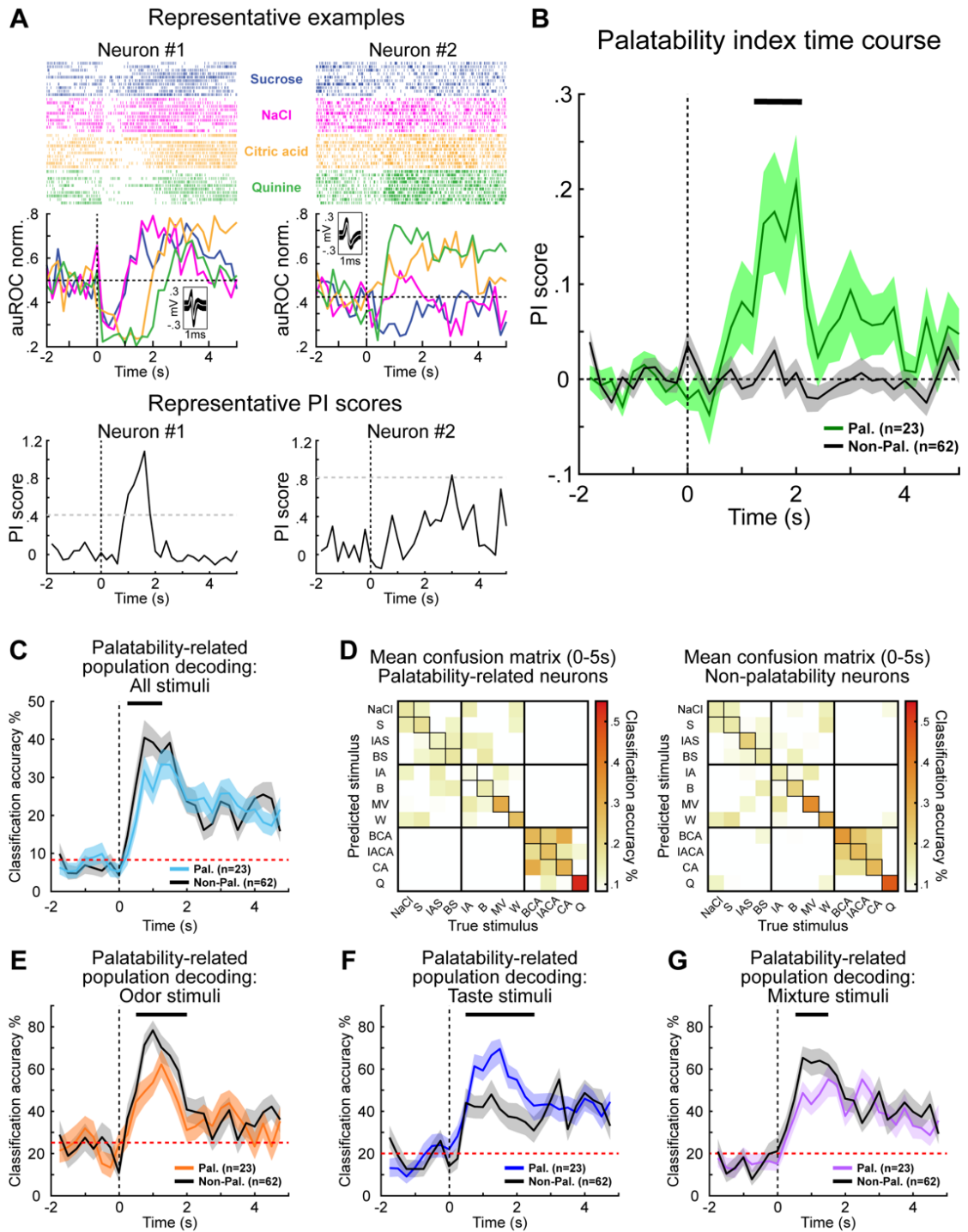
Figure 10. Processing of taste palatability by neurons in the mediodorsal thalamus. A. *Top:* Raster plots and auROC normalized PSTHs from two neurons in the mediodorsal thalamus that represent the palatability-related features of

tastes. Vertical dashed lines indicate stimulus delivery (time = 0). Horizontal dashed lines indicate baseline. Insets: average action potential waveforms for each neuron. *Bottom:* PI scores of the two representative neurons. Grey dashed lines indicate the significance threshold (baseline PI score + 6 times the standard deviation). **B.** Time course of the average palatability index (PI) score of the 23 palatability-related neurons (green line) and 62 non-palatability neurons (black line) 2 s before to 5 s after intraoral delivery (200 ms bins). The response of the palatability-related population significantly differs from baseline from 1.4–2 s (black bar) after stimulus delivery, while the average PI score of the non-palatability population never differs from baseline. The vertical dashed line indicates stimulus delivery (time = 0). The horizontal dashed line indicates baseline. The shaded area represents the SEM. **C.** The population decoding performance for all 12 intraoral stimuli over time by palatability-related (n = 23) and non-palatability-related neurons (n = 62). Note that the decoding performance for the 12 stimuli by the population of non-palatability-related neurons is significantly greater than that of the palatability-related population (black bar; permutation test, $p < 0.05$). The red dashed line indicates chance level. The vertical dashed line indicates stimulus delivery (time = 0). The shaded area represents a 99.5% bootstrapped confidence interval. **D.** Confusion matrices of the palatability-related (left) and non-palatability-related neurons (right) showing the average classification accuracy over the 5 s after stimulus delivery. Colors represent the classification accuracy, with white squares representing performance less than chance and darker hues indicating a greater fraction of correct trials. The diagonal squares highlight the proportion in

which the classifier correctly assigned the predicted stimulus to its true stimulus.

E–G. The population decoding performance over time by the palatability-related and non-palatability-related neurons for the three categories of chemosensory stimuli: **E.** odors, **F.** tastes, and **G.** odor-taste mixtures.
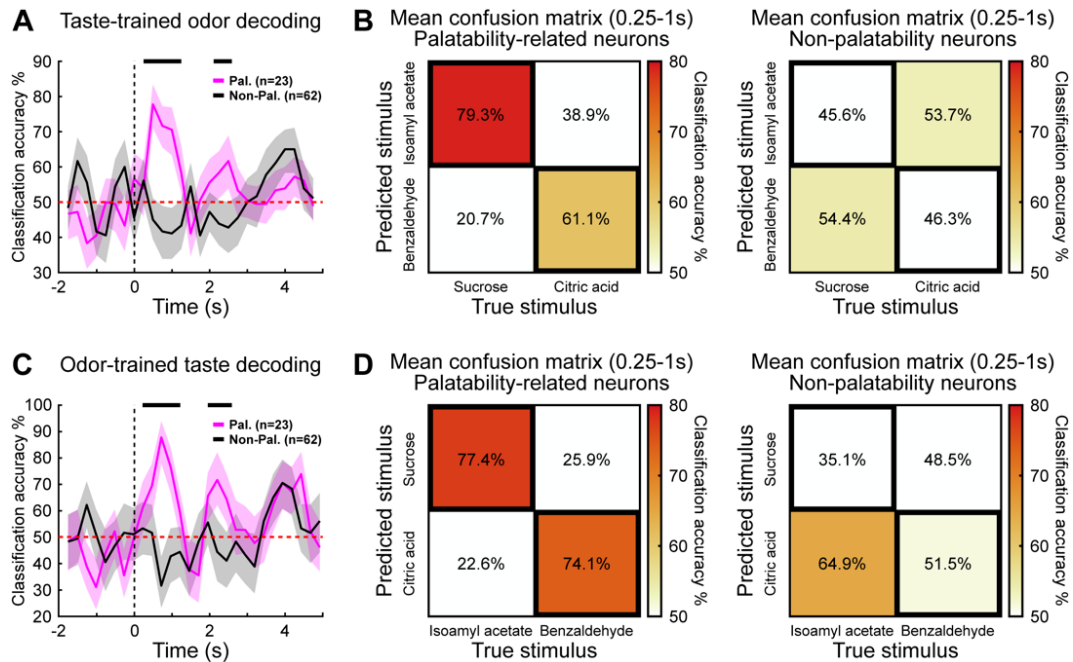
Figure 11. The population activity of palatability-related neurons represents the association between previously experienced odor-taste pairs. A. Population decoding performance over time of the palatability-related (n = 23) and non-palatability-related neurons (n = 62) when responses to sucrose and citric acid were used to train the classifier (true stimulus), but testing it with responses to isoamyl acetate and benzaldehyde (predicted stimulus). The vertical dashed line indicates stimulus delivery (time = 0). The red dashed line indicates chance level performance (50%). The shaded area represents a 99.5% bootstrapped confidence interval. The horizontal black bar above the trace denotes bins in which the classification accuracy significantly differed between the two populations (permutation test, *p* < 0.05). **B.** Confusion matrices showing the average classification accuracy during the initial peak 0.25–1 s after stimulus delivery for

the palatability-related neurons (left) and non-palatability-related neurons (right). Colors represent the classification accuracy, with darker hues indicating a greater fraction of correct trials. The diagonal highlights the proportion of trials in which the classifier correctly assigned the paired odor stimulus (predicted stimulus) to the correct paired taste (true stimulus). **C.** Population decoding performance when responses to isoamyl acetate and benzaldehyde were used to train the classifier (true stimulus), but testing it with responses to sucrose and citric acid (predicted stimulus). **D.** Confusion matrices showing the average classification accuracy during the initial peak 0.25–1 s after stimulus delivery for the palatability-related neurons (left) and non-palatability-related neurons (right). The diagonal highlights the proportion of trials in which the classifier correctly assigned the paired taste (predicted stimulus) to the correct paired odor (true stimulus).

Discussion

The thalamic subnuclei can be divided into two categories based on their functional connections with subcortical and cortical areas. First-order thalamic nuclei primarily process peripheral sensory input from subcortical regions before relaying it to the cortex, while higher-order thalamic nuclei process and communicate information between cortical areas (Sherman, 2016; Nakajima and Halassa, 2017; Halassa and Sherman, 2019). Higher-order thalamic areas, such as the mediodorsal thalamus, are thought to modulate, synchronize, and transmit behaviorally-relevant information between sensory and prefrontal cortical areas (Theyel et al., 2010; Saalmann et al., 2012; Stroh et al., 2013; Mease et al., 2016; Zhou et al., 2016; Schmitt et al., 2017; Rikhye et al., 2018). By sustaining communication across cortical regions, these cortico-thalamo-cortical (i.e., transthalamic) circuits separate potentially overlapping information and enable rapid behavioral changes based on environmental demands (Saalmann, 2014; Sherman, 2016; Rikhye et al., 2018). Given its connectivity, the mediodorsal thalamus may perform a similar function by communicating behaviorally-relevant chemosensory information between prefrontal cortical areas and principal regions of the olfactory and gustatory systems (Price and Slotnick, 1983; Kuroda et al., 1992; Ray and Price, 1992; Shi and Cassell, 1998; Kuramoto et al., 2017; Pelzer et al., 2017). However, a crucial step to understanding its role in chemosensory processing is determining how neurons represent orally-sourced odor, taste, and odor-taste mixture signals. Using tetrode recordings in behaving rats, our results indicate that most mediodorsal thalamus neurons respond broadly across intraoral

stimuli with time-varying multiphasic changes in activity. Furthermore, we demonstrate that the population activity of chemoselective neurons reliably encodes unimodal and multimodal chemosensory signals over time, representing both stimulus identity and stimulus palatability. Altogether, our findings further demonstrate the multidimensionality of the mediodorsal thalamus and provide novel evidence of its involvement in processing chemosensory information important to ingestive behaviors.

As a multimodal region, the mediodorsal thalamus responds to visual, auditory, somatosensory, and olfactory stimuli, but its role in processing gustatory signals is unknown (Yarita et al., 1980; Imamura et al., 1984; Oyoshi et al., 1996; Yang et al., 2006; Courtiol and Wilson, 2016). To our knowledge, the only study to provide evidence of taste-evoked activity in the mediodorsal thalamus showed that neurons responded to sucrose given as a reward for the correct choice in a sensory-discrimination task (Oyoshi et al., 1996). In addition to using only one taste stimulus, the complex nature of the task prevented determining whether responses were somatosensory-, reward-, or taste-dependent. The present results are the first to demonstrate how neurons in the mediodorsal thalamus process the sensory and palatability-related features of tastes. Half of the total population of recorded neurons responded to the intraoral delivery of taste stimuli, with the majority of this chemoselective population responding to multiple taste qualities (i.e., broadly tuned). This population also reflected possible differences between palatable and unpalatable tastes, with a significantly greater proportion of neurons responding to citric acid than to either sucrose or NaCl, but not to quinine.

Many electrophysiological studies of cortical and subcortical regions throughout the gustatory system, including the gustatory thalamus, lateral hypothalamus, basolateral amygdala, central amygdala, gustatory cortex, and prefrontal cortex, have demonstrated that neurons encode taste palatability (Katz et al., 2001; Fontanini et al., 2009; Sadacca et al., 2012; Jezzini et al., 2013; Li et al., 2013; Samuelsen and Fontanini, 2017). Thus, we expected that mediodorsal thalamus neurons would also represent the palatability-related features of tastes. Similar to previous studies, we used a PI analysis to identify neurons that represent taste palatability and examine the temporal evolution of palatability-related activity in the mediodorsal thalamus. More than one-quarter of chemoselective neurons represented taste palatability, with palatability-related information primarily represented 1.2–2 s after stimulus delivery. Population decoding analyses of the 12 intraoral stimuli showed that the neurons representing the palatability-related features of tastes performed significantly worse than the remaining chemoselective population ~0.25–1 s after stimulus delivery. Surprisingly, this deficit in decoding performance was not due to poor taste coding but was likely caused by "confusion" between the components of experienced odor-taste mixtures.

Because odor-taste mixture experience generates associations between the quality and value of an odor and a taste (Fanselow and Birk, 1982; Holder, 1991; Stevenson et al., 1995; Prescott et al., 2004; Gautam and Verhagen, 2010; Green et al., 2012; McQueen et al., 2020), we hypothesized that the deficit in overall decoding performance by the palatability-related population may be due to

similar responses evoked by the components of experienced odor-taste mixtures. When training the classifier with the activity evoked by paired tastes but eliciting predictions using the activity evoked by paired odors (and vice versa), the peak decoding performance of odor-taste pairs occurred simultaneously with the deficit in the overall decoding performance, ~0.25–1 s after stimulus delivery. Although our results are consistent with the subpopulation of neurons that represents taste palatability also representing the relationship between experienced odor-taste pairs, it is possible that the response similarities observed represent an innate relationship between sucrose and isoamyl acetate and between citric acid and benzaldehyde. Future experiments employing a larger battery of odor-taste mixtures would help to elucidate whether mediodorsal thalamus neurons represent associations between experienced odor-taste pairs.

Convergence of chemosensory signals occurs in numerous subcortical and cortical areas (Di Lorenzo and Garcia, 1985; Maier et al., 2012; Escanilla et al., 2015; Maier, 2017; Samuelsen and Fontanini, 2017). These multimodal responses are thought to enhance detectability and discriminability across the network to better represent behaviorally-relevant environmental features (Ohshiro et al., 2011). The population activity of mediodorsal thalamus neurons accurately classified the four odor-taste mixtures, even when they consisted of only two odors and two tastes. Furthermore, the MCD analysis showed that nearly two-thirds of chemoselective neurons responded to an odor-taste mixture differently than at least one of its odor or taste components. This means that one-third of chemoselective neurons responded similarly to odor-taste mixtures and their

components, suggesting that some chemoselective neurons faithfully represent individual odors and tastes even when they are presented as part of an odor-taste mixture. This coding scheme would allow ensembles of neurons in the mediodorsal thalamus to consistently represent unimodal information, while enabling flexibility when responding to multimodal signals. Alternatively, experience itself may be how neurons disambiguate mixtures with overlapping representations of odors and tastes. Future studies using novel odor-taste pairs for every session would allow determination of whether the convergent representation across mixtures is experience-dependent or a summation of olfactory and gustatory signals.

Although identifying the sources of chemosensory input to the mediodorsal thalamus is outside the scope of this study, the temporal dynamics of chemosensory-evoked activity indicate likely sources. The thalamic representation of chemosensory information is rapid and persistent, with responses to the various stimuli mostly overlapping in time. Chemoselective neurons begin to represent the chemical identity of odor-containing stimuli (odors and odor-taste mixtures) ~250 ms after intraoral delivery but take an additional ~250 ms to encode the identity of tastes alone. However, the palatability-related features of tastes are represented by a neuron subpopulation much later, between ~1.2 and 2 s after stimulus delivery. These response dynamics indicate the piriform cortex, gustatory cortex, and basolateral amygdala as likely sources of chemosensory input to the mediodorsal thalamus.

Both chemosensory cortical areas project to the mediodorsal thalamus and represent stimulus identity more quickly, where the piriform cortex encodes odor

101

identity in ~100 ms (Bolding and Franks, 2017) and the gustatory cortex encodes taste identity in ~175–250 ms (Katz et al., 2001; Jezzini et al., 2013; Bouaichi and Vincis, 2020). However, another cortical region with dense reciprocal connections to the mediodorsal thalamus, the medial prefrontal cortex, does not represent taste identity until ~575 ms after intraoral delivery (Jezzini et al., 2013). Therefore, it is unlikely that the medial prefrontal cortex is a source of chemosensory input, but it may represent an important cortical feedback site for chemosensory information to the mediodorsal thalamus. Similar network interactions may be responsible for communicating the palatability-related features of tastes, as both the basolateral amygdala and gustatory cortex form dense reciprocal connections and represent the palatability-related features of tastes faster than the mediodorsal thalamus (Katz et al., 2001; Fontanini et al., 2009; Jezzini et al., 2013; Samuelsen and Fontanini, 2017). Together, the temporal dynamics of chemosensory processing suggest a mechanism whereby the mediodorsal thalamus receives chemosensory information from the piriform cortex, gustatory cortex, and/or basolateral amygdala, while dynamic multiphasic activity arises via recurrent interactions with prefrontal cortical areas. This transthalamic circuit could facilitate large-scale integration of chemosensory information across multiple cortical circuits (Saalmann, 2014). Future studies selectively targeting neuronal populations with cell-specific viral manipulations (e.g., optogenetics) would help to identify the contribution of these regions to chemosensory processing by the mediodorsal thalamus.

In summary, despite its robust connectivity with olfactory and gustatory areas, involvement in olfactory-dependent behaviors, and importance for the perception of flavors, the mediodorsal thalamus remains an understudied area of network processing of chemosensory information. Our results show that mediodorsal thalamus neurons dynamically encode the sensory and palatability-related features of chemosensory signals originating from the mouth. Future studies probing cortico-thalamo-cortical interactions in behaving animals are necessary to determine the contribution of the mediodorsal thalamus to chemosensory-dependent behaviors.

CHAPTER 4

THE ROLE OF THE MEDIODORSAL THALAMUS IN THE CONSUMMATORY

CHOICE OF ODORS, TASTES, AND ODOR-TASTE MIXTURES

Introduction

Experience with flavors (i.e., odor-taste mixtures) is an essential factor

guiding choices of what to eat or drink (i.e., consummatory choice) (Barnett and

Spencer, 1953; Partridge, 1981). Sampling an odor-taste mixture initiates

multisensory processes that generate robust odor-taste associations between the

odor and the taste's quality (i.e., chemical identity) and hedonic value (i.e.,

pleasantness or unpleasantness) (Stevenson et al., 1995; Sakai and Imada, 2003;

Prescott et al., 2004; Gautam and Verhagen, 2010; Green et al., 2012). These

experiences lead to preferences for odors experienced with pleasant tastes, and

the avoidance of odors experienced with unpleasant tastes (Fanselow and Birk,

1982; Holder, 1991; Schul et al., 1996; Sakai and Yamamoto, 2001; Gautam and

Verhagen, 2010; Green et al., 2012; McQueen et al., 2020). Processing odor-taste

associations that guide consummatory choices involves a complex network of

brain areas (Small, 2012; Samuelsen and Vincis, 2021). One such region, the

mediodorsal thalamus, is known to play a crucial role in the perception of odors

and odor-taste mixtures in humans (Rousseaux et al., 1996; Sela et al., 2009; Tham et al., 2011a).

The mediodorsal thalamus is integral to an array of cognitive functions, including working memory (Slotnick and Risser, 1990; Han et al., 2013; Bolkan et al., 2017; Scott et al., 2020), sensory attention (Plailly et al., 2008; Tham et al., 2009, 2011a; Veldhuizen and Small, 2011; Schmitt et al., 2017; Rikhye et al., 2018), and action-outcome associations (Slotnick and Kaneko, 1981; Gaffan and Murray, 1990; Oyoshi et al., 1996; Corbit et al., 2003; Kawagoe et al., 2007; Mitchell, 2015; Courtiol and Wilson, 2016). More specifically, the mediodorsal thalamus is involved in many experience-dependent olfactory behaviors (Courtiol and Wilson, 2015), such as odor attention (Plailly et al., 2008; Tham et al., 2011a; Veldhuizen and Small, 2011), odor discrimination (Eichenbaum et al., 1980; Sapolsky and Eichenbaum, 1980; Staubli et al., 1987; Sela et al., 2009), and odor-reward associations (Oyoshi et al., 1996; Kawagoe et al., 2007; Courtiol and Wilson, 2016). Our recent findings showed that neurons in the mediodorsal thalamus not only represent the sensory and affective properties of individual odors, but also properties of tastes and odor-taste mixtures (Fredericksen and Samuelsen, 2022). A recent study by Scott et al. (2020) found that pharmacological inactivation of the mediodorsal thalamus significantly disrupted working memory for olfactory-dependent foraging. Additionally, psychophysical experiments show that people with lesions of mediodorsal thalamus have an altered hedonic perception of odors and odor-taste mixtures, exhibiting a reduction in consumption (Rousseaux et al., 1996; Asai et al., 2008; Sela et al., 2009). While

evidence suggests the mediodorsal thalamus is involved in processing chemosensory information, its role in consummatory choice is unknown.

To investigate its role in the consummatory choice of experienced odors, tastes, and odor-taste mixtures, we pharmacologically inactivated the mediodorsal thalamus during a 2-bottle brief-access task (Fredericksen et al., 2019; McQueen et al., 2020). Rats were given experience with two odor-taste mixtures: benzaldehyde-saccharin and isoamyl-acetate-stevia. Both saccharin and stevia are noncaloric sweeteners that rats prefer to water, but saccharin is preferred to stevia (Sclafani et al., 2010). Before each 2-bottle brief-access task, the mediodorsal thalamus was bilaterally infused with either saline or pharmacologically inactivated with NBQX disodium salt hydrate (AMPA/kainite glutamate receptor antagonist). We found that inactivating the mediodorsal thalamus eliminated the odor-taste mixture preference, significantly reduced the consumption of the preferred saccharin but did not alter taste preference. Moreover, it significantly increased the within-trial sampling from both bottles. These results suggest that the mediodorsal thalamus plays a critical role in chemosensory preference and attention.

Materials and Methods

Animals. All experimental procedures were performed according to university, state, and federal regulations regarding research animals. Procedures were approved by University of Louisville Institutional Animal Care and Use Committee. Nine female Long-Evans rats (250-350 g; Charles Rivers) were single-housed and maintained on a 12/12-h light-dark cycle with ad libitum access to food and water unless otherwise specified.

Chemosensory stimuli. Chemical stimuli were selected based on their previous use in research involving rats (Aimé et al., 2007; Sclafani et al., 2010; Gautam and Verhagen, 2012; Samuelsen and Fontanini, 2017; Fredericksen et al., 2019; McQueen et al., 2020; Fredericksen and Samuelsen, 2022). At the concentrations used here, the non-caloric sweeteners 0.1% saccharin sodium salt hydrate (Sigma-Aldrich, S1002) and 0.1% stevia (Stevia Canada) are preferred to water, but saccharin is preferred to stevia (Sclafani et al., 2010). At the concentrations used here, the odorants 0.01% isoamyl acetate and 0.01% benzaldehyde (Sigma-Aldrich) are tasteless (Aimé et al., 2007; Gautam and Verhagen, 2010; Samuelsen and Fontanini, 2017). All stimuli were prepared with distilled water.

The 2-bottle brief-access task. All experiments were completed using a computer-controlled 2-bottle brief-access apparatus directed by custom-written LabVIEW scripts (National Instruments, Austin, TX) (Fredericksen et al., 2019; McQueen et

107

al., 2020). The apparatus consists of a testing chamber, two motorized port doors allowing stimulus port access, and a motorized stage for stimulus bottle positioning at the two ports. A session began with the opening of the motorized port doors allowing access to two sipper tubes. Once opened, the rats had approximately 20 seconds to engage in a trial by licking either bottle. If a bottle was contacted, the port doors remained open for approximately 20 seconds. Only the first 15 seconds of sampling was analyzed to ensure consistency across trials and comparability to previous studies (McQueen et al., 2020). The large sampling window afforded time for switching between ports within a trial. Licks were recorded using a grounded circuit. To ensure that only tongue contacts were recorded as licks, we removed artifacts that occurred faster than 10 Hz (faster than the lick rate of a rat) (Lin et al., 2013) and licks that occurred simultaneously on both ports. The rat had to lick a spout at least 3 times to qualify as an engaged trial. If no contact was made during the contact window, the port doors would close, and a new trial would begin. At the completion of the trial, the doors closed and a 30 second intertrial interval began. Bottles were counterbalanced and chemosensory stimuli were presented 10 times at each port for a total of 20 trials. This paradigm gives rats a limited amount of time in a fixed number of trials to drink from two simultaneously presented bottles containing different chemosensory stimuli. Rats were water regulated during training and experimental days, receiving a maximum of 30 ml per day, or 20 ml in addition to the liquid consumed during the 2-bottle brief-access task.

Data are presented as the number of total licks, licks per engaged trial, number of engaged trials, initiation time, number of switches, proportion of switched trials, preference ratio, and absolute change in preference ratio. Preference ratio was calculated as (S1 − S2) / (S1 + S2), where S1 is the total number of licks for bottles containing stimulus 1, and S2 is the total number of licks for bottles containing stimulus 2. Thus, a positive preference ratio indicates a preference for stimulus 1, and a negative preference ratio indicates a preference for stimulus 2. The absolute change in preference ratio was calculated as the absolute difference between the preference ratio during the Saline and NBQX conditions.

Pre-surgery 2-bottle brief-access task training. Rats were placed on a water regulation regime and trained to drink water during a 2-bottle brief-access task. For the first three days, rats were habituated to the 2-bottle brief-access apparatus for two minutes before being presented with the choice of drinking distilled water from either port during 10 trials. After each session, rats were given a maximum of 20 ml of distilled water in their home cage overnight. Following this initial training, rats were given ad libitum access to water for four days before beginning the chemosensory experience and behavioral training protocol (Fig. 12). First, rats were water restricted for three days receiving a maximum of 30 ml distilled water access in their home cage each day. To reduce the impact of neophobia (Barnett, 1958; Corey, 1978; Demattè et al., 2014), rats were given their primary experience with chemosensory stimuli in the homecage the day immediately prior to receiving

109

it in the 2-bottle brief-access apparatus (Fig. 12A). Each 2-bottle brief-access session consisted of 20 trials. After each session, rats received one-hour access in their home cage to bottles of chemosensory stimuli or water. After the final chemosensory experience session, rats returned to *ad libitum* water in preparation for surgery.

Bilateral cannula implantation surgery. Rats were anesthetized with isoflurane (induction: 5%, maintenance: 2-5%). Animals were secured in a stereotaxic device (KOPF) and given subcutaneous injections of atropine sulfate (0.03 mg/kg), dexamethasone (0.2 mg/kg), and the analgesic buprenorphine HCl (0.03 mg/kg). The scalp was shaved, sterilized with 70% ethanol and povidone-iodine solution, and excised to reveal the skull. Small craniotomies were made to secure five anchoring screws (SMPPS0002, Micro Fasteners) into the skull. Two additional craniotomies were made for the placement of 26 ga guide cannulas (7 mm, Plastics One, Protech International, Inc.) into the mediodorsal thalamus (coordinates: 10° angle, AP: -3.3 mm, ML: ± 1.80 mm from bregma, DV: -5.20 mm from dura). Guide cannulas were implanted at a 10-degree angle to avoid the superior sagittal sinus and cemented to the skull with dental acrylic. Dummy stylets (7 mm, Plastics One, Protech International, Inc.) were inserted into the guide cannulas. A head-restraint bolt was attached posteriorly to the guide cannulas to allow for head-restraint. Rats were allowed a recovery period of 7-13 days before behavioral training resumed.

Post-surgery head-restraint and 2-bottle brief-access training. Rats were placed on a water regulation schedule where they received access to 30 ml of water each day in their home cage for three days. To prepare them for the pharmacological inactivation experiment, rats underwent six days of head-restraint training without infusion. During each session, rats were head restrained for 4 minutes, placed in the 2-bottle brief-access apparatus, and allowed 2 minutes to habituate before beginning a 20-trial 2-bottle brief-access task. Stimuli provided during the six head-restraint training sessions consisted of water on day 1, odor-taste mixtures on days 2-4, odors on day 5, and tastes on day 6 (Fig. 12B). After each session, rats were given 20 ml of water in their home-cage. Following the final head-restraint training session, rats received access to 30 ml of distilled water in in their home cage for three days before beginning the twelve-day pharmacological inactivation experiment (Fig. 12C).

Pharmacological inactivation of the mediodorsal thalamus during 2-bottle brief-access task. Rats underwent the same procedure prior to each 2-bottle brief-access behavioral session. Rats were head-restrained, the dummy stylets were removed, and 33 ga injection cannulas (7 mm, Plastics One, Protech International, Inc.) were inserted through guide cannula into the mediodorsal thalamus. The injection cannulas were attached to polyethylene (PE)-50 tubing (A-M Systems) attached to 10 μl Hamilton syringes backfilled with mineral oil in a dual syringe pump (Pump 11 Elite, Harvard Apparatus). The syringe pump was used to infuse 400 nl of sterile saline or 400 nl of NBQX disodium salt hydrate (Sigma-Aldrich,

N183-5MG) at a rate of 200 nl/minute. Two additional minutes were allotted for diffusion of the fluid into the brain before the removal of the injection cannulas and replacement of the dummy stylets. The rats were removed from the head-restraint box and placed in the test chamber of the 2-bottle brief-access apparatus. Rats were given a further two minutes to acclimate to the test chamber before starting the 2-bottle brief-access task. The four chemosensory choice tasks were consistent across the three consecutive infusion conditions: Day-1) water vs. water, Day-2) benzaldehyde-saccharin vs. isoamyl acetate-stevia, Day-3) benzaldehyde vs. isoamyl acetate, and Day-4) saccharin vs. stevia (Fig. 12C). Saline was infused into the mediodorsal thalamus for the first 4 chemosensory choice task sessions (Saline-1), followed by 4 days of NBQX inactivation of the mediodorsal thalamus during the 4 chemosensory choice task sessions (NBQX). The second round of saline infusion sessions (Saline-2) were performed to examine whether consummatory behaviors were impacted by the previous NBQX sessions or the repeated experience in the 2-bottle brief-access task. One rat was unable to complete the second saline sessions due to a head-cap failure.

Histology. After completing the pharmacological inactivation experiment, rats were anesthetized with a mixture of ketamine, xylazine, and acepromazine (100, 5.2, and 1 mg/kg) and 400 nl of biotinylated dextran amine (BDA; Invitrogen, D1956) was bilaterally infused (200 nl/minute) into the mediodorsal thalamus. Two additional minutes were allotted for diffusion of the fluid into the brain before removing the injection cannulas. Rats were then transcardially perfused with cold

0.1 M phosphate buffer solution (PBS) and cold 4% paraformaldehyde. Brains were removed, post-fixed for 24 hours, cryoprotected in 30% sucrose, and cut into 70 μm thick sections. Sections were washed three times (10 minutes) in PBS before being incubated in 1:100 Alexa Fluor488-conjugated streptavidin (Invitrogen, S11223) in PBS with 0.2% Triton X-100 for 2 hours in the dark. Next, sections were washed in a PBS and 0.2% Triton X-100 solution for 10 minutes, then washed twice (10 minutes) in PBS, followed by three washes (10 minutes) in 0.1M PB. Sections incubated for 30 minutes in solution 0.1 M PB with DAPI (Invitrogen, D1306). Finally, sections were washed three times (10 minutes) with 0.1 M PB and mounted with Fluormount-G medium (SouthernBiotech). Only animals with cannula placement within the mediodorsal thalamus were included in the study (Fig. 13).

Data analysis. All statistical analyses were performed using GraphPad Prism (GraphPad Software, Inc.). Repeated-measures comparisons across control conditions (i.e., non-infusion, Saline-1, and Saline-2) were performed using a mixed-effects model analysis because one rat did not complete the Saline-2 condition due to a head-cap failure. Overall comparisons between infusion conditions (i.e., Saline and NBQX) were tested with a 2-tailed paired *t*-test. Two-way repeated-measures analysis of variance (ANOVA) were used to test the effects of infusion condition and stimulus category on the number of total licks, licks per engaged trial, number of engaged trials, initiation time, number of switches, and preference ratios. Kruskal–Wallis tests were used to compare the

absolute change in preference ratio between stimulus category. *Post hoc* analyses were performed using Tukey's HSD tests to correct for familywise error. χ^2 tests (*p* < 0.05) were used to compare the overall proportion of switched trials between infusion conditions. Fisher's exact tests with Dunn–Sidak correction for familywise errors were used to compare the proportion of switched trials within each stimulus category.

Results

Electrophysiological recordings in behaving rats have shown that neurons in the mediodorsal thalamus represent the sensory and affective properties of individual odors, tastes, and odor-taste mixtures (Fredericksen and Samuelsen, 2022). It is also known that people with lesions of the mediodorsal thalamus have an altered hedonic perception of odors and odor-taste mixtures, exhibiting a reduction in consumption (Rousseaux et al., 1996; Asai et al., 2008; Sela et al., 2009). However, it is unclear what role the mediodorsal thalamus plays in consummatory choices between experienced odors, tastes, and odor-taste mixtures. To this aim, we pharmacologically inactivated the mediodorsal thalamus during a 2-bottle brief-access task to investigate the area's role in the consummatory choice of odors, tastes, and odor-taste mixtures. Figure 12 shows the behavioral paradigm schedule. First, rats were given experience with odors, tastes, and odor-taste mixtures and trained to drink from the 2-bottle brief-access apparatus (Figure 12A). Following surgical implantation of guide cannulas into the mediodorsal thalamus, rats underwent head-restraint training without infusion while being retrained in the 2-bottle brief-access task (Figure 12B). The pharmacological inactivation experiment consisted of twelve sessions divided into three infusion conditions (Figure 12C). The choices between chemosensory stimuli in the 2-bottle brief-access task was consistent for each 4-day condition. The first day was water vs. water, the second day was benzaldehyde-saccharin vs. isoamyl acetate-stevia, the third day was isoamyl acetate vs. benzaldehyde, and the fourth day was saccharin vs. stevia. The first 4-day condition consisted of head-restraint

115

with infusion of saline (i.e., Saline-1), the second 4-day condition was head-restraint with infusion of NBQX disodium salt hydrate (i.e., NBQX), and the third 4-day condition was head-restraint with infusion of saline (i.e., Saline-2). Figure 13 shows a representative example of the bilateral infusion area in the mediodorsal thalamus.

Infusion of saline did not significantly impact consummatory behavior

After surgical implantation of cannulas, rats were trained to sit calmly in a head-restrained position without infusion (non-infusion condition) for 4 minutes and then placed in the 2-bottle brief-access apparatus to perform a preference task. This training procedure ensured rats were accustomed to head-restraint before beginning the experiment protocol. The saline sessions before (Saline-1 condition) and after (Saline-2 condition) the NBQX sessions enabled us to investigate whether infusion of NBQX affected preferences and whether a greater amount of experience in the 2-bottle brief-access task influenced consummatory choices. We specifically examined whether there were any significant differences in total licks, licks per engaged trial, and number of engaged trials across the non-infusion, Saline-1, and Saline-2 conditions.

Repeated-measures comparisons across non-infusion, Saline-1, and Saline-2 conditions were performed using a mixed-effects model analyses because one rat was unable to complete the Saline-2 condition due to a head-cap failure. We found no significant differences in the total licks across the three conditions for odor-taste mixture [$F_{(2,15)} = 0.5604$, $p = 0.5825$], odor [$F_{(2,15)} =$

0.9868, p = 0.3957], or taste sessions [F (2,15) = 0.1013, p = 0.9042]. Next, we performed two-way repeated measures mixed-effects analyses to examine the effects of condition on licks per engaged trial within each stimulus category. For odor-taste mixtures, there was no effect of condition [F (2,16) = 1.946, p = 0.1752] and no interaction [F (2, 14) = 0.7592, p = 0.759], but there was a main effect of odor-taste mixture [F (1,8) = 19.03, p = 0.0024]. For odors, there was no main effect of condition [F (2,16) = 0.6494, p = 0.5356], odor stimuli [F (1,8) = 2.961, p = 0.1236], and no interaction [F (2, 14) = 0.609, p = 0.558]. For tastes, there was no main effect of condition [F (2,16) = 0.04935, p = 0.9520] and no interaction [F (2, 14) = 0.844, p = 0.451], but there was a main effect of taste stimuli [F (1,8) = 17.45, p = 0.0031]. We also examined whether task engagement was consistent across these three conditions. A mixed-effects model analysis revealed that the total number of engaged trials was similar across conditions and found no significant differences for odor-taste mixture [F (2,15) = 0.6952, p = 0.5144], odor [F (2,15) = 0.9555, p = 0.4068], or taste sessions [F (2,15) = 0.4969, p = 0.6181].

These results indicate that the different control conditions did not alter consummatory behaviors. In fact, the only significant effects were dependent upon stimulus category, which reflect differences in preference between the chemosensory stimuli. Importantly the consistency across conditions indicates that neither the infusion of saline into the mediodorsal thalamus, nor the greater amount of experience in the 2-bottle brief-access task significantly affected consummatory behaviors. Therefore, the results of the two saline infusion conditions were averaged (i.e., Saline) for further analyses.

***Inactivation of the mediodorsal thalamus with NBQX impacts consummatory
behavior***

To determine the role of the mediodorsal thalamus in guiding
consummatory choice, we pharmacologically inactivated the mediodorsal
thalamus with infusion of NBQX during the choice between chemosensory stimuli
in a 2-bottle brief-access task. We hypothesized that, compared to the Saline
condition, there would be significant decreases in consumption and engagement
during the inactivation of the mediodorsal thalamus because of its known
involvement in processing the hedonic value of odors and odor-taste mixtures
(Rousseaux et al., 1996; Asai et al., 2008; Sela et al., 2009; Tham et al., 2011a)
and its role in olfactory attention (Plailly et al., 2008; Tham et al., 2009, 2011a;
Veldhuizen and Small, 2011; Schmitt et al., 2017; Rikhye et al., 2018). First, we
compared the total licks between Saline and NBQX infusion conditions and found
that rats performed significantly fewer licks during the NBQX condition than the
Saline condition (Saline: 1003.15 ± 87.69 vs. NBQX: 823.06 ± 119.94, $t_{(8)}$ = 3.054,
p = 0.0157) (Fig. 14A). Next, we used a two-way repeated-measures ANOVA to
determine whether the number of total licks differed between the infusion
conditions during the four 2-bottle brief-access sessions (i.e., water, odor-taste
mixtures, odors, or tastes) (Fig. 14B). There were significant main effects of
infusion condition [F (1,8) = 9.325, p = 0.0157] and stimulus category [F (3,24) =
12.25, p < 0.0001], but no significant interaction [F (3,24) = 1.837, p = 0.1674]. A
Tukey's HSD test of multiple comparison revealed a significant difference in the

total licks between infusion conditions for tastes (Saline: 1288.39 ± 101.67 vs. NBQX: 904.22 ± 150.32, p = 0.032), but not water (Saline: 776.0 ± 100.33 vs. NBQX: 726.0 ± 170.92), odor-taste mixtures (Saline: 1065.78 ± 97.11 vs. NBQX: 969.44 ± 122.82), or odors (Saline: 882.44 ± 98.92 vs. NBQX: 969.44 ± 122.82). Contrary to our expectations, these data indicate that inactivation of the mediodorsal thalamus led to a significant decrease in the sampling of taste stimuli, while having little impact on the overall consumption of water, odor-taste mixtures, or odors.

To better understand how inactivation of the mediodorsal thalamus influenced the consummatory choice between chemosensory stimuli, we performed two-way repeated measures analyses examining the effects of infusion condition on licks per engaged trial within each stimulus category (Fig. 15). For the choice between odor-taste mixtures, there was a significant main effect for infusion condition [F (1,8) = 7.905, p = 0.0228] and between benzaldehyde-saccharin and isoamyl acetate-stevia [F (1,8) = 9.889, p = 0.0137], but no significant interaction [F (1,8) = 0.1912, p = 0.6735]. A Tukey's HSD *post hoc* analyses showed that during the Saline condition, rats sampled significantly more benzaldehyde-saccharin than isoamyl acetate-stevia (41.43 ± 2.06 vs. 24.94 ± 2.60, p = 0.044). However, there was no difference between the two odor-taste mixtures during the NBQX condition (33.09 ± 5.77 vs. 19.69 ± 2.59) (Fig. 15A). For the odors, there was a significant main effect between infusion condition [F (1,8) = 11.10, p = 0.0104], but no effect between benzaldehyde and isoamyl acetate [F (1,8) = 1.546, p = 0.2489] and no significant interaction [F (1,8) = 0.9674, p = 0.3541] (Fig. 15B).

For tastes, there were significant main effects of infusion condition [$F_{(1,8)}$ = 28.90, p = 0.0007] and between saccharin and stevia [$F_{(1,8)}$ = 6.995, p = 0.0295], but no interaction [$F_{(1,8)}$ = 2.222, p = 0.1744] (Fig. 15C). *Post hoc* analysis revealed that rats sampled significantly more saccharin than stevia during both the Saline (45.03 ± 3.27 vs. 28.40 ± 2.91, p = 0.002) and NBQX conditions (30.45 ± 4.84 vs. 20.02 ± 2.96, p = 0.031). However, rats sampled significantly less saccharin during the NBQX condition compared to the Saline condition (p = 0.005) (Fig. 15C). These data show that rats preferred to consume saccharin-containing over stevia-containing stimuli during the Saline condition. During inactivation of the mediodorsal thalamus, rats no longer preferred to sample benzaldehyde-saccharin to isoamyl acetate-stevia and significantly reduced their consumption of the preferred saccharin taste.

Next, we examined the impact of mediodorsal thalamus inactivation on stimulus preference (Fig. 16). A preference ratio indicates which of the 2 stimuli were sampled more during each 2-bottle choice; a positive ratio indicates a preference for stimuli containing benzaldehyde-saccharin or its components, and a negative ratio indicates a preference for stimuli containing isoamyl acetate-stevia or its components. There was no difference in the mean preference ratios between infusion conditions for any of the stimulus categories (Fig. 16A-C). However, visual inspection of the individual preference ratios indicated that some scores greatly changed between conditions. Therefore, we calculated the absolute difference in preference ratio between infusion conditions for each stimulus category (Fig. 16D). This measures the change in the preference ratio when the mediodorsal thalamus

was inactivated. The results of a Kruskal–Wallis test revealed a significant difference between the three stimulus categories (H (2) = 7.27, p = 0.0264). A Tukey's HSD test for multiple comparisons showed that the absolute change in preference ratio was significantly smaller for taste stimuli (0.12 ± 0.03) compared to odors (0.40 ± 0.11, p = 0.027), but not odor-taste mixtures (0.32 ± 0.07, p = 0.122) (Fig. 16D). These results indicate that the taste preference remained consistent during inactivation of NBQX.

Since the mediodorsal thalamus is known to be involved in olfactory attention (Plailly et al., 2008; Tham et al., 2011a; Veldhuizen and Small, 2011), it is possible that the reduced sampling during the NBQX condition is related to a decrease in task engagement. One measure of task engagement is the number of trials in which the rat chooses to engage. A two-way repeated measures ANOVA verified that there was no significant main effect between Saline and NBQX infusion conditions [F (1,8) = 0.8149, p = 0.3930] or interaction [F (3,24) = 1.935, p = 0.1509], but there was a main effect between stimulus categories [F (3,24) = 4.927, p = 0.0083]. However, a Tukey's HSD analyses found no significant difference in the number of engaged trials between conditions for any stimulus category (Fig. 17A). These findings indicate that the rats consistently participated in the 2-bottle brief-access task regardless of infusion condition or chemosensory choice. However, inactivation of the mediodorsal thalamus could have impacted the motivation or ability to initiate a trial. As an alternative assessment of task engagement, we measured the time it took to engage in a trial by determining the duration until the first spout contact (i.e., initiation time) (Fig. 17B). The results of

a two-way repeated-measures ANOVA showed no significant main effect of infusion condition [$F_{(1,8)}$ = 0.007894, p = 0.9314] or interaction [$F_{(3,24)}$ = 0.4474, p = 0.7214]. However, there was a significant main effect of initiation time for chemosensory stimulus category [$F_{(3,24)}$ = 5.636, p = 0.0045]. A Tukey's HSD *post hoc* test showed that in the Saline condition, trials were initiated more quickly for the taste stimuli (1.18 ± 0.11) compared to water (2.32 ± 0.50, p = 0.019) and odors (2.31 ± 0.29, p = 0.019), but not odor-taste mixtures (1.70 ± 0.29, p = 0.681). There were no significant differences between infusion conditions for any chemosensory category, indicating that the inactivation of the mediodorsal thalamus did not alter the rat's motivation or ability to initiate trials.

Our results show that rats initiated and engaged in a similar number of trials regardless of infusion condition but consumed significantly less during the inactivation of the mediodorsal thalamus. One possibility is that increased switching between ports within each 15 second trial window reduced the amount of time rats could sample from the spouts. First, we compared the total number of switches between Saline and NBQX infusion conditions and found that rats switched between the two ports significantly more during the NBQX condition (Saline: 6.07 ± 1.95 vs. NBQX: 16.47 ± 5.30, $t_{(8)}$ = 2.769, p = 0.0243) (Fig. 18A). Next, we used a two-way repeated-measures ANOVA to determine whether the number of switches differed between the infusion conditions during the 2-bottle brief-access sessions (Fig. 18B). There was a significant main effect of infusion condition [$F_{(1,8)}$ = 7.666, p = 0.0243] and a significant interaction between condition and stimulus category [$F_{(3,24)}$ = 3.772, p = 0.0238], but no main effect

122

of stimulus category [F (3,24) = 1.571, p = 0.2222]. A Tukey's HSD test revealed that rats switched between bottles significantly more often during the NBQX condition for odor-taste mixtures (Saline: 5.78 ± 2.09 vs. NBQX: 16.22 ± 6.06, p = 0.002), odors (Saline: 6.28 ± 2.19 vs. NBQX: 20.00 ± 5.93, p < 0.001), and tastes (Saline: 4.55 ± 1.69 vs. NBQX: 17.56 ± 5.62, p < 0.001), but not for water (Saline: 7.67 ± 2.28 vs. NBQX: 12.11 ± 4.55). Interestingly, this identifies that increased switching between ports is a chemosensory specific behavior that is impacted by inactivation of the mediodorsal thalamus.

Next, we examined whether the behavior of increased in switching between ports observed in the NBQX condition was widespread across trials by determining the proportion of engaged trials that rats sampled from both ports (Fig. 18C). A χ^2 test revealed a significant difference between infusion conditions in the proportion of trials rats switched between ports (Saline: 28.2% vs. NBQX: 56.7%, χ^2= 144.7, p < 0.001). *Post hoc* analyses showed that the proportion of switched trials was significantly higher during NBQX than Saline condition for water (Saline: 33.1% vs. NBQX: 51.1%, Fisher's exact test, p < 0.001), odor-taste mixtures (Saline: 26.9% vs. NBQX: 52.5%, Fisher's exact test, p < 0.001), odors (Saline: 31.6% vs. NBQX: 62.6%, Fisher's exact test, p < 0.001), and tastes (Saline: 22.2% vs. NBQX: 60.3%, Fisher's exact test, p < 0.001). These results indicate that inactivating the mediodorsal thalamus led to rats switching between ports during a greater proportion of trials regardless of the choice of chemosensory stimuli.
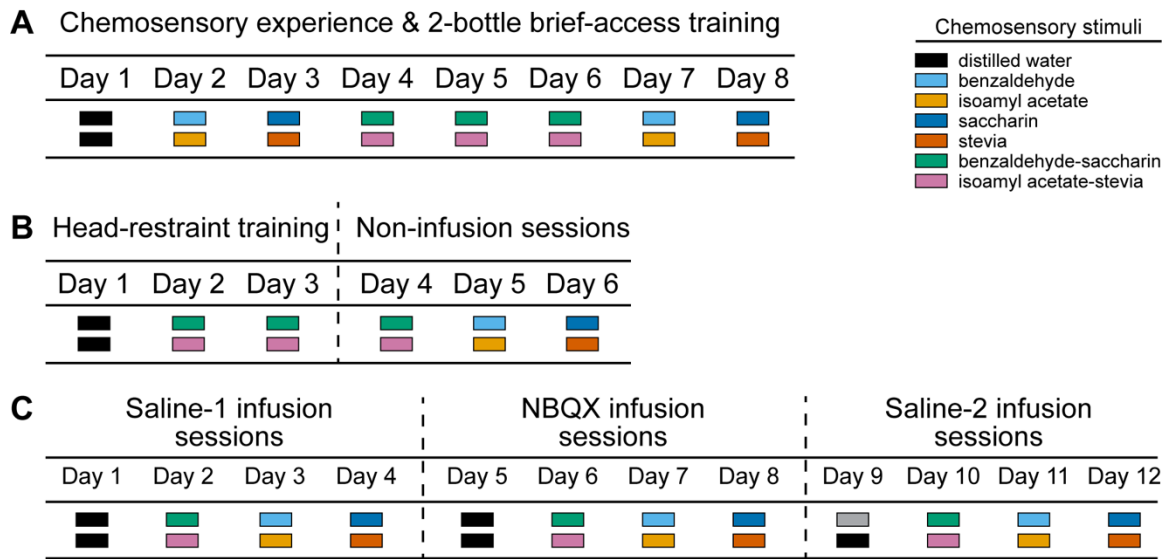
Figure 12. Schematic outline of training and experimental sessions. A. Rats were given 1-hour home-cage access to the two odors, two tastes, or the two odor-taste mixtures the day before the stimuli were presented in the 2-bottle brief-access task. Rats chose between two lick ports of water on day 1, experienced benzaldehyde-saccharin and isoamyl acetate-stevia odor-taste mixtures on days 4-6, experienced benzaldehyde and isoamyl acetate odors on days 2 and 7, experienced saccharin and stevia tastes on days 3 and 8. **B.** Rats were trained to be head-restrained for four minutes before the 2-bottle brief-access task. Rats chose between two lick ports of water on day 1, odor-taste mixtures on days 2-4, odors on day 5, days tastes on day 6. **C.** Rats were head-restrained and the mediodorsal thalamus was infused with saline on days 1-4 (Saline-1 condition) and days 9-12 (Saline-2 condition), and NBQX on days 5-8 (NBQX condition). Rats

chose between two lick ports of water on days 1, 5, and 9, odor-taste mixtures on days 2, 6, and 10, odors on days 3, 7, and 11, and tastes on days 4, 8, and 12.
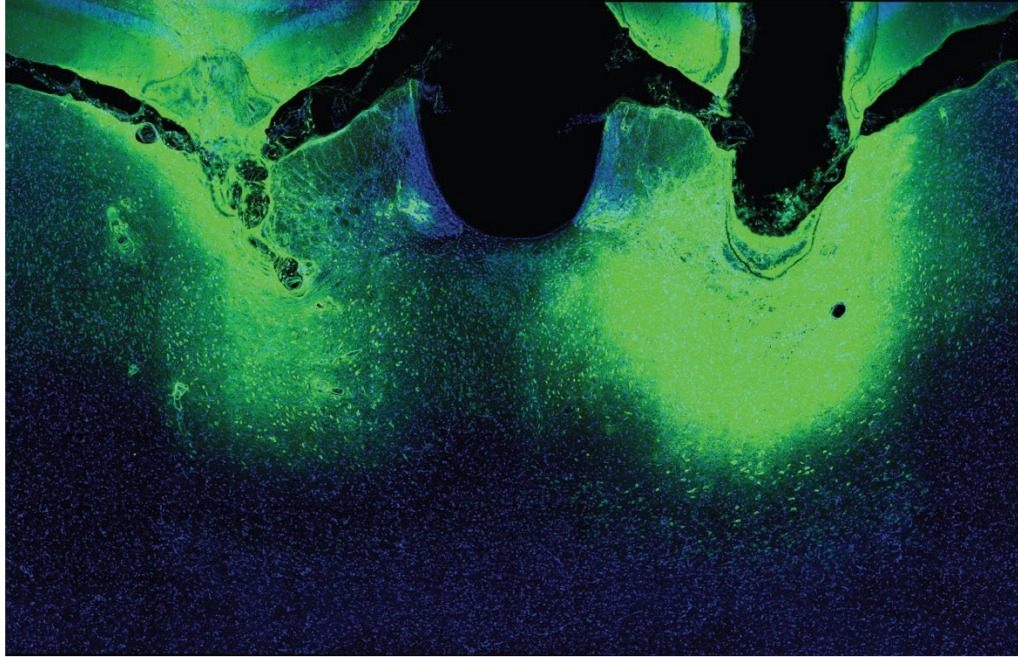
Figure 13. Representative image of targeted infusion in the mediodorsal thalamus. Prior to perfusion, biotinylated dextran amine (BDA, green) was bilaterally infused into the mediodorsal thalamus to estimate the spread of saline and NBQX infusions. Sections were stained with DAPI (blue). Only rats with cannula placement within the mediodorsal thalamus were included in the study.
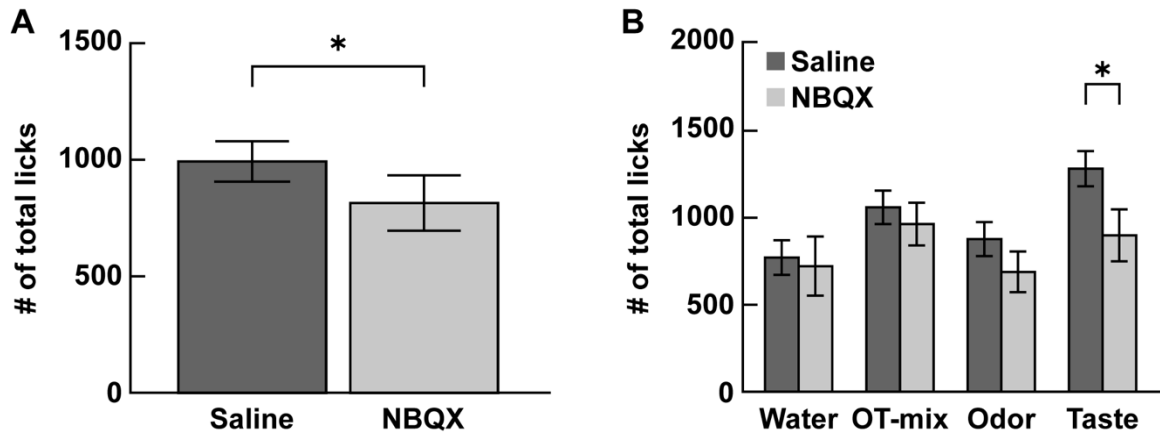
Figure 14. Inactivation of the mediodorsal thalamus reduces overall consumption. A. Rats performed significantly fewer licks (± SEM) overall during the NBQX condition (dark grey bars) than the Saline condition (light grey bars). **B.** During the NBQX condition, rats performed significantly fewer licks for tastes, but not for water, odor-taste mixtures, or odors. *$p < 0.05$.
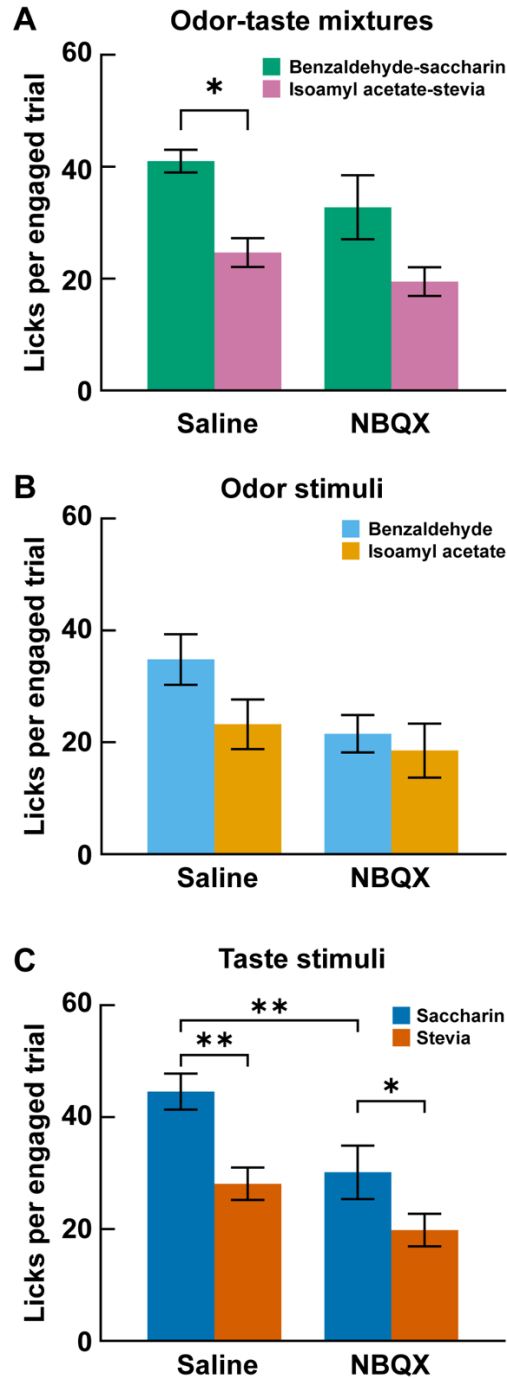
Figure 15. Mediodorsal thalamus inactivation alters consummatory behaviors. A. Rats performed significantly more licks per engaged trial (± SEM) of benzaldehyde-saccharin (green bars) than isoamyl acetate-stevia (pink bars)

during the Saline condition, but showed no preference for sampling either odor-taste mixture during the NBQX condition. **B.** Rats performed equal licks per engaged trial for benzaldehyde (cyan bars) and isoamyl acetate (yellow bars) odors during both Saline and NBQX conditions. **C.** Rats performed significantly more licks per engaged trial of saccharin (dark blue bars) than stevia (orange bars) taste during both Saline and NBQX conditions. Rats performed significantly fewer licks per engaged trial for saccharin during the NBQX condition than during the Saline condition. **$p < 0.01$. *$p < 0.05$.
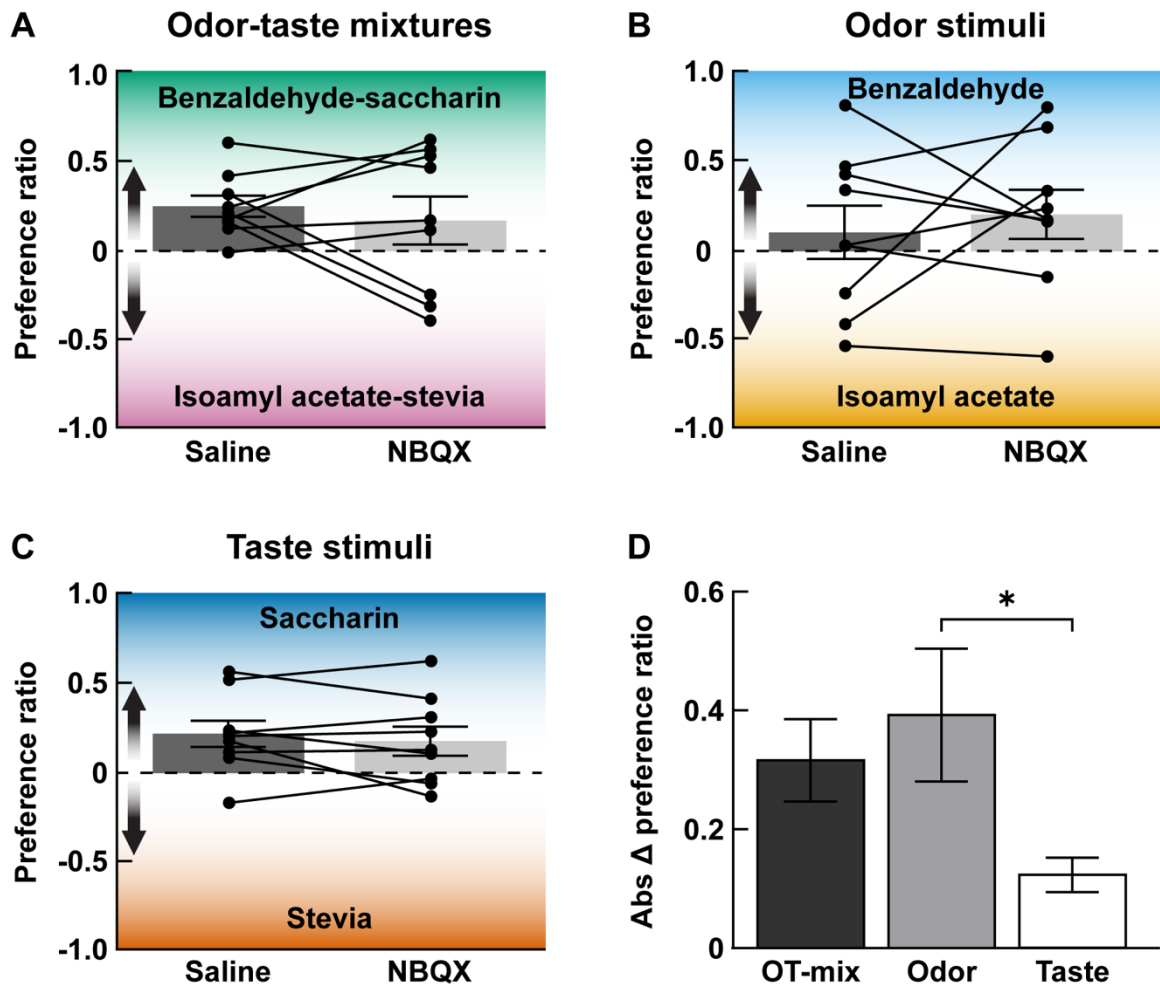
Figure 16. Taste preference is the least impacted by mediodorsal thalamus inactivation. Preference ratios ($\pm$ SEM) did not significantly differ across conditions for **A.** odor-taste mixture stimuli, **B.** odor stimuli, or **C.** taste stimuli. **D.** The absolute difference in preference ratio ($\pm$ SEM) was significantly smaller for tastes (white bar) compared to odors (light grey bar), but not odor-taste mixtures (dark grey bar), indicating preference was most consistent for tastes. *$p < 0.05$.
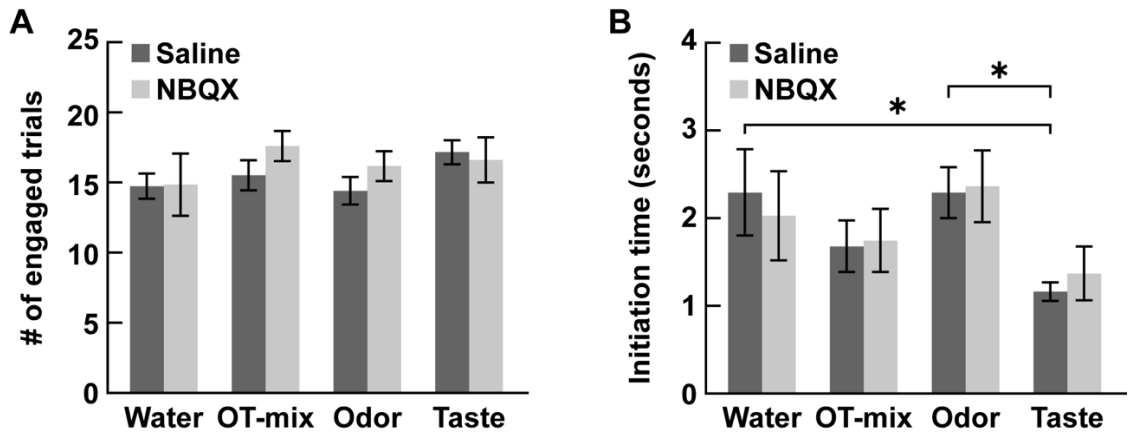
Figure 17. Rats initiated and engaged in a similar number of trials regardless of infusion condition. A. There was no significant difference in the number of engaged trials ($\pm$ SEM) between Saline and NBQX conditions for water, odor-taste mixtures, odors, or tastes. **B.** Initiation time ($\pm$ SEM) was significantly faster in the Saline condition for tastes compared to odors and water, but not odor-taste mixtures. There were no significant differences across stimulus categories between infusion conditions. *$p < 0.05$.
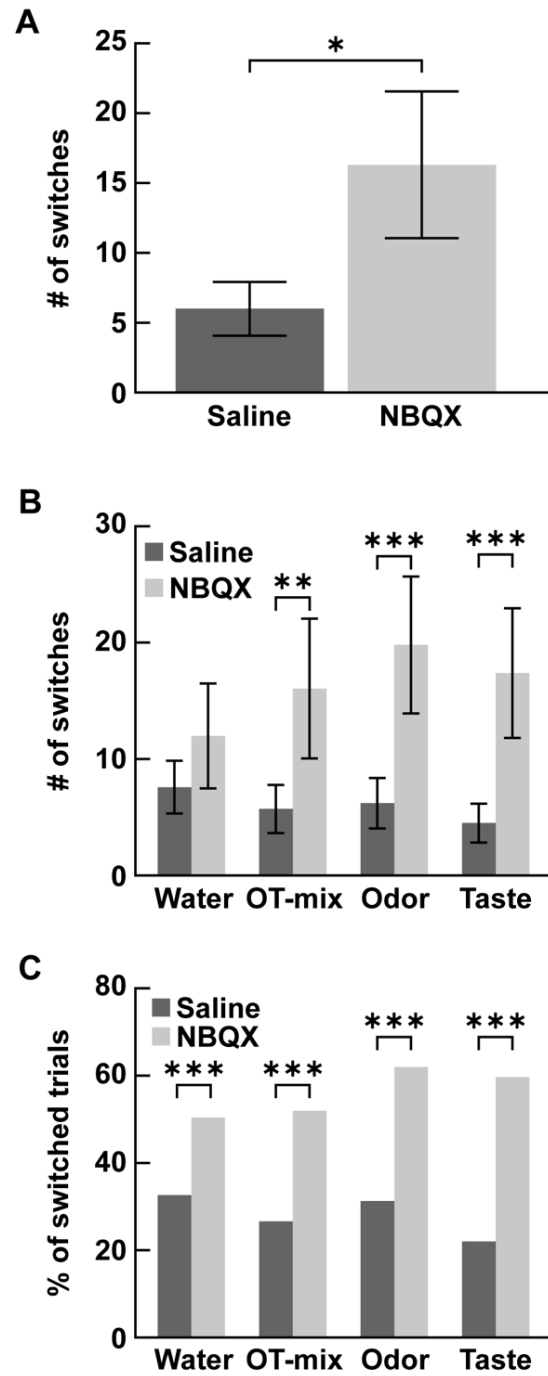
Figure 18. Inactivation of the mediodorsal thalamus increases within-trial switching between ports. A. The mean number of switches (± SEM) between the two ports in the 2-bottle brief-access task was significantly higher during NBQX

condition than the Saline condition. **B.** The mean number of switches ($\pm$ SEM) was significantly higher during the NBQX condition than Saline condition for odor-taste mixtures, odors, and tastes, but not for water. **C.** The proportion of switched trials was significantly higher during NBQX than Saline condition across all stimulus categories. ***$p < 0.001$. **$p < 0.01$. *$p < 0.05$

Discussion

In this study, we investigated the role of the mediodorsal thalamus in consummatory choice during a 2-bottle brief-access task. We found that inactivation of the mediodorsal thalamus significantly decreased the consumption of the preferred saccharin taste and eliminated the preference for benzaldehyde-saccharin over isoamyl acetate-stevia. These findings suggest that perturbing the activity of the mediodorsal thalamus may alter the hedonic perception of chemosensory stimuli. However, our results also show that mediodorsal thalamus inactivation increased within-trial switching between stimuli, indicating possible attentional deficits or indecision. While there was overall less consumption, rats engaged in a similar number of trials with similar trial initiation times, indicating that inactivation of the mediodorsal thalamus does not disrupt the rats' willingness to engage in the task. Our findings align with previous literature that suggests the involvement of the mediodorsal thalamus in both hedonic value and sensory attention (Rousseaux et al., 1996; Asai et al., 2008; Plailly et al., 2008; Sela et al., 2009; Tham et al., 2009, 2011a, 2011b; Veldhuizen and Small, 2011; Schmitt et al., 2017; Rikhye et al., 2018).

To investigate the role of the mediodorsal thalamus in consummatory choice, we chose to give rats experience with odor-taste mixtures containing tastes with the same quality, but slightly different hedonic values. At the concentration used here, both noncaloric sweeteners are preferred to water but saccharin is preferred to stevia (Sclafani et al., 2010). Our results confirmed the taste preference and showed that rats also prefer a mixture of benzaldehyde-saccharin

to one of isoamyl acetate-stevia. Numerous animal and human studies have demonstrated that experience with odor-taste mixtures leads to associations between the odor and the paired taste's quality and hedonic value (Fanselow and Birk, 1982; Holder, 1991; Stevenson et al., 1998, 1995; Schul et al., 1996; Sakai and Yamamoto, 2001; Prescott et al., 2004; Gautam and Verhagen, 2010; Green et al., 2012; Blankenship et al., 2019; McQueen et al., 2020). Therefore, we expected that rats would prefer to consume benzaldehyde over isoamyl acetate but found no significant odor preference. This could be due to saccharin and stevia having similar positive hedonic values or due to the nature of the 2-bottle brief-access task. It employs a fixed number of trials with a limited sampling period, thus the consequence of sampling the "wrong" less preferred odor may be outweighed by the drive to consume. Furthermore, we expected that chemosensory preferences would be eliminated by inactivation of the mediodorsal thalamus because people with lesions of the mediodorsal thalamus report decreases in the pleasantness of both odors and odor-taste mixtures (Tham et al., 2011a). We found that rats no longer preferred to consume the benzaldehyde-saccharin mixture to the isoamyl acetate-stevia mixture during the inactivation of the mediodorsal thalamus. Additionally, while the rats still preferred to consume the saccharin taste, they sampled significantly less saccharin during the NBQX condition. The changes in consummatory behavior during mediodorsal thalamic inactivation were likely related to the reduced sampling time caused by the increased switching between bottles.

Previous studies highlight two likely reasons for the increased switching during inactivation of the mediodorsal thalamus. The first suggests that inactivation of the mediodorsal thalamus altered the perceived value of the chemosensory stimuli (Rousseaux et al., 1996; Asai et al., 2008; Sela et al., 2009; Tham et al., 2011a), resulting in rats switching between ports to repeatedly "test" the stimuli due to an incongruity in their hedonic expectations. Future studies using odor-taste mixtures with opposite hedonic values could help to determine whether increased switching during mediodorsal thalamus inactivation is due to altered stimulus hedonics. If the mediodorsal thalamus is required for the perceptual value of chemosensory stimuli, then inactivation would still result in increased switching between ports regardless of the hedonic value of the stimuli.

A second possible reason for the increased switching between ports during inactivation of the mediodorsal thalamus is related to its role in sensory attention (Plailly et al., 2008; Tham et al., 2009, 2011a, 2011b; Veldhuizen and Small, 2011; Schmitt et al., 2017; Rikhye et al., 2018). It is known that the mediodorsal thalamus plays a crucial role in directing attention towards relevant sensory stimuli (Plailly et al., 2008; Schmitt et al., 2017). For example, during an olfactory attention task, neural coupling increases between the piriform cortex and mediodorsal thalamus, as well as the mediodorsal thalamus and orbitofrontal cortex (Plailly et al., 2008). Therefore, the increase in the proportion of switched trials during the NBQX sessions may be due to indecision or attentional deficits, as rats struggle to focus on one sensory stimulus over another. Interestingly, studies of attention deficit hyperactivity disorder (ADHD) have revealed that individuals with ADHD exhibit

increased brain activity in the mediodorsal thalamus during a conscious resting-state, compared to those without ADHD (Tian et al., 2008). This suggests that individuals with ADHD may be processing more sensory information during a resting state, which is consistent with their symptoms of inattention and distraction by environmental stimuli. These studies suggest that abnormal activity in the mediodorsal thalamus, whether overactive or inactivated, can cause attentional issues, and that a balanced relationship between the cortex and thalamus is needed for optimal attention. To further investigate the role of the mediodorsal thalamus in attention during a two-bottle choice task, researchers could require that rats hold a position for a set time before stimulus delivery. If rats are unable to hold the position during inactivation of the mediodorsal thalamus, this would suggest that the mediodorsal thalamus is important for attending to a single stimulus without switching in a two-bottle brief-access task. Further studies are needed to fully understand the mechanisms underlying the involvement of the mediodorsal thalamus in sensory attention and its impact on consummatory behavior.

In conclusion, our findings implicate the mediodorsal thalamus in the consummatory choice of experienced odors, tastes, and odor-taste mixtures. Our results show that the inactivation of the mediodorsal thalamus decreases overall consumption and increases the amount of switching between two stimuli. These results suggest the importance of the mediodorsal thalamus in appropriate hedonic value of chemosensory stimuli and sensory attention during consummatory choice

tasks. Future research will aim to elucidate the neural mechanisms underlying its

involvement in attention related to consummatory behavior.

CHAPTER 5

SUMMARY AND CONCLUSIONS

In this dissertation, I provided anatomical, electrophysiological, and behavioral evidence supporting the involvement of the mediodorsal thalamus in processing chemosensory signals and informing consummatory choice.

In chapter 2, I employed an intersectional viral method to compare the cortico-thalamic connectivity between the chemosensory cortices and mediodorsal thalamus. Contrary to my hypothesis, I discovered that the gustatory cortex forms more connections with the mediodorsal thalamus than the posterior piriform cortex. For the reasons discussed, I focused on characterizing the connections from the posterior piriform cortex. However, it is important to note that the projections from anterior piriform cortex were not characterized, and likely contribute input to the mediodorsal thalamus as well. Although anatomical differences do not necessarily indicate functional differences, this result suggests that input from the gustatory cortex could broadly influence processing in the mediodorsal thalamus. To further understand the circuitry between the gustatory cortex and the mediodorsal thalamus, future studies employing electron microscopy or optogenetic circuitry-based recordings would help define the anatomical and functional relationship between these regions and their respective roles in chemosensory processing.

In chapter 3, I used awake behaving electrophysiology to demonstrate that neurons in the mediodorsal thalamus dynamically encode chemosensory signals originating from the mouth. The chemoselective population is broadly tuned, exhibits excited and suppressed responses, and responds to odor-taste mixtures differently than their odor or taste component alone. A subset of these neurons also represented the palatability-related features of tastes. These results provide evidence of the multidimensionality of the mediodorsal thalamus in processing chemosensory information. This heavy taste-based physiology parallels my anatomical findings in chapter II demonstrating the dense cortico-thalamic connectivity between the gustatory cortex and mediodorsal thalamus.

In chapter 4, I used pharmacological inactivation during a 2-bottle brief-access task to determine the role of the mediodorsal thalamus in the consummatory choice of experienced odors, tastes, and odor-taste mixtures. I found that inactivating the mediodorsal thalamus significantly decreased consumption of the preferred saccharin taste and eliminated the preference for the odor-taste mixture benzaldehyde-saccharin over isoamyl acetate-stevia. Furthermore, inactivation increased the amount of within trial switches between chemosensory stimuli. Future investigations combining electrophysiology recordings as in chapter 3 with optogenetic perturbation of specific circuits during 2-bottle brief-access tasks as in chapter 4 would provide insight into the functional role of the mediodorsal thalamus during consummatory choice.

In conclusion, my findings suggest that the mediodorsal thalamus is an important region for the processing of chemosensory signals. The robust

connectivity between the gustatory cortex and the mediodorsal thalamus, as well as its heavy taste-based physiology and role in taste preferences, indicate its significant contribution to taste processing. While the field thus far has focused on the role of the mediodorsal thalamus in odor processing, these results emphasize the necessity of future studies on taste processing by the mediodorsal thalamus. Additionally, the role of the mediodorsal thalamus in sustaining attention to sensory stimuli is also crucial, as evidenced by the increase in switching between chemosensory stimuli during mediodorsal thalamic inactivation. The centralized connectivity of the mediodorsal thalamus may be essential to the network directing sensory attention, providing bottom-up information regarding stimulus type and value and top-down information regarding memory and cognitive behaviors from the prefrontal and orbitofrontal cortices that together inform the decision-making processes. I believe that the mediodorsal thalamus is critical for the modulation and transmission of behaviorally relevant sensory information that informs consummatory choices.

REFERENCES

Aimé P, Duchamp-Viret P, Chaput MA, Savigner A, Mahfouz M, Julliard AK (2007) Fasting increases and satiation decreases olfactory detection for a neutral odor in rats. Behav Brain Res 179:258–264.

Albertella L, Boakes RA (2006) Persistence of conditioned flavor preferences is not due to inadvertent food reinforcement. J Exp Psychol Anim Behav Process 32:386–395.

Alcaraz F, Marchand AR, Courtand G, Coutureau E, Wolff M (2016) Parallel inputs from the mediodorsal thalamus to the prefrontal cortex in the rat. Eur J Neurosci 44:1972–1986.

Allen G V., Saper CB, Hurley KM, Cechetto DF (1991) Organization of visceral and limbic connections in the insular cortex of the rat. J Comp Neurol 311:1–16.

Asai H, Udaka F, Hirano M, Ueno S (2008) Odor abnormalities caused by bilateral thalamic infarction. Clin Neurol Neurosurg 110:500–501.

Bäck S, Necarsulmer J, Whitaker LR, Hamra FK, Richie CT, Correspondence BKH (2019) Neuron-Specific Genome Modification in the Adult Rat Brain Using CRISPR-Cas9 Transgenic Rats. Neuron 102:105-119.e8.

Bamji-Stocke S, Biggs BT, Samuelsen CL (2018) Experience-dependent c-Fos expression in the primary chemosensory cortices of the rat. Brain Res 1701:189-195.

Barnett SA (1958) Experiments on neophobia in wild and laboratory rats. Br J Psychol 49:195–201.

Barnett SA, Spencer MM (1953) Experiments on the food preferences of wild rats (Rattus norvegicus Berkenhout). J Hyg (Lond) 51:16–34.

Bartoshuk LM, Sims CA, Colquhoun TA, Snyder DJ (2019) What Aristotle didn't know about flavor. Am Psychol 74:1003–1011.

Beckstead RM, Morse JR, Norgren R (1980) The nucleus of the solitary tract in the monkey: projections to the thalamus and brain stem nuclei. J Comp Neurol 190:259–282.

Bickford ME (2015) Thalamic Circuit Diversity: Modulation of the Driver/Modulator Framework. Front Neural Circuits 9:86.

Blankenship ML, Grigorova M, Katz DB, Maier JX (2019) Retronasal Odor Perception Requires Taste Cortex, but Orthonasal Does Not. Curr Biol 29:62-69.e3.

Bolding KA, Franks KM (2017) Complementary codes for odor identity and intensity in olfactory cortex. Elife 6.e22630

Bolkan SS, Stujenske JM, Parnaudeau S, Spellman TJ, Rauffenbart C, Abbas AI, Harris AZ, Gordon JA, Kellendonk C (2017) Thalamic projections sustain prefrontal activity during working memory maintenance. Nat Neurosci 20:987–996.

Bonanomi D (2019) Axon pathfinding for locomotion. Semin Cell Dev Biol 85:26–35.

Bouaichi CG, Vincis R (2020) Cortical processing of chemosensory and hedonic features of taste in active licking mice. J Neurophysiol 123:1995–2009.

Budisantoso T, Matsui K, Kamasawa N, Fukazawa Y, Shigemoto R (2012) Mechanisms underlying signal filtering at a multisynapse contact. J Neurosci 32:2357–2376.

Calu DJ, Roesch MR, Stalnaker TA, Schoenbaum G (2007) Associative encoding in posterior piriform cortex during odor discrimination and reversal learning. Cereb Cortex 17:1342–1349.

Chakraborty S, Ouhaz Z, Mason S, Mitchell AS (2019) Macaque parvocellular mediodorsal thalamus: dissociable contributions to learning and adaptive decision-making. Eur J Neurosci 49:1041–1054.

Cohen JY, Haesler S, Vong L, Lowell BB, Uchida N (2012) Neuron-type-specific signals for reward and punishment in the ventral tegmental area. Nature 482:85–88.

Corbit LH, Muir JL, Balleine BW (2003) Lesions of mediodorsal thalamus and anterior thalamic nuclei produce dissociable effects on instrumental conditioning in rats. Eur J Neurosci 18:1286–1294.

Corey DT (1978) The determinants of exploration and neophobia. Neurosci Biobehav Rev 2:235–253.

Courtiol E, Neiman M, Fleming G, Teixeira CM, Wilson DA (2019) A specific olfactory cortico-thalamic pathway contributing to sampling performance during odor reversal learning. Brain Struct Funct 224:961-971.

Courtiol E, Wilson DA (2014) Thalamic olfaction: characterizing odor processing in the mediodorsal thalamus of the rat. J Neurophysiol 111:1274–1285.

Courtiol E, Wilson DA (2015) The olfactory thalamus: unanswered questions about the role of the mediodorsal thalamic nucleus in olfaction. Front Neural Circuits 9:49.

Courtiol E, Wilson DA (2016) Neural Representation of Odor-Guided Behavior in the Rat Olfactory Thalamus. J Neurosci 36:5946–5960.

Datiche F, Cattarelli M (1996) Reciprocal and topographic connections between the piriform and prefrontal cortices in the rat: a tracing study using the B subunit of the cholera toxin. Brain Res Bull 41:391–398.

Demattè ML, Endrizzi I, Gasperi F (2014) Food neophobia and its relation with olfaction. Front Psychol 5:127.

DeNicola AL, Park MY, Crowe DA, MacDonald AW, Chafee M V. (2020) Differential roles of mediodorsal nucleus of the thalamus and prefrontal cortex in decision-making and state representation in a cognitive control task measuring deficits in schizophrenia. J Neurosci 40:1650–1667.

Di Lorenzo PM, Garcia J (1985) Olfactory responses in the gustatory area of the parabrachial pons. Brain Res Bull 15:673–676.

Eichenbaum H, Shedlack KJ, Eckmann KW (1980) Thalamocortical mechanisms in odor-guided behavior: I. Effects of lesions of the mediodorsal thalamic nucleus and frontal cortex on olfactory discrimination in the rat. Brain Behav Evol 17:255–275.

Erişir A, Van Horn SC, Bickford ME, Sherman SM (1997) Immunocytochemistry and distribution of parabrachial terminals in the lateral geniculate nucleus of the cat: a comparison with corticogeniculate terminals. J Comp Neurol 377:535–549.

Escanilla OD, Victor JD, Di Lorenzo PM (2015) Odor-taste convergence in the nucleus of the solitary tract of the awake freely licking rat. J Neurosci 35:6284–6297.

Fanselow MS, Birk J (1982) Flavor-flavor associations induce hedonic shifts in taste preference. Anim Learn Behav 10:223–228.

Fontanini A, Grossman SE, Figueroa JA, Katz DB (2009) Distinct subtypes of basolateral amygdala taste neurons reflect palatability and reward. J Neurosci 29:2486–2495.

Fredericksen KE, McQueen KA, Samuelsen CL (2019) Experience-Dependent c-Fos Expression in the Mediodorsal Thalamus Varies with Chemosensory Modality. Chem Senses 44:41–49.

Fredericksen KE, Samuelsen CL (2022) Neural representation of intraoral olfactory and gustatory signals by the mediodorsal thalamus in alert rats. J Neurosci 42:8136–8153.

Gaffan D, Murray EA (1990) Amygdalar interaction with the mediodorsal nucleus of the thalamus and the ventromedial prefrontal cortex in stimulus-reward associative learning in the monkey. J Neurosci 10:3479–3493.

Gardner MPH, Fontanini A (2014) Encoding and Tracking of Outcome-Specific Expectancy in the Gustatory Cortex of Alert Rats. J Neurosci 34:13000–13017.

Gautam SH, Verhagen J V. (2010) Evidence that the sweetness of odors depends on experience in rats. Chem Senses 35:767–776.

Gautam SH, Verhagen J V. (2012) Direct behavioral evidence for retronasal olfaction in rats. PLoS One 7:e44781.

Ghosh S, Larson SD, Hefzi H, Marnoy Z, Cutforth T, Dokka K, Baldwin KK (2011) Sensory maps in the olfactory cortex defined by long-range viral tracing of single neurons. Nature 472:217–222.

González F, Morillas E, Hall G (2016) The extinction procedure modifies a conditioned flavor preference in nonhungry rats only after revaluation of the unconditioned stimulus. J Exp Psychol Anim Learn Cogn 42:380–390.

Green BG, Nachtigal D, Hammond S, Lim J (2012) Enhancement of retronasal odors by taste. Chem Senses 37:77–86.

Haberly LB, Price JL (1977) The axonal projection patterns of the mitral and tufted cells of the olfactory bulb in the rat. Brain Res 129:152–157.

Halassa MM, Sherman SM (2019) Thalamocortical Circuit Motifs: A General Framework. Neuron 103:762–770.

Hammer S, Carrillo GL, Govindaiah G, Monavarfeshani A, Bircher JS, Su J, Guido W, Fox MA (2014) Nuclei-specific differences in nerve terminal distribution, morphology, and development in mouse visual thalamus. Neural Dev 9:16.

Hammer S, Monavarfeshani A, Lemon T, Su J, Fox MA (2015) Multiple Retinal Axons Converge onto Relay Cells in the Adult Mouse Thalamus. Cell Rep 12:1575–1583.

Han J, Lee JH, Kim MJ, Jung MW (2013) Neural activity in mediodorsal nucleus of thalamus in rats performing a working memory task. Front Neural Circuits 7:128.

Hanamori T, Kunitake T, Kato K, Kannan H (1998) Responses of neurons in the insular cortex to gustatory, visceral, and nociceptive stimuli in rats. J Neurophysiol 79:2535–2545.

Hikosaka O, Kim HF, Amita H, Yasuda M, Isoda M, Tachibana Y, Yoshida A (2019) Direct and indirect pathways for choosing objects and actions. Eur J Neurosci 49:637–645.

Holder MD (1991) Conditioned preferences for the taste and odor components of flavors: Blocking but not overshadowing. Appetite 17:29–45.

Idris A, Christensen BA, Walker EM, Maier JX (2023) Multisensory integration of orally-sourced gustatory and olfactory inputs to the posterior piriform cortex in awake rats. J Physiol 601:151–169.

Ifuku H, Nakamura T, Hirata S, Ogawa H (2006) Neuronal activities in the reward phase in primary and higher-order gustatory cortices of monkeys. Neurosci Res 55:54–64.

Illig KR (2005) Projections from Orbitofrontal Cortex to Anterior Piriform Cortex in the Rat Suggest a Role in Olfactory Information Processing. J Comp Neurol 488:224.

Imamura K, Onoda N, Takagi SF (1984) Odor response characteristics of thalamic mediodorsal nucleus neurons in the rabbit. Jpn J Physiol 34:55–73.

Iwai H, Kuramoto E, Yamanaka A, Sonomura T, Uemura M, Goto T (2015) Ascending parabrachio-thalamo-striatal pathways: potential circuits for integration of gustatory and oral motor functions. Neuroscience 294:1–13.

Jezzini A, Mazzucato L, La Camera G, Fontanini A (2013) Processing of Hedonic and Chemosensory Features of Taste in Medial Prefrontal and Insular Networks. J Neurosci 33:18966–18978.

Johnson DMG, Illig KR, Behan M, Haberly LB (2000) New Features of Connectivity in Piriform Cortex Visualized by Intracellular Injection of Pyramidal Cells Suggest that "Primary" Olfactory Cortex Functions Like "Association" Cortex in Other Sensory Systems. J Neurosci 20:6974–6982.

Jones LM, Fontanini A, Sadacca BF, Miller P, Katz DB (2007) Natural stimuli evoke dynamic sequences of states in sensory cortical ensembles. Proc Natl Acad Sci U S A 104:18772–18777.

Julliard AK, Chaput MA, Apelbaum A, Aimé P, Mahfouz M, Duchamp-Viret P (2007) Changes in rat olfactory detection performance induced by orexin and leptin mimicking fasting and satiation. Behav Brain Res 183:123–129.

Kadohisa M, Rolls ET, Verhagen J V. (2005) Neuronal representations of stimuli in the mouth: the primate insular taste cortex, orbitofrontal cortex and amygdala. Chem Senses 30:401–419.

Kadohisa M, Wilson DA (2006) Separate encoding of identity and similarity of complex familiar odors in piriform cortex. Proc Natl Acad Sci U S A 103:15206.

Katz DB, Simon SA, Nicolelis MAL (2001) Dynamic and Multimodal Responses of Gustatory Cortical Neurons in Awake Rats. J Neurosci 21:4478–4489.

Kawagoe T, Tamura R, Uwano T, Asahi T, Nishijo H, Eifuku S, Ono T (2007) Neural correlates of stimulus-reward association in the rat mediodorsal thalamus. Neuroreport 18:683–688.

Kirchgessner MA, Franklin AD, Callaway EM (2021) Distinct "driving" versus "modulatory" influences of different visual corticothalamic pathways. Curr Biol 31:5121-5137.e7.

Krettek JE, Price JL (1977) The cortical projections of the mediodorsal nucleus and adjacent thalamic nuclei in the rat. J Comp Neurol 171:157–191.

Krushel LA, van Der Kooy D (1988) Visceral cortex: integration of the mucosal senses with limbic information in the rat agranular insular cortex. J Comp Neurol 270:39–54.

Kuramoto E, Pan S, Furuta T, Tanaka YR, Iwai H, Yamanaka A, Ohno S, Kaneko T, Goto T, Hioki H (2017) Individual mediodorsal thalamic neurons project to multiple areas of the rat prefrontal cortex: A single neuron-tracing study using virus vectors. J Comp Neurol 525:166–185.

Kuroda M, Murakami K, Kishi K, Price JL (1992) Distribution of the piriform cortical terminals to cells in the central segment of the mediodorsal thalamic nucleus of the rat. Brain Res 595:159–163.

Levitan D, Lin JY, Wachutka J, Mukherjee N, Nelson SB, Katz DB (2019) Single and population coding of taste in the gustatory cortex of awake mice. J Neurophysiol 122:1342–1356.

Li H, Penzo MA, Taniguchi H, Kopec CD, Huang ZJ, Li B (2013) Experience-dependent modification of a central amygdala fear circuit. Nat Neurosci 16:332–339.

Lim J, Johnson MB (2011) Potential mechanisms of retronasal odor referral to the mouth. Chem Senses 36:283–289.

Lin X Bin, Pierce DR, Light KE, Hayar A (2013) The fine temporal structure of the rat licking pattern: what causes the variabiliy in the interlick intervals and how is it affected by the drinking solution? Chem Senses 38:685–704.

Lin JY, Roman C, Reilly S (2009) Taste-potentiated odor aversion learning in rats with lesions of the insular cortex. Brain Res 1297:135–142.

Litaudon P, Amat C, Bertrand B, Vigouroux M, Buonviso N (2003) Piriform cortex functional heterogeneity revealed by cellular responses to odours. Eur J Neurosci 17:2457–2461.

Liu H, Fontanini A (2015) State dependency of chemosensory coding in the gustatory thalamus (VPMpc) of alert rats. J Neurosci 35:15479–15491.

MacKinnon CD (2018) Sensorimotor anatomy of gait, balance, and falls. Handb Clin Neurol 159:3–26.

Maier JX (2017) Single-neuron responses to intraoral delivery of odor solutions in primary olfactory and gustatory cortex. J Neurophysiol 117:1293–1304.

Maier JX, Blankenship ML, Li JX, Katz DB (2015) A multisensory network for olfactory processing. Curr Biol 25:2642.

Maier JX, Wachowiak M, Katz DB (2012) Chemosensory convergence on primary olfactory cortex. J Neurosci 32:17037–17047.

Majak K, Rönkkö S, Kemppainen S, Pitkänen A (2004) Projections from the amygdaloid complex to the piriform cortex: A PHA-L study in the rat. J Comp Neurol 476:414–428.

McQueen KA, Fredericksen KE, Samuelsen CL (2020) Experience Informs Consummatory Choices for Congruent and Incongruent Odor-Taste Mixtures in Rats. Chem Senses 45:371–382.

Mease RA, Metz M, Groh A (2016) Cortical Sensory Responses Are Enhanced by the Higher-Order Thalamus. Cell Rep 14:208–215.

Meyers EM (2013) The neural decoding toolbox. Front Neuroinform 7:8.

Miller JS, Nonneman AJ, Kelly KS, Neisewander JL, Isaac WL (1986) Disruption of neophobia, conditioned odor aversion, and conditioned taste aversion in rats with hippocampal lesions. Behav Neural Biol 45:240–253.

Mitchell AS (2015) The mediodorsal thalamus as a higher order thalamic relay nucleus important for learning and decision-making. Neurosci Biobehav Rev 54:76–88.

Mitchell AS, Gaffan D (2008) The magnocellular mediodorsal thalamus is necessary for memory acquisition, but not retrieval. J Neurosci 28:258–263.

Miyamichi K, Amat F, Moussavi F, Wang C, Wickersham I, Wall NR, Taniguchi H, Tasic B, Huang ZJ, He Z, Callaway EM, Horowitz MA, Luo L (2011) Cortical representations of olfactory input by transsynaptic tracing. Nature 472:191.

Nakajima M, Halassa MM (2017) Thalamic control of functional cortical connectivity. Curr Opin Neurobiol 44:127–131.

Neville KR, Haberly LB (2003) Beta and gamma oscillations in the olfactory system of the urethane-anesthetized rat. J Neurophysiol 90:3921–3930.

Norgren R (1978) Projections from the nucleus of the solitary tract in the rat. Neuroscience 3:207–218.

Norgren R (1983) The gustatory system in mammals. Am J Otolaryngol 4:234–237.

Ohshiro T, Angelaki DE, Deangelis GC (2011) A normalization model of multisensory integration. Nat Neurosci 14:775–782.

Ojala M, Garriga GC (2010) Permutation Tests for Studying Classifier Performance. J Mach Learn Res 11:1833–1863.

Oyoshi T, Nishijo H, Asakura T, Takamura Y, Ono T (1996) Emotional and behavioral correlates of mediodorsal thalamic neurons during associative learning in rats. J Neurosci 16:5812–5829.

Parnaudeau S, O'Neill PK, Bolkan SS, Ward RD, Abbas AI, Roth BL, Balsam PD, Gordon JA, Kellendonk C (2013) Inhibition of mediodorsal thalamus disrupts thalamofrontal connectivity and cognition. Neuron 77:1151–1162.

Partridge L (1981) Increased preferences for familiar foods in small mammals. Anim Behav 29:211–216.

Pelzer P, Horstmann H, Kuner T, Feldmeyer D, Krieger P, Wozny C, Hallermann S (2017) Ultrastructural and Functional Properties of a Giant Synapse Driving the Piriform Cortex to Mediodorsal Thalamus Projection. Front Synaptic Neurosci 9:3.

Petersen SE, Robinson DL, Morris JD (1987) Contributions of the pulvinar to visual spatial attention. Neuropsychologia 25:97–105.

Piette CE, Baez-Santiago MA, Reid EE, Katz DB, Moran A (2012) Inactivation of basolateral amygdala specifically eliminates palatability-related information in cortical sensory responses. J Neurosci 32:9981–9991.

Plailly J, Howard JD, Gitelman DR, Gottfried JA (2008) Attention to odor modulates thalamocortical connectivity in the human brain. J Neurosci 28:5257–5267.

Potter H, Butters N (1980) An assessment of olfactory deficits in patients with damage to prefrontal cortex. Neuropsychologia 18:621–628.

Prescott J (2012) Chemosensory learning and flavour: perception, preference and intake. Physiol Behav 107:553–559.

Prescott J (2015) Multisensory processes in flavour perception and their influence on food choice. Curr Opin Food Sci 3:47–52.

Prescott J, Johnstone V, Francis J (2004) Odor-taste interactions: Effects of attentional strategies during exposure. Chem Senses 29:331–340.

Price JL, Slotnick BM (1983) Dual olfactory representation in the rat thalamus: An anatomical and electrophysiological study. J Comp Neurol 215:63–77.

Prillwitz CC, David B, Schlaug G, Deller T, Schramm J, Lindenberg R, Hattingen E, Weber B, Surges R, Elger CE, Rüber T (2021) Functional redundancy of the premotor network in hemispherotomy patients. Ann Clin Transl Neurol 8:1796–1808.

Ray JP, Price JL (1992) The organization of the thalamocortical connections of the mediodorsal thalamic nucleus in the rat, related to the ventral forebrain-prefrontal cortex topography. J Comp Neurol 323:167–197.

Rebello MR, Kandukuru P, Verhagen J V. (2015) Direct behavioral and neurophysiological evidence for retronasal olfaction in mice. PLoS One 10:e0117218.

Reilly S (1999) The parabrachial nucleus and conditioned taste aversion. Brain Res Bull 48:239–254.

Rikhye R V., Gilra A, Halassa MM (2018) Thalamic regulation of switching between cortical representations enables cognitive flexibility. Nat Neurosci 21:1753–1763.

Rousseaux M, Muller P, Gahide I, Mottin Y, Romon M (1996) Disorders of smell, taste, and food intake in a patient with a dorsomedial thalamic infarct. Stroke 27:2328–2330.

Roy DS, Zhang Y, Halassa MM, Feng G (2022) Thalamic subnetworks as units of function. Nat Neurosci 25:140–153.

Rozin P (1982) "Taste-smell confusions" and the duality of the olfactory sense. Percept Psychophys 31:397–401.

Saalmann YB (2014) Intralaminar and medial thalamic influence on cortical synchrony, information transmission and cognition. Front Syst Neurosci 8:83.

Saalmann YB, Pinsk MA, Wang L, Li X, Kastner S (2012) The pulvinar regulates information transmission between cortical areas based on attention demands. Science 337:753–756.

Sadacca BF, Rothwax JT, Katz DB (2012) Sodium concentration coding gives way to evaluative coding in cortex and amygdala. J Neurosci 32:9999–10011.

Sakai N, Imada S (2003) Bilateral lesions of the insular cortex or of the prefrontal cortex block the association between taste and odor in the rat. Neurobiol Learn Mem 80:24–31.

Sakai N, Yamamoto T (2001) Effects of excitotoxic brain lesions on taste-mediated odor learning in the rat. Neurobiol Learn Mem 75:128–139.

Samuelsen CL, Fontanini A (2017) Processing of Intraoral Olfactory and Gustatory Signals in the Gustatory Cortex of Awake Rats. J Neurosci 37:244–257.

Samuelsen CL, Gardner MPH, Fontanini A (2012) Effects of Cue-Triggered Expectation on Cortical Processing of Taste. Neuron 74:410–422.

Samuelsen CL, Gardner MPH, Fontanini A (2013) Thalamic contribution to cortical processing of taste and expectation. J Neurosci 33:1815–1827.

Samuelsen CL, Vincis R (2021) Cortical Hub for Flavor Sensation in Rodents. Front Syst Neurosci 15:77286.

Sapolsky RM, Eichenbaum H (1980) Thalamocortical mechanisms in odor-guided behavior. II. Effects of lesions of the mediodorsal thalamic nucleus and frontal cortex on odor preferences and sexual behavior in the hamster. Brain Behav Evol 17:276–290.

Scalia F, Winans SS (1975) The differential projections of the olfactory bulb and accessory olfactory bulb in mammals. J Comp Neurol 161:31–55.

Schmitt LI, Wimmer RD, Nakajima M, Happ M, Mofakham S, Halassa MM (2017) Thalamic amplification of cortical connectivity sustains attentional control. Nature 545:219–223.

Schoenbaum, Roesch, Stalnaker, Takahashi (2011) Orbitofrontal Cortex and Outcome Expectancies: Optimizing Behavior and Sensory Perception. In: Neurobiology of Sensation and Reward, pp 349–370.

Schul R, Slotnick BM, Dudai Y (1996) Flavor and the frontal cortex. Behav Neurosci 110:760–765.

Sclafani A (2001) Psychobiology of food preferences. Int J Obes Relat Metab Disord 25 Suppl 5:S13–S16.

Sclafani A, Bahrani M, Zukerman S, Ackroff K (2010) Stevia and Saccharin Preferences in Rats and Mice. Chem Senses 35:433–443.

Scott GA, Liu MC, Tahir NB, Zabder NK, Song Y, Greba Q, Howland JG (2020) Roles of the medial prefrontal cortex, mediodorsal thalamus, and their combined circuit for performance of the odor span task in rats: Analysis of memory capacity and foraging behavior. Learn Mem 27:67–77.

Sela L, Sacher Y, Serfaty C, Yeshurun Y, Soroker N, Sobel N (2009) Spared and impaired olfactory abilities after thalamic lesions. J Neurosci 29:12059–12069.

Sewards T V., Sewards MA (2001) Cortical association areas in the gustatory system. Neurosci Biobehav Rev 25:395–407.

Shan G, Gerstenberger S (2017) Fisher's exact approach for post hoc analysis of a chi-squared test. PLoS One 12:e0188709.

Sherman SM (2016) Thalamus plays a central role in ongoing cortical functioning. Nat Neurosci 19:533–541.

Sherman SM, Guillery RW (1998) On the actions that one nerve cell can have on another: distinguishing "drivers" from "modulators." Proc Natl Acad Sci U S A 95:7121–7126.

Shi C-J, Cassell MD (1998) Cortical, thalamic, and amygdaloid connections of the anterior and posterior insular cortices. J Comp Neurol 399:440–468.

Slotnick BM, Kaneko N (1981) Role of mediodorsal thalamic nucleus in olfactory discrimination learning in rats. Science 214:91–92.

Slotnick BM, Risser JM (1990) Odor memory and odor learning in rats with lesions of the lateral olfactory tract and mediodorsal thalamic nucleus. Brain Res 529:23–29.

Small DM (2012) Flavor is in the brain. Physiol Behav 107:540–552.

Small DM, Green BG (2012) A Proposed Model of a Flavor Modality. Neural Bases Multisensory Process:717–738.

Small DM, Veldhuizen MG, Felsted J, Mak YE, McGlone F (2008) Separable Substrates for Anticipatory and Consummatory Food Chemosensation. Neuron 57:786–797.

Snow JC, Allen HA, Rafal RD, Humphreys GW (2009) Impaired attentional selection following lesions to human pulvinar: evidence for homology between human and monkey. Proc Natl Acad Sci U S A 106:4054–4059.

Staubli U, Schottler F, Nejat-Bina D (1987) Role of dorsomedial thalamic nucleus and piriform cortex in processing olfactory information. Behav Brain Res 25:117–129.

Stevenson RJ, Boakes RA, Prescott J (1998) Changes in Odor Sweetness Resulting from Implicit Learning of a Simultaneous Odor-Sweetness Association: An Example of Learned Synesthesia. Learn Motiv 29:113–132.

Stevenson RJ, Prescott J, Boakes RA (1995) The acquisition of taste properties by odors. Learn Motiv 26:433–455.

Stroh A, Adelsberger H, Groh A, Rühlmann C, Fischer S, Schierloh A, Deisseroth K, Konnerth A (2013) Making waves: initiation and propagation of corticothalamic Ca2+ waves in vivo. Neuron 77:1136–1150.

Tham WWP, Stevenson RJ, Miller LA (2009) The functional role of the medio dorsal thalamic nucleus in olfaction. Brain Res Rev 62:109–126.

Tham WWP, Stevenson RJ, Miller LA (2011a) The impact of mediodorsal thalamic lesions on olfactory attention and flavor perception. Brain Cogn 77:71–79.

Tham WWP, Stevenson RJ, Miller LA (2011b) The role of the mediodorsal thalamic nucleus in human olfaction. Neurocase 17:148–159.

Theyel BB, Llano DA, Sherman SM (2010) The corticothalamocortical circuit drives higher-order cortex in the mouse. Nat Neurosci 13:84–88.

Tian L, Jiang T, Liang M, Zang Y, He Y, Sui M, Wang Y (2008) Enhanced resting-state brain activities in ADHD patients: a fMRI study. Brain Dev 30:342–348.

Tokita K, Inoue T, Boughter JD (2009) Afferent connections of the parabrachial nucleus in C57BL/6J mice. Neuroscience 161:475.

Tong J, Mannea E, Aimé P, Pfluger PT, Yi CX, Castaneda TR, Davis HW, Ren X, Pixley S, Benoit S, Julliard K, Woods SC, Horvath TL, Sleeman MM, D'Alessio D, Obici S, Frank R, Tschöp MH (2011) Ghrelin enhances olfactory sensitivity and exploratory sniffing in rodents and humans. J Neurosci 31:5841–5846.

Veldhuizen MG, Small DM (2011) Modality-specific neural effects of selective attention to taste and odor. Chem Senses 36:747–760.

Verhagen J V., Engelen L (2006) The neurocognitive bases of human multimodal food perception: Sensory integration. Neurosci Biobehav Rev 30:613–650.

Vincis R, Fontanini A (2016) Associative learning changes cross-modal representations in the gustatory cortex. Elife 5:e16420.

Wesson DW, Wilson DA (2011) Sniffing out the contributions of the olfactory tubercle to the sense of smell: hedonics, sensory integration, and more? Neurosci Biobehav Rev 35:655.

Wilson DA, Fleming G, Vervoordt SM, Coureaud G (2020) Cortical processing of configurally perceived odor mixtures. Brain Res 1729.

Wilson DA, Sullivan RM (2011) Cortical Processing of Odor Objects. Neuron 72:506.

Witter MP, Doan TP, Jacobsen B, Nilssen ES, Ohara S (2017) Architecture of the Entorhinal Cortex A Review of Entorhinal Anatomy in Rodents with Some Comparative Notes. Front Syst Neurosci 11:46.

Yang JW, Shih HC, Shyu BC (2006) Intracortical circuits in rat anterior cingulate cortex are activated by nociceptive inputs mediated by medial thalamus. J Neurophysiol 96:3409–3422.

Yarita H, Iino M, Tanabe T, Kogure S, Takagi SF (1980) A transthalamic olfactory pathway to orbitofrontal cortex in the monkey. J Neurophysiol 43:69–85.

Yeomans MR, Mobini S, Elliman TD, Walker HC, Stevenson RJ (2006) Hedonic and sensory characteristics of odors conditioned by pairing with tastants in humans. J Exp Psychol Anim Behav Process 32:215–228.

Zhou H, Schafer RJ, Desimone R (2016) Pulvinar-Cortex Interactions in Vision and Attention. Neuron 89:209–220.

Zingg B, Chou X lin, Zhang Z gang, Mesik L, Liang F, Tao HW, Zhang LI (2017) AAV-Mediated Anterograde Transsynaptic Tagging: Mapping Corticocollicular Input-Defined Neural Pathways for Defense Behaviors. Neuron 93:33–47.

CURRICULUM VITAE

NAME: Kelly E. Fredericksen

ADDRESS: Department of Anatomical Sciences and Neurobiology
                    511 South Floyd Street, Room 433
                    University of Louisville School of Medicine
                    Louisville, KY 40202

DOB: Elk Grove Village, Illinois – September 9, 1993

EDUCATION &   **B.S., Psychology**
TRAINING: Elmhurst University
                    2011-2015

                    M.S./Ph.D., Anatomical Sciences and Neurobiology
                    University of Louisville
                    2017-2023

AWARDS: Doctoral Dissertation Completion Award for Spring 2023,
                    University of Louisville (2022)

                    Writing in the Sciences (with Honors) Certification,
                    Stanford ONLINE (2022)

                    University of Louisville Graduate School Council Travel
                    Scholarship Award (2021)

                    Cum Laude Honors Award, Elmhurst University (2015)

                    Student Athlete CCIW Academic All-Conference Award,
                    Elmhurst University (2012-2015)

PROFESSIONAL SOCIETIES:	American Medical Writers Association
	Kentucky Academy of Science
	Neuroscience and Anatomical Sciences Student Association (NASSA), University of Louisville
	Association for Chemoreception Sciences
	Society for Neuroscience
	Local Chapter Society for Neuroscience, Louisville, KY
TEACHING:	Anatomical Sciences and Neurobiology Anatomy Seminar, Guest Lecturer, Fall 2022
	Synaptic Organization of the Central Nervous System, Graduate Teaching Assistant, Spring 2021
	Developmental Neurobiology, Reviewer for Mock Study Session, Spring 2020
	Neuroanatomy, Graduate Teaching Assistant, Fall 2020 and 2018
MENTORSHIPS:	Rose Hudson- Louisville Science Pathways, High School Student, Summer 2022
	Elizabeth Johnson- Louisville Science Pathways, High School Student, 2018-2019
	Taylor Hood- University of Louisville School of Medicine, Medical Student, Fall 2020
	Saphira (Mimi) Chiu- Department of Anatomical Sciences and Neurobiology, Master's Student, 2019-2021
	Kelsey McQueen- Department of Anatomical Sciences and Neurobiology, Master's Student, 2017-2019
PUBLICATIONS:	**Fredericksen KE**, Samuelsen CL. Neural representation of intraoral olfactory and gustatory signals by the

mediodorsal thalamus in alert rats. *J Neurosci. 2022;* 42 (43) 8136-8153. PMID: 36171086.

McQueen KA*, **Fredericksen KE***, Samuelsen CL. Experience informs consummatory choices for congruent and incongruent odor-taste mixtures. *Chem Senses* 2020; 45(5):371-382. *authors contributed equally. PMID: 32239150.

Fredericksen KE, McQueen KA, Samuelsen CL. Experience-Dependent c-Fos Expression in the Mediodorsal Thalamus Varies with Chemosensory Modality. *Chem Senses* 2019; 44(1):41-49. PMID: 30388214.

ORAL PRESENTATIONS (SELECT FEW):	**Fredericksen KE,** Chemosensory processing by the mediodorsal thalamus, Taste section presentation (03/2023)
	Fredericksen KE, Direct anatomical connectivity from the chemosensory cortices to neurons in the mediodorsal thalamus, Taste section presentation (08/2022)
	Fredericksen KE, The role of the mediodorsal thalamus in the consummatory choice of odors, tastes, and odor-tastemixtures, Taste section presentation (05/2022)
	Fredericksen KE, Chemosensory processing by the mediodorsal thalamus, Department-wide thesis defense (03/2021)
	Fredericksen KE, Flavor evoked responses in thalamus, Taste section presentation (05/2020)
	Fredericksen KE, Bilateral mediodorsal thalamus electrode implant surgery, Anatomy seminar presentation (02/2018)
POSTER PRESENTATIONS (NATIONAL/ INTERNATIONAL):	**Fredericksen KE**, Samuelsen CL. Processing of multimodal chemosensory stimuli by the mediodorsal thalamus. Society for Neuroscience (SfN). Virtual meeting. 11/2021.

Fredericksen KE, Samuelsen CL. Single-unit responses in the mediodorsal thalamus to orally consumed chemosensory stimuli. International Symposium on Olfaction and Taste (ISOT). Virtual meeting. 08/2020.

Fredericksen KE, Samuelsen CL. Single-unit responses to the intraoral delivery of chemosensory stimuli in the mediodorsal thalamus. Association for Chemoreception Sciences (AChemS) XLI. Bonita Springs, FL. 04/2019.

Bamji-Stocke SK, **Fredericksen KE**, Samuelsen CL. Subpopulations of Chemoresponsive Neurons in Gustatory Cortex Represent Different Properties of Flavors. Association for Chemoreception Sciences (AChemS) XL. Bonita Springs, FL. 04/2018.

POSTER PRESENTATIONS (LOCAL/ REGIONAL):	**Fredericksen KE**, Samuelsen CL. An anatomical study of synaptic connections from the chemosensory cortices to the mediodorsal thalamus. Sensorium. Cincinnati, OH. 11/2022.

Fredericksen KE, Samuelsen CL. Chemosensory coding in the mediodorsal thalamus. Neuroscience Day, Local Chapter of Society for Neuroscience. Louisville, KY. 04/2022.

Fredericksen KE, Samuelsen CL. Single-unit responses to the intraoral delivery of chemosensory stimuli in the mediodorsal thalamus. Neuroscience Day, Local Chapter of Society for Neuroscience. Louisville, KY. 04/2019.

Martinez A, **Fredericksen K**, Zuluaga E, Alejandria L, Moore K. Color and Memory: The Effect of Color Hue on Word Recall. Research and Performance Showcase at Elmhurst University. Elmhurst, IL. 05/2015.